

Ref

NBS
Publi-
cations

NATL INST. OF STAND & TECH



A11106 978560

NBSIR 77-1289

~~A11101 726388~~

The Measurement of Wind Loads On A Full-Scale Mobile Home

Richard D. Marshall

Center for Building Technology
Institute for Applied Technology
National Bureau of Standards
Washington, D.C. 20234

September 1977

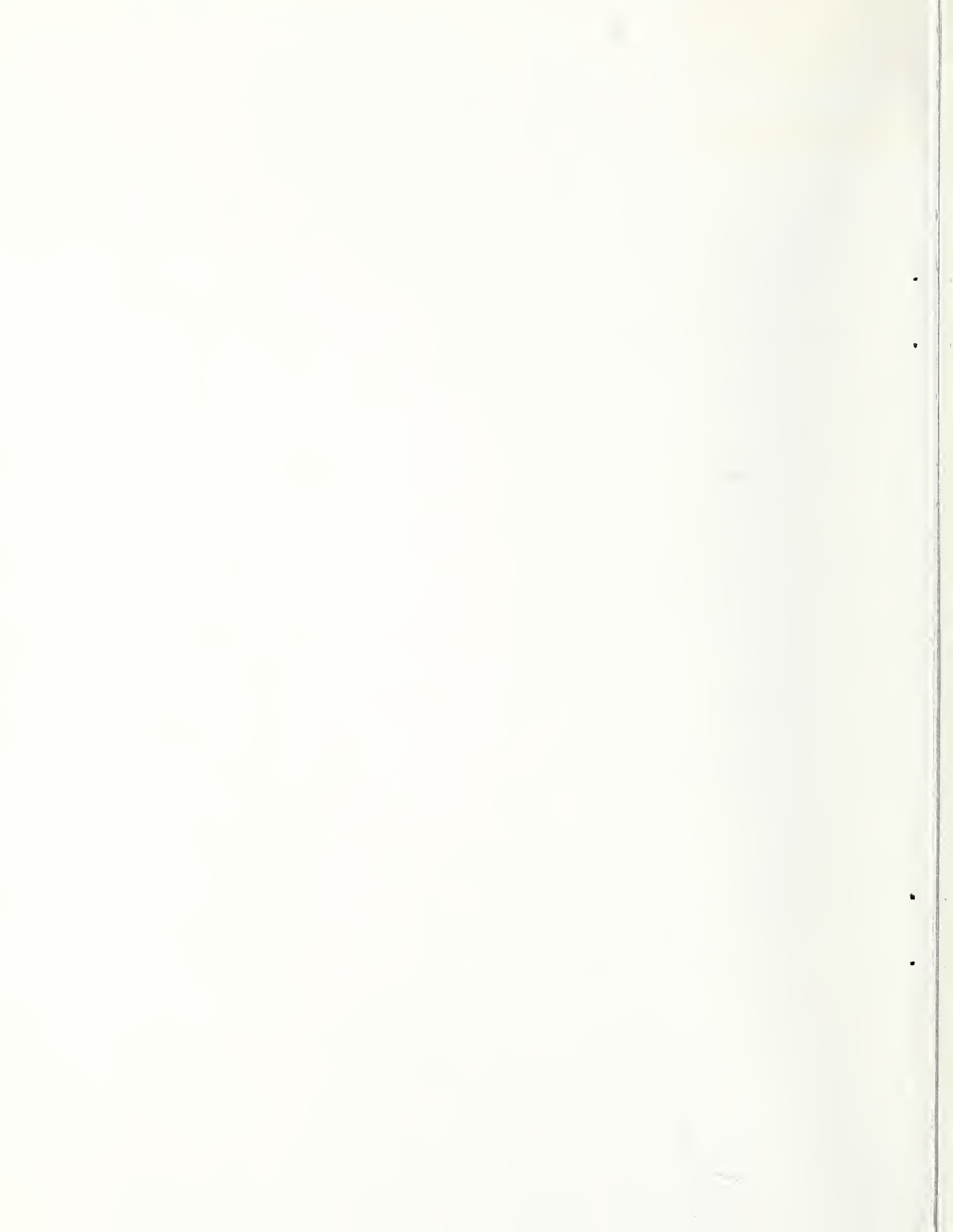
Prepared for
**Division of Energy, Building Technology and Standards
Office of Policy Development and Research
Department of Housing and Urban Development
Washington, D.C. 20410**

QC

100

.U56

77-1298



DEC 12 1979

NOT ACCEPTED

QC100

US6

77-1289

NBSIR 77-1289

**THE MEASUREMENT OF WIND
LOADS ON A FULL-SCALE MOBILE
HOME**

Richard D. Marshall

Center for Building Technology
Institute for Applied Technology
National Bureau of Standards
Washington, D.C. 20234

September 1977

Prepared for
Division of Energy, Building Technology and Standards
Office of Policy Development and Research
Department of Housing and Urban Development
Washington, D.C. 20410



U.S. DEPARTMENT OF COMMERCE, Juanita M. Kreps, *Secretary*

Dr. Sidney Harman, *Under Secretary*

Jordan J. Baruch, *Assistant Secretary for Science and Technology*

NATIONAL BUREAU OF STANDARDS, Ernest Ambler, *Acting Director*



SI Conversion Units

In view of the present accepted practice in this country for building technology, common U. S. units of measurement have been used throughout this publication. In recognition of the position of the United States as a signatory to the General Conference on Weights and Measures, which gave official status to the metric SI system of units in 1960, appropriate conversion factors have been provided in the table below. The reader interested in making further use of the coherent system of SI units is referred to:

NBS SP 330, 1972 Edition, "The International System of Units"

ASTM E380-75/IEEE Std. 268-1976 ASTM/IEEE, "Standard Metric Practice Guide"

Table of Conversion Factors to Metric (S.I.) Units

Physical Quantity	To Convert From	To	Multiply By
Length	inch (in)	meter (m)	2.540×10^{-2} *
	foot (ft)	meter (m)	3.048×10^{-1} *
Area	inch ²	meter ² (m ²)	6.4516×10^{-4} *
	foot ²	meter ² (m ²)	9.290×10^{-2}
Volume	inch ³	meter ³ (m ³)	1.639×10^{-5}
	foot ³	meter ³ (m ³)	2.832×10^{-2}
Force	pound (lbf)	newton (N)	4.448
Pressure or Stress	psi	pascal (Pa) or	6.895×10^3
	psf	newton/meter ² (N/m ²)	4.788×10^1
Mass	pound (lbm)	kilogram (kg)	4.536×10^{-1}
Unit Weight	pcf	kilogram/meter ³ (kg/m ³)	1.602×10^1
Velocity	mile/hr (mph)	meter/sec (m/s)	4.470×10^{-1}
Acceleration	foot/sec ²	meter/sec ² (m/s ²)	3.048×10^{-1}

*Exact value.



Abstract

An experimental investigation of wind loads acting on a full-scale mobile home is reported. The objectives of the investigation were (1) the direct measurement of surface pressures and overall drag and lift forces, (2) the formulation of recommended loads for the design of mobile homes and their anchoring systems to resist forces due to wind and (3) the measurement of deflections and the identification of failure modes with application of simulated wind loads.

Measurements were obtained for a variety of wind speeds and relative wind directions using a mobile home with nominal plan dimensions of 12 by 60 ft (3.7 by 18.3 m). Wind speeds were measured at five levels ranging from 1.5 to 18 m and the mean velocity profiles were found to be best described by a power law with exponent $\alpha = 0.18$.

Extreme negative pressure fluctuations were found to occur on the end walls and along the perimeter of the roof. The resonant component of response of the mobile home to drag and lift forces is negligible for basic wind speeds up to 90 mph (40 m/s) and the average maximum lift loads are not strongly influenced by the presence or absence of skirting.

Recommended design loads are based on the average maximum event in a time interval of 1000 seconds and are tabulated for assumed basic wind speeds of 70 and 90 mph (31 and 40 m/s) and a moderately open wind exposure.

Keywords: Aerodynamics; buildings; codes and standards; full-scale testing; mobile homes; wind loads.



TABLE OF CONTENTS

	Page
SI CONVERSION UNITS	iii
ABSTRACT	v
NOTATION	ix
LIST OF TABLES	xi
LIST OF FIGURES.	xiii
SUMMARY.	xv
1. INTRODUCTION	1
2. FULL-SCALE MEASUREMENT PROGRAM	1
2.1 The Mobile Home.	2
2.2 The Test Site.	2
2.3 Support Frame and Turntable.	5
3. INSTRUMENTATION.	12
3.1 Wind Speed	12
3.2 Pressure	12
3.3 Drag and Lift.	17
3.4 Acceleration	19
3.5 Data Acquisition	19
4. DATA REDUCTION AND ANALYSIS.	21
4.1 A-D Conversion	21
4.2 Mean and Standard Deviation.	21
4.3 Peak Values.	23
4.4 Spectral Analysis.	23
5. TEST RESULTS	24
5.1 Wind Speed	24
5.2 Time Histories and Spectra of Wind Speed and Pressure.	27
5.3 Pressure Coefficients.	38
5.4 Drag and Lift Coefficients	55
5.5 Structural Damping	62
6. RECOMMENDED DESIGN WIND LOADS.	66
6.1 Basic Wind Speeds.	66
6.2 Design Wind Speeds	66
6.3 Selection of Peak Factors.	67
6.4 Internal and External Pressures.	69
6.5 Maximum Drag and Lift Coefficients	74
6.6 Design Wind Loads.	78
7. LOAD-DEFLECTION STUDIES.	84
7.1 Experimental Setup	84
7.2 Load-Deflection Measurements and Failure Modes	89
7.3 Stiffness Coefficients	104
7.4 Forces in Tie-Down Cables.	104

	Page
8. CONCLUSIONS AND RECOMMENDATIONS.	109
9. ACKNOWLEDGMENTS.	111
10. REFERENCES	112
11. APPENDIX A: Illustrative Example - Determination of Design Loads.	115
12. APPENDIX B: Recommended Revisions of Wind Load Requirements for Federal Mobile Home Construction and Safety Standards.	117

NOTATION

- A = area
- a = amplitude level at upcrossing
- c = Weibull parameter
- \bar{C}_d = mean drag coefficient
- \bar{C}_l = mean lift coefficient
- \bar{C}_p = mean pressure coefficient
- $C_{p\sigma}$ = r.m.s. pressure coefficient (similarly for drag and lift)
- \hat{C}_p = maximum or minimum pressure coefficient as appropriate (similarly for drag and lift)
- g = peak factor = (peak value - mean)/(standard deviation)
- h = reference height (top of mobile home)
- H = height of mobile home superstructure (floor to ceiling)
- I = intensity of turbulence (percent)
- k = Weibull parameter
- L = length of member
- n = frequency (Hz)
- n_a = upcrossings of amplitude level "a" per unit time
- n_o = upcrossings of the mean per unit time
- n_p = average rate of occurrence of positive or negative peaks in the record
- \bar{p} = mean pressure over record length
- \hat{p} = maximum or minimum pressure as appropriate
- p' = maximum or minimum pressure between successive upcrossings of the mean
- p_o = freestream static pressure
- $P(>X)$ = complementary cumulative distribution function of X.
- \bar{q}_h = reference dynamic pressure at height h
- S = spectral density
- t = time
- \bar{u} = mean velocity over record length
- \hat{u} = maximum velocity observed in record
- u_{FM} = speed based on fastest mile of wind
- V_R = coefficient of variation of resistance

w_n = weight factor

W = width of mobile home

α = mean wind speed profile index

$\bar{\beta}$ = mean wind direction relative to true north

$\bar{\theta}$ = mean wind direction relative to axis of mobile home measured clockwise from front

ρ = mass density of air

σ = standard deviation

ϕR = factored ultimate resistance

$\gamma_d D$ = factored dead load

$\gamma_w W$ = factored wind load

LIST OF TABLES

- TABLE 1. Test Configuration and Characteristics of Records
2. Wind Characteristics From 1.5 to 18 Meters as Measured by Propeller Anemometers
 3. Single-Point Pressure Coefficients
 4. Multiple-Point Pressure Coefficients
 5. Individual Drag Coefficients
 6. Combined Drag Coefficients
 7. Lift Coefficients
 8. Damping Ratios
 9. Average Maximum Single-Point Pressure Coefficients
 10. Average Maximum Multiple-Point Pressure Coefficients
 11. Average Maximum Combined Pressures
 12. Average Maximum Drag Coefficients (Individual)
 13. Average Maximum Drag Coefficients (Combined)
 14. Average Maximum Lift Coefficients
 15. Recommended Design Loads for Standard and Hurricane Wind Zones



LIST OF FIGURES

- Fig. 2.1 - Mobile Home Installed on Test Frame
- Fig. 2.2 - Mobile Home Layout and Pressure Tap Designations
- Fig. 2.3 - Test Site Plan
- Fig. 2.4 - Details of Foundation System
- Fig. 2.5 - Layout of Main Support Frame and Turntable
- Fig. 2.6 - Jackscrews Used to Level Main Support Frame
- Fig. 2.7 - View of Vertical Force Link
- Fig. 3.1 - View of 18 m Meteorological Mast
- Fig. 3.2 - Pressure Transducer and Solenoid Valve Arrangement
- Fig. 3.3 - Details of Pressure Tap
- Fig. 3.4 - Transducer - Valve Assembly
- Fig. 3.5 - Ambient Pressure Probe
- Fig. 3.6 - Data Acquisition System
- Fig. 4.1 - Data Acquisition and Analysis Flow Chart
- Fig. 5.1 - Typical Mean Velocity Profiles - Power Law Representation
- Fig. 5.2 - Estimates of Mean Wind Speed Profile Index α for Various Wind Directions
- Fig. 5.3 - Typical Time Histories of Wind Speed and Pressure, Record No. 10-4
- Fig. 5.4(a) - Spectrum of Wind Speed at 3 Meters
- Fig. 5.4(b) to 5.4(f) - Spectra of Wind Pressures on Mobile Home
- Fig. 5.5 - Definition Sketch of Mean, Standard Deviation and Peak Factor
- Fig. 5.6 - Probability Distribution of Peak Values, Record No. 10-5, Tap 64
- Fig. 5.7 - Probability Distribution of Peak Values, Record No. 12-5, Tap R4
- Fig. 5.8 - Distribution of Mean Pressure Coefficients, Skirting Installed
- Fig. 5.9 - Distribution of Mean Pressure Coefficients, Skirting Removed
- Fig. 5.10 - Spectrum of Drag Load, Record No. 8-2, Force Link No. 9
- Fig. 5.11 - Analysis of Acceleration Time History
- Fig. 6.1 - Variation of Maximum Wind Speed With Averaging Time
- Fig. 6.2 - Variation of Peak Factor With Averaging Time
- Fig. 6.3 - Loading Diagrams for Recommended Design Loads Listed in Table 15
- Fig. 7.1 - Loading Scheme for Load-Deflection Studies
- Fig. 7.2 - View Showing Booms and Tension Rods
- Fig. 7.3 - View Showing Whiffletrees on "Windward" Side
- Fig. 7.4 - View of Whiffletree System for Applying Uplift Forces
- Fig. 7.5 - Locations of Load Points and Deflection Measurement Sections
- Fig. 7.6 - Load versus Deflection for Load Case No. 1
- Fig. 7.7 - Load versus Deflection for Load Case No. 2
- Fig. 7.8 - Load versus Deflection for Load Case No. 3
- Fig. 7.9 - Load versus Diagonal Displacement for Load Case No. 3
- Fig. 7.10 - View of Failure in Roof-to-Wall Connection (load applied)
- Fig. 7.11 - View of Top Plate and Header (facia strip and roof membrane removed)
- Fig. 7.12 - Load versus Diagonal Displacement for Load Case No. 4

LIST OF FIGURES (continued)

Fig. 7.13 - Yield Lines in Web of Underframe Stringer at Load Point No. 1

Fig. 7.14 - Load versus Deflection for Load Case No. 5

Fig. 7.15 - Condition of Front End Wall at Maximum Load

Fig. 7.16 - Load versus Diagonal Displacement for Load Case No. 5

Fig. 7.17 - Forces in Tie-Down Cables for Load Case No. 3

Fig. 7.18 - Forces in Tie-Down Cables for Load Case No. 4

SUMMARY

This report describes instrumentation, experimental techniques and test results obtained from a study of wind forces acting on a full-scale mobile home. The information presented herein forms the basis for recommended revisions of Section 280.305 "Structural Design Requirements," Part (c) "Wind, Snow, and Roof Loads," Subsections (1), (2), and (3) of the federal Mobile Home Construction and Safety Standards, dated December 18, 1975. These recommended revisions are included as an appendix to this report and are intended as minimum requirements for the design of mobile homes to resist wind loads.



1. INTRODUCTION

Although the general area of wind research has made tremendous advances over the past decade, most of the effort has been concentrated on tall buildings and other major engineering structures. Only recently have wind loading problems associated with low-rise buildings begun to receive proper attention. There are several reasons for this set of circumstances, among them the lack of economic incentive for seeking design refinements in individual buildings of relatively low initial cost and a prevailing belief that conventional low-rise buildings, single-family dwellings in particular, do not merit the same concern for structural integrity that is associated with larger buildings. Studies of damage caused by hurricanes, tornadoes and other strong winds consistently point to housing as the major contributor to economic loss and in the case of mobile homes, wind is second only to fire in causing deaths, injuries and property damage [1, 2, 3]^{1/}. As mobile homes currently account for 20 to 30 percent of single-family housing production in the United States [4], the benefits to be derived from better load definition are substantial.

The determination of wind forces on mobile homes is complicated by the fact that, near ground level, the local terrain and adjacent buildings can have a pronounced effect on the mean wind speeds and on the intensity of wind gusts (turbulence). In addition, the relatively high ratio of wind load to dead load and the limited physical size of mobile homes tend to make them more sensitive to wind effects than is the case for buildings of larger dimensions where spatial averaging can substantially reduce the effectiveness of gusts in producing load fluctuations.

The purpose of this research effort is to document both localized and overall loading due to wind, to provide a rational basis for the determination of wind forces acting on mobile homes and their anchoring systems, to develop specific wind load requirements on which to base revisions of the federal Mobile Home Construction and Safety Standards [5], and to provide reference data for future investigations of wind forces on mobile homes and similar low-rise buildings. This study was sponsored by the Energy, Building Technology and Standards Division of the Office of Policy Development and Research, Department of Housing and Urban Development (HUD) as part of its series of research projects directed towards the improvement of the federal Mobile Home Construction and Safety Standards as required by Title VI of the Housing and Development Act of 1974.

2. FULL-SCALE MEASUREMENT PROGRAM

The systematic investigation of wind forces acting on a structure and the response of the structure to those forces can most conveniently be carried out in a wind tunnel. To be valid, this approach requires that certain features of the atmospheric surface flow be

^{1/} Figures in brackets indicate literature reference on page 112.

adequately simulated at some reduced scale and that the structure under consideration be modeled at this same scale. Adequate wind tunnel simulations of atmospheric surface flows have been accomplished at scale ratios of from 1:200 to 1:500 which would make it extremely difficult to construct and instrument models of mobile homes and their supports and tie-down systems at the required scale. For the measurement of surface pressures a simple geometric model is usually sufficient, but for those cases in which the dynamic response is of concern, structural characteristics such as stiffness, mass distribution and damping must also be modeled. If load-deflection relationships and failure modes are of interest, individual structural members and connections must be modeled and this is usually done at scale ratios of from 1:3 to 1:10.

In view of these problems associated with model studies, it was decided early in the program that a comprehensive set of wind load measurements should be obtained in full scale to provide the basis for design load recommendations for conventional "single-wide" units and to provide a means for checking the validity of any future wind tunnel studies of more complex mobile home geometries and various types of wind exposure. The experimental techniques and test results described in this report consist of two distinct phases; a first phase involving the measurement of wind loads on a full-scale mobile home under strong wind conditions, and a second phase in which simulated wind loads were applied to the mobile home to establish load-deflection relationships and to identify failure modes. It is important to understand that the results of the first phase form the basis for the design load recommendations contained in this report and that these recommendations are in no way related to the results obtained in the second phase. The specimen mobile home and experimental setup are described in the following sections. Consultations were held with the project sponsor and technical representatives of the mobile home manufacturing industry to reach a consensus on the choice of the specimen mobile home and the experimental setup prior to conducting the full-scale measurement program.

2.1 The Mobile Home - The mobile home used in this study was obtained from the HUD inventory at Wilkes-Barre, Pennsylvania, where several thousand units had been stored following deployment as temporary shelter for victims of Hurricane Agnes in 1972. Nominal plan dimensions are 12 by 60 ft (3.7 by 18.3 m) and an overall view of the mobile home installed at the test site is shown in Figure 2.1. The floor plan and a typical cross-section are shown in Figures 2.2 and 7.1, respectively. The dead load with furnishings removed averaged 260 lbf/ft (3.8 kN/m). Thus the exterior geometry and mass distribution (those parameters which largely govern the wind loads and response to those loads for a given wind condition) of the specimen mobile home are typical of current "single-wide" units. Details of the mobile home construction, which are pertinent to the load-deflection studies carried out following completion of the wind load measurements, are presented in Section 7.

2.2 The Test Site - A parking area at the south end of the Gaithersburg Campus of the National Bureau of Standards (NBS) was selected for the field test site. The availability of electric service lines and a flat, paved surface on which to rotate the mobile home greatly

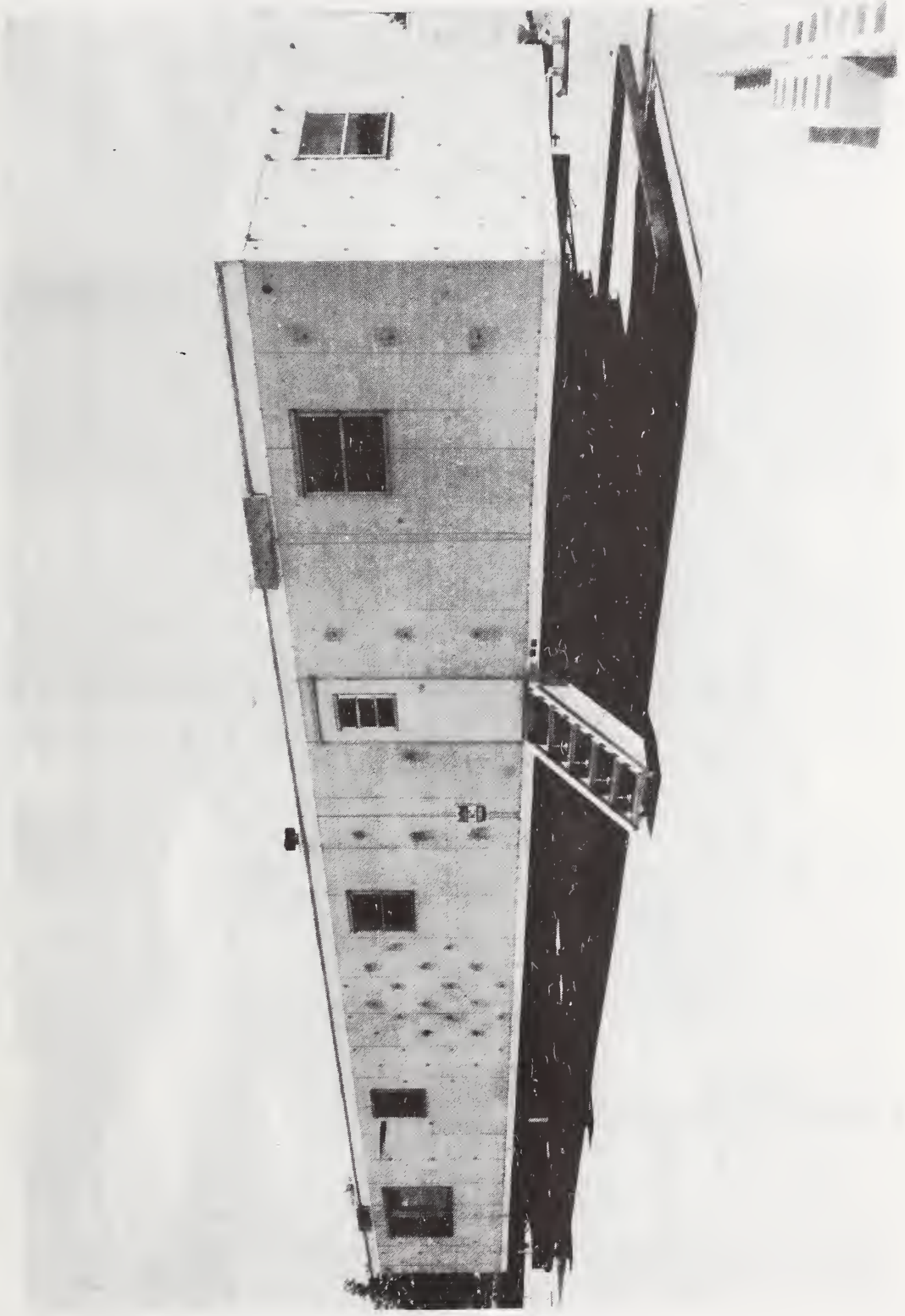


Fig. 2.1 - Mobile Home Installed on Test Frame

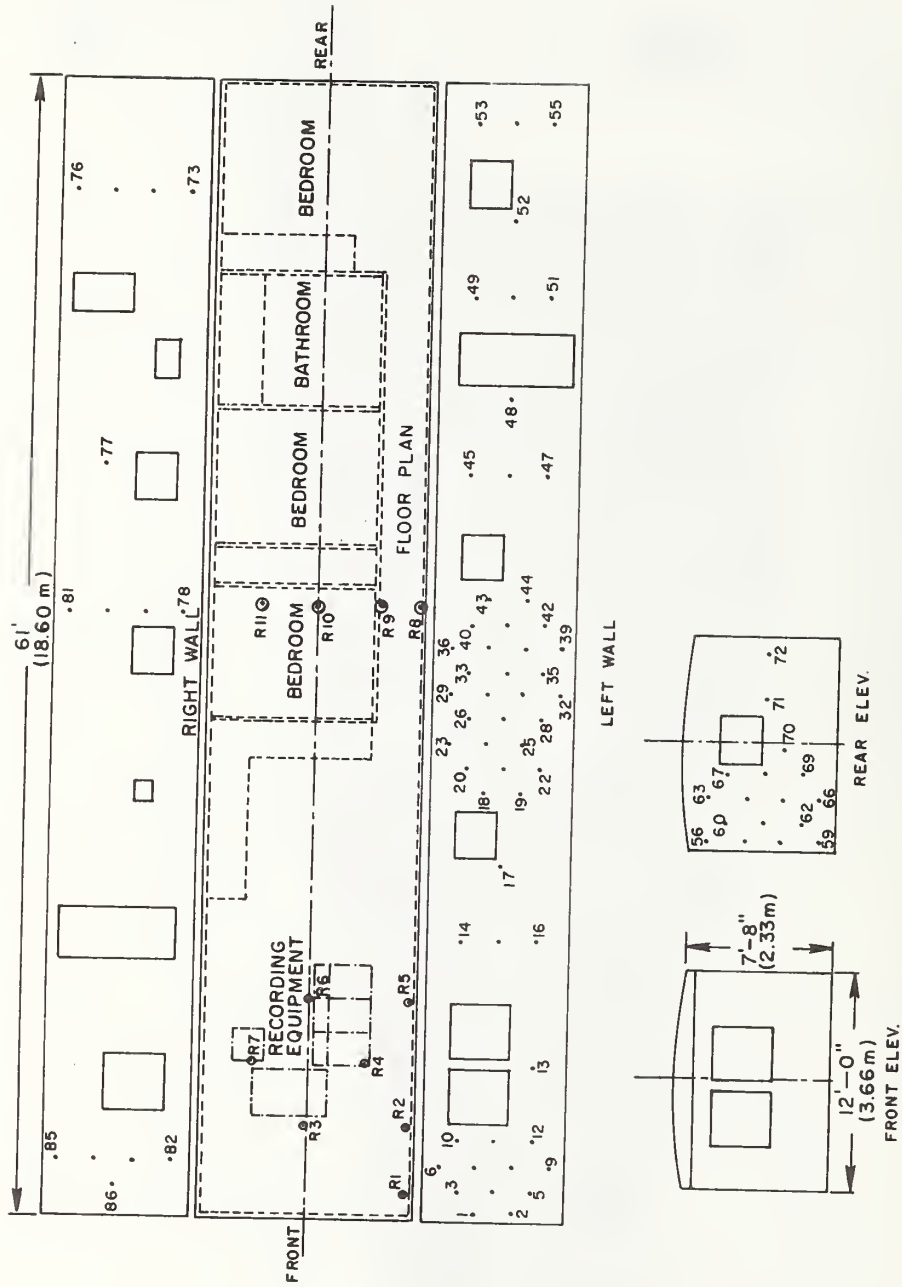


Fig. 2.2 - Mobile Home Layout and Pressure Tap Designations

simplified the experimental setup. The surrounding terrain in the direction of the prevailing winds can best be described as gently rolling grassland and cultivated fields with a few scattered trees. Two buildings are located adjacent to the test site as shown in Figure 2.3. However, for the records discussed in this report, the influence of these buildings on the wind field around the mobile home was insignificant. Strong winds in the Gaithersburg area are most frequent during the winter months from November through March and usually come from the west-northwest although several events can be expected each winter from the southwest. Maximum gusts of 45 to 60 mph (20 to 27 m/s) are normal.

2.3 Support Frame and Turntable - The criteria for the design of the mobile home support frame were as follows: (1) that rotation of the mobile home and support frame be possible under strong-wind conditions in order to change the relative wind direction, (2) that the support frame provide a realistic simulation of the in-service foundation conditions of a typical mobile home installation, and (3) that the stiffness of the support frame be much greater than that of the mobile home to avoid resonance problems.

The first criterion was important because of the limited range of wind directions that could reasonably be expected to occur at the test site during the winter months and the need to complete the field studies in a relatively short period of time. The support frame can best be described as three separate components; the foundation system, the force measurement system and the main support frame. The foundation system consists of four identical steel beam and column assemblies which simulate footings and piers and include diagonal and over-the-top tie-downs as shown in Figure 2.4. The force measurement system consists of four force links to measure horizontal forces (drag) and eight force links to measure vertical forces (lift). These force links transmit the loads acting on the beam and column assemblies to the main frame which is supported by four leveling jacks and a turntable as shown in Figures 2.4 and 2.5. To rotate the mobile home the jacks are retracted and the load is transferred to a set of casters located at the front end of the main support frame (Figure 2.6). A manometer system installed in the mobile home facilitated adjustment of the leveling jacks after rotation. The turntable-caster arrangement allowed 216 degrees of rotation (Figure 2.3) and a set of guide rollers kept the main support frame centered on the turntable during rotation.

In designing the various components of the support frame the lowest first-mode natural frequencies (both vertical and horizontal) were required to be at least $\sqrt{2}$ times the highest first-mode natural frequencies of the mobile home. This requirement prevented resonance of the mobile home and foundation system and approximately uncoupled the dynamic response of the mobile home and the support frame. The mobile home natural frequencies were determined by temporarily mounting the home on piers located as shown in Figure 2.4, exciting the home and measuring the free vibration with an accelerometer. The highest first-mode natural frequencies were approximately 8 Hz vertical and 4 Hz horizontal.

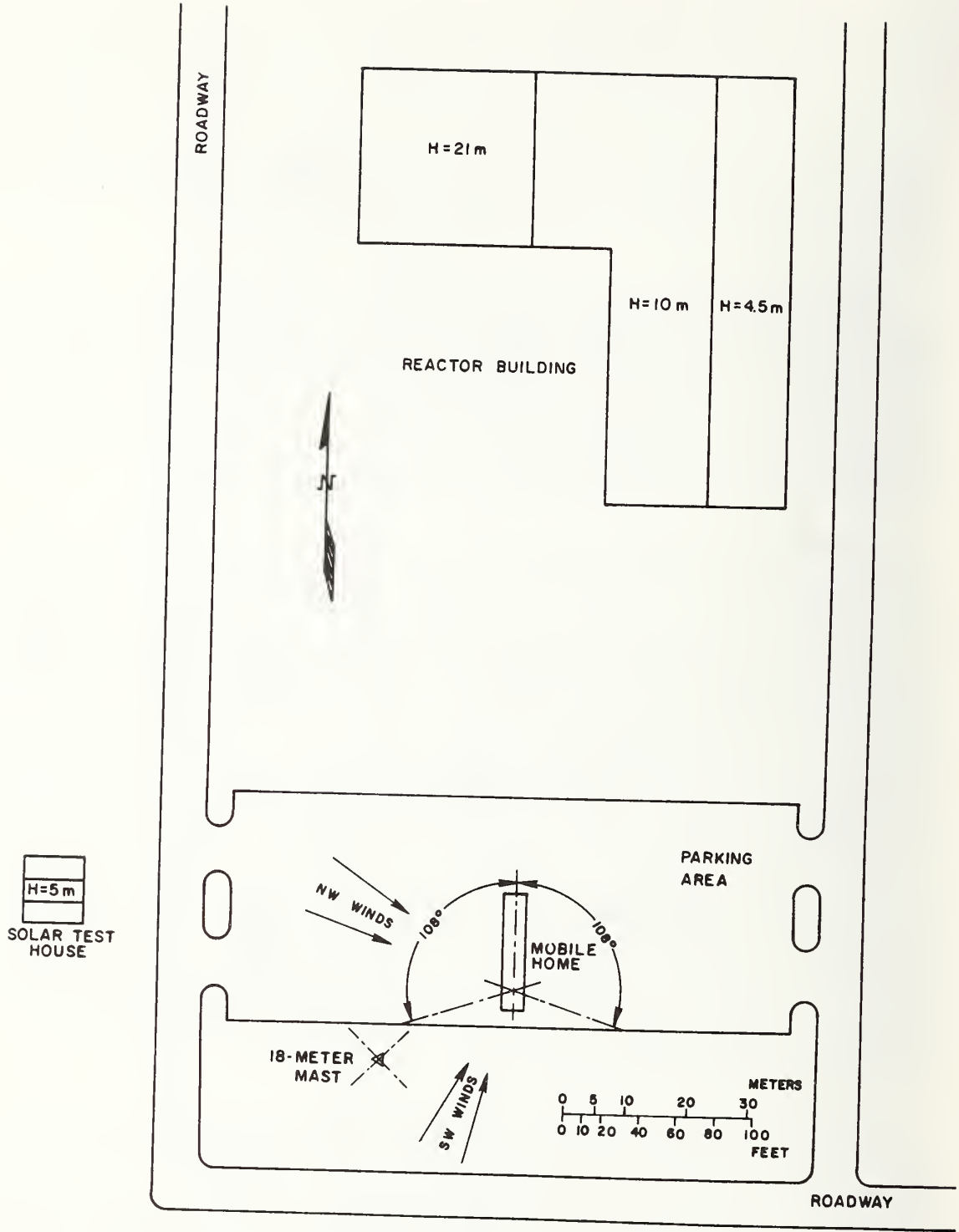


Fig. 2.3 - Test Site Plan

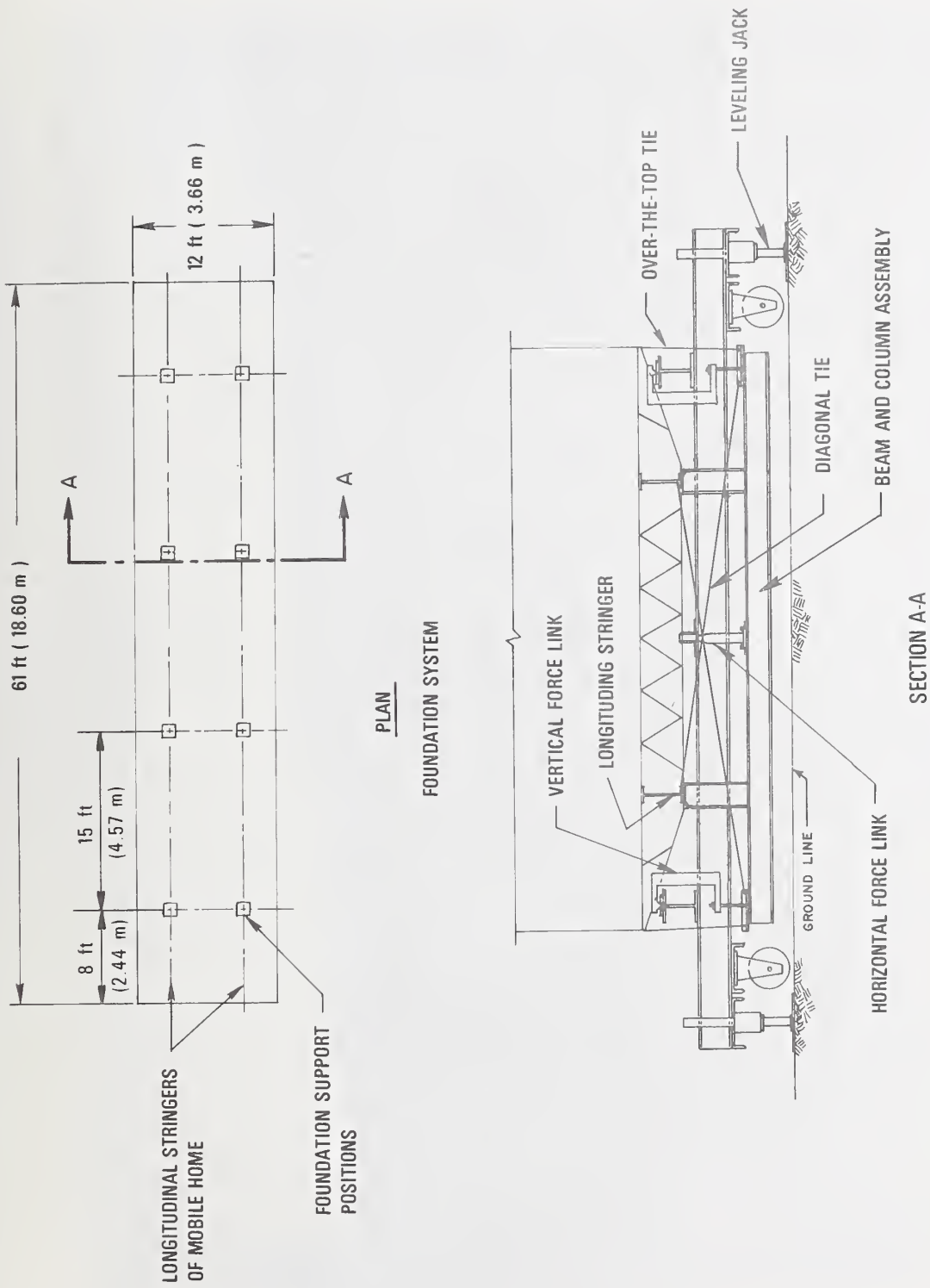
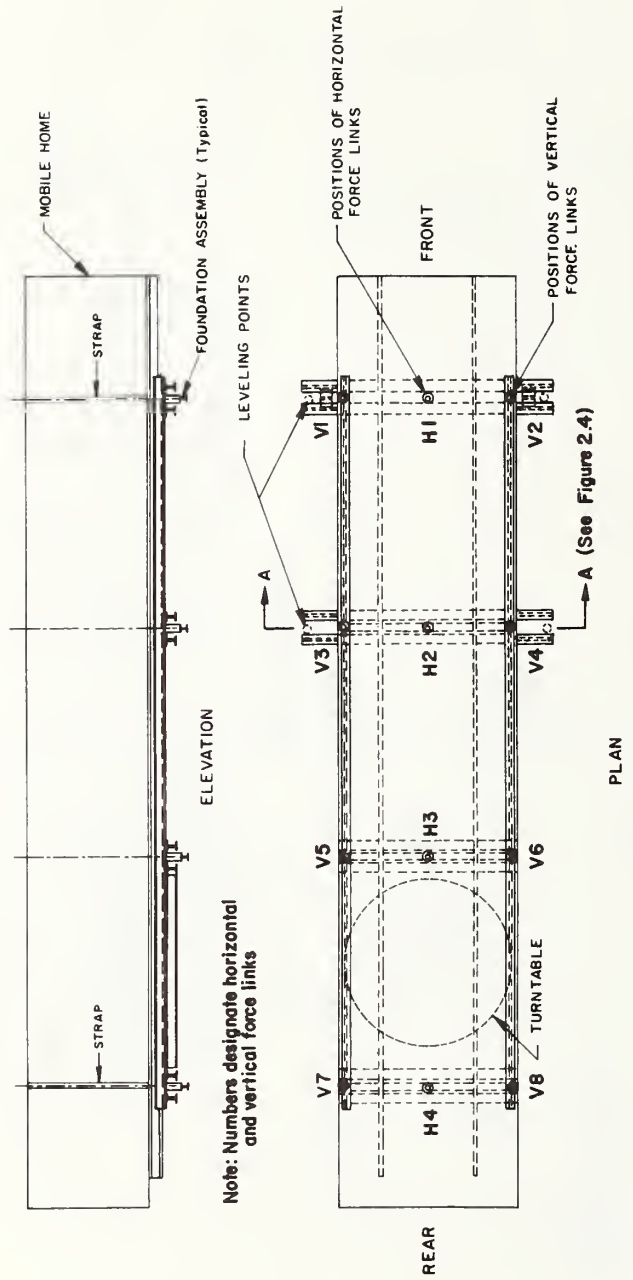


Fig. 2.4 - Details of Foundation System



Note: Numbers designate horizontal and vertical force links

Fig. 2.5 - Layout of Main Support Frame and Turntable

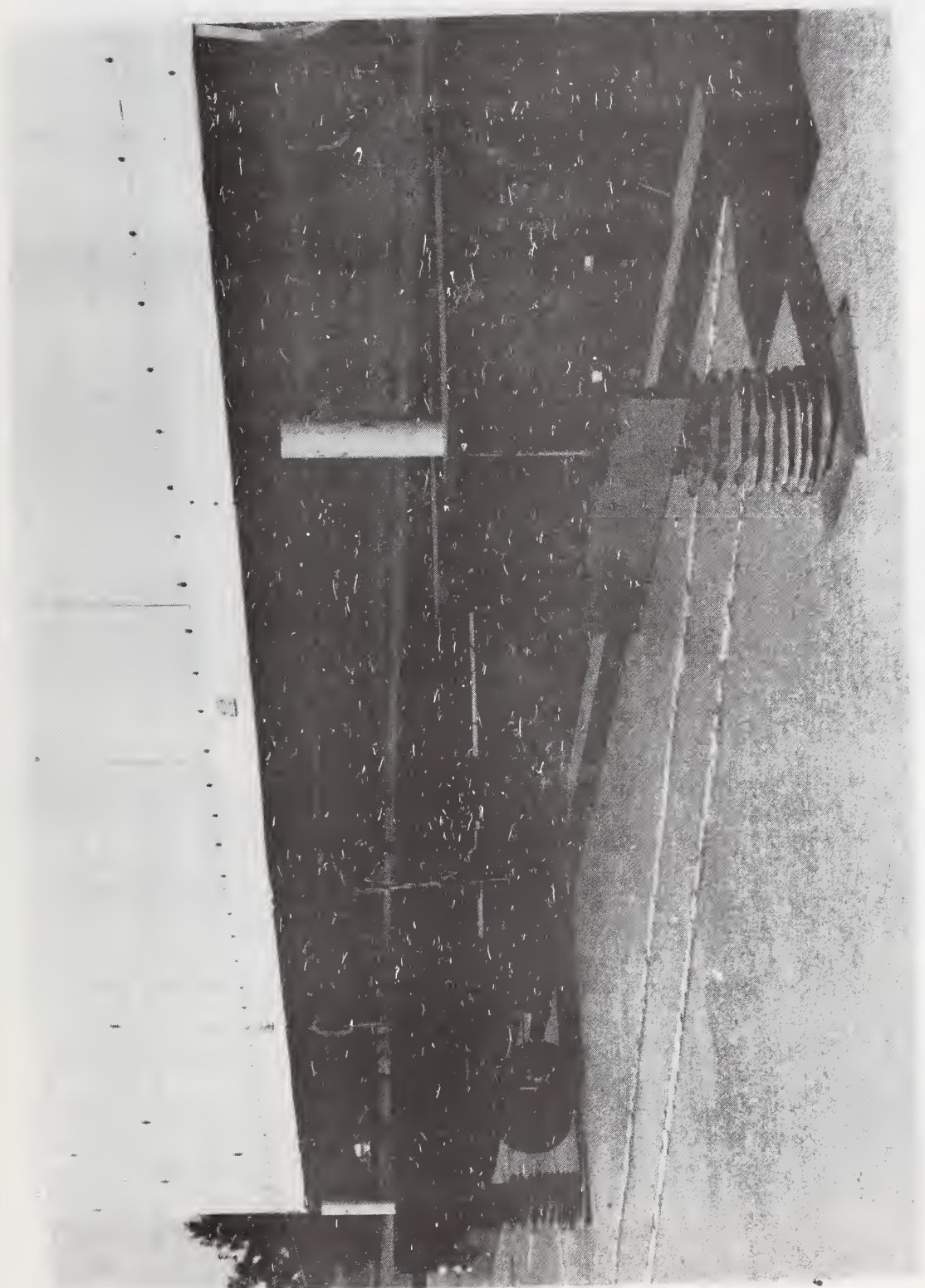


Fig. 2.6 - Jackscrews Used to Level Main Support Frame

Locations of the force links are shown in Figures 2.4 and 2.5 and a view of a vertical force link is shown in Figure 2.7. A knife edge welded to the top arm and a ball joint mounted on the bottom arm allow the transmission of vertical forces only. The channel section at the bottom of Figure 2.7 supports plywood skirting (removed). Both skirted and unskirted configurations were investigated. The horizontal force links were designed to act as cantilevers, being clamped to the main support frame at the top and contacting the beam and column assembly of the foundation system through knife edges at the bottom as shown in Figure 2.4.

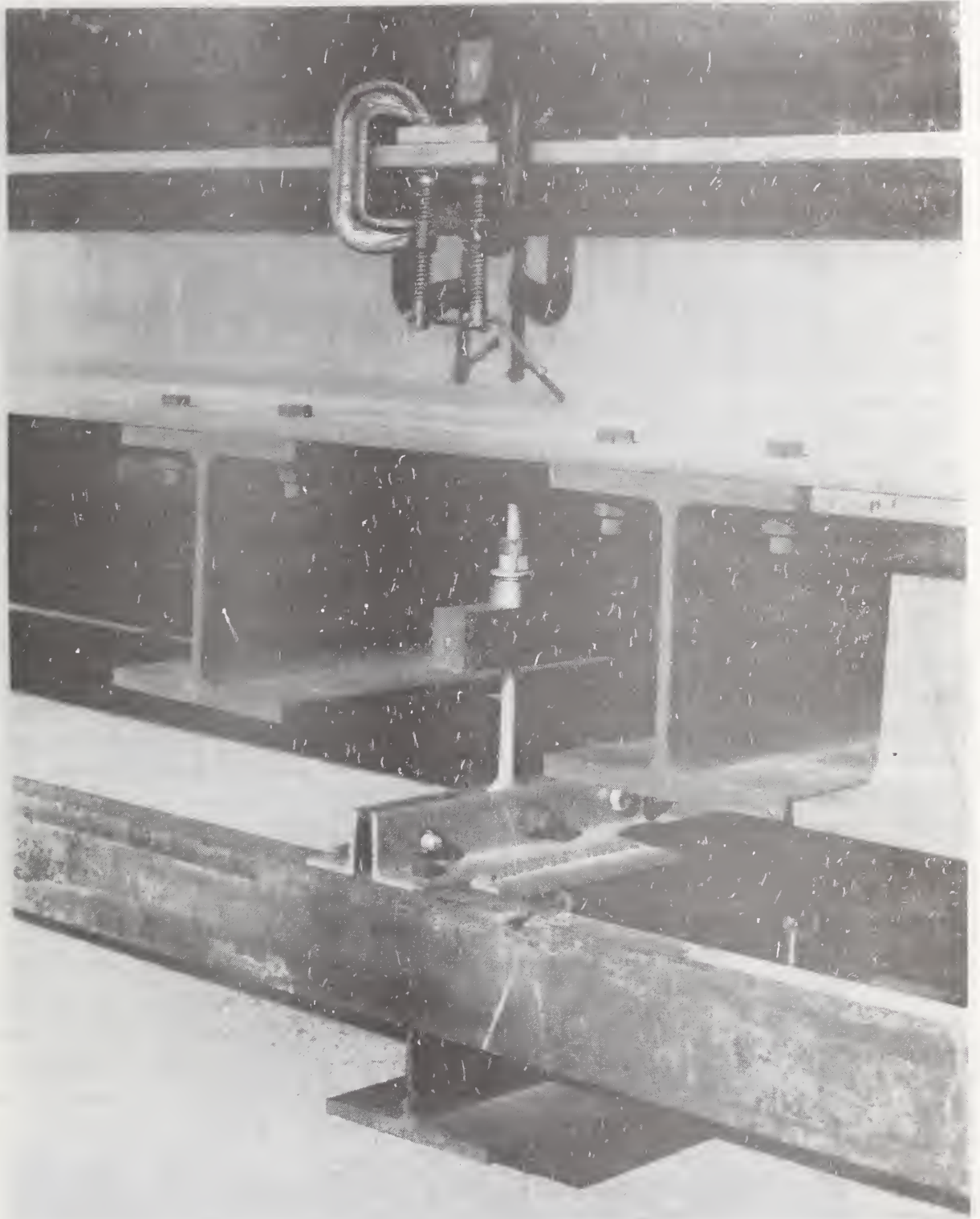


Fig. 2.7 - View of Vertical Force Link

3. INSTRUMENTATION

The following sections describe the arrangement and essential characteristics of instrumentation used to obtain measurements of wind speed, pressure, drag, lift and acceleration in the first phase of the study.

3.1 Wind Speed - An 18 m guyed mast was located to the southwest of the mobile home (Figure 3.1) and instrumented with propeller anemometers (Gill Mod. 27100 equipped with 4-blade propellers) at the 18, 10, 5, 3 and 1.5 m levels. The anemometers were clamped to a pipe running the height of the mast so that they could be manually aligned with a wind direction vane mounted at the top of the mast. So that wind speed data could be correlated with National Weather Service records, a standard 3-cup anemometer (Mod. F420-C) was mounted on a boom at the 10 m level. This anemometer provided the signal for triggering the data acquisition system while operating in the automatic mode and a continuous stripchart record of wind speed was obtained from this anemometer during the course of the study. In addition to the mast-mounted anemometers, two propeller anemometers were mounted on portable tripods which were usually located directly upwind of the mobile home. The heights of these anemometers were adjustable from 1.5 to 2.5 m.

The anemometer signals were filtered by means of a simple RC network to remove brush ripple and the output voltages were trimmed to a nominal sensitivity of 10 mv/mph (22 mv/ms^{-1}). The output impedance of the signal conditioning circuit required a sensitivity correction of approximately 5 percent when operating with analog tape recorders. The anemometers were calibrated in a wind tunnel prior to being installed on the mast and were periodically calibrated in place during the study using synchronous motors. Maximum changes in sensitivity of the anemometer circuits during the study were of the order of ± 2 percent.

3.2 Pressure- Pressures on the exterior surfaces of the mobile home and the internal pressure were measured by means of differential pressure transducers of the variable-reluctance type that had been used successfully in previous NBS studies of wind loading [6, 7]. To account for changes in the zero readings due to thermal drift and repositioning of the transducers a scheme developed at the Building Research Station (U.K.) [8] for obtaining transducer offsets under windy conditions was used in this study. A solenoid valve is placed in the reference pressure line and normally transmits the reference pressure to the back side of the transducer. When actuated, the valve connects the back side of the transducer to the active pressure line, thus providing a net transducer electrical offset for a zero pressure differential. The transducer-valve arrangement and details of the pressure taps used in this study are shown in Figures 3.2 and 3.3. The complete assembly was mounted in a bracket as shown in Figure 3.4 and this allowed the transducer array to be changed in a matter of a few minutes between recordings.

An ambient pressure probe developed at the NBS [9] was mounted on the anemometer mast at a height of 11 m and served all of the pressure taps through a manifold system of 3/16-in

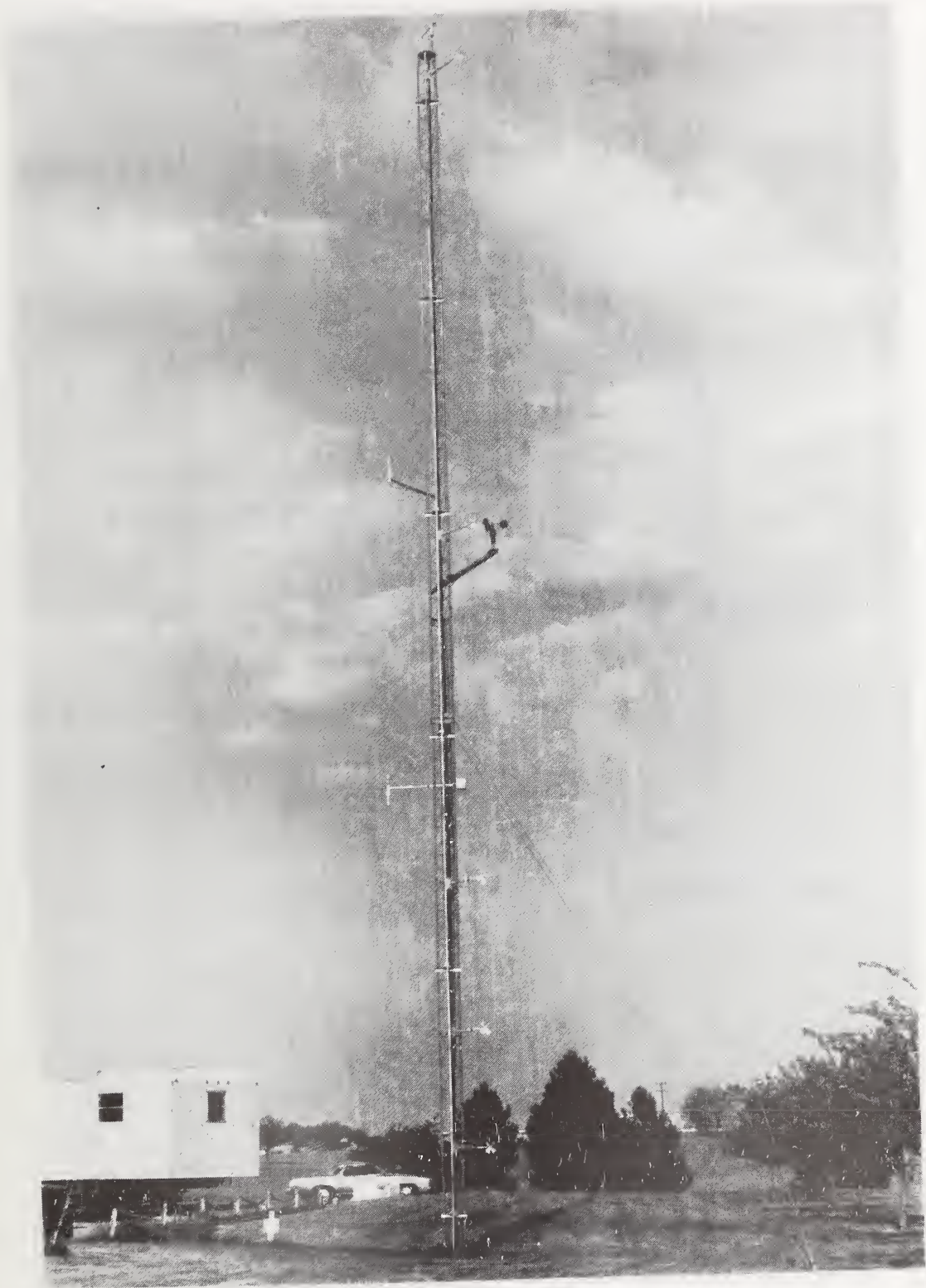


Fig. 3.1 - View of 18 m Meteorological Mast

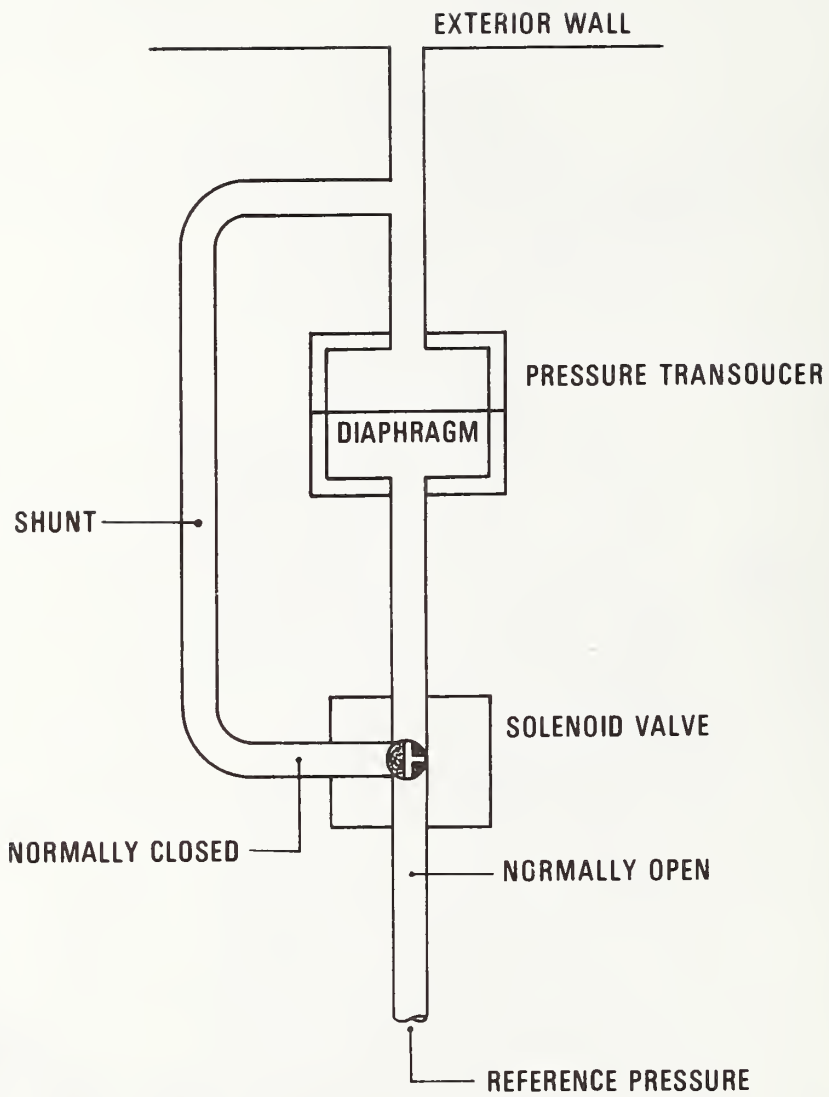


Fig. 3.2 - Pressure Transducer and Solenoid Valve Arrangement

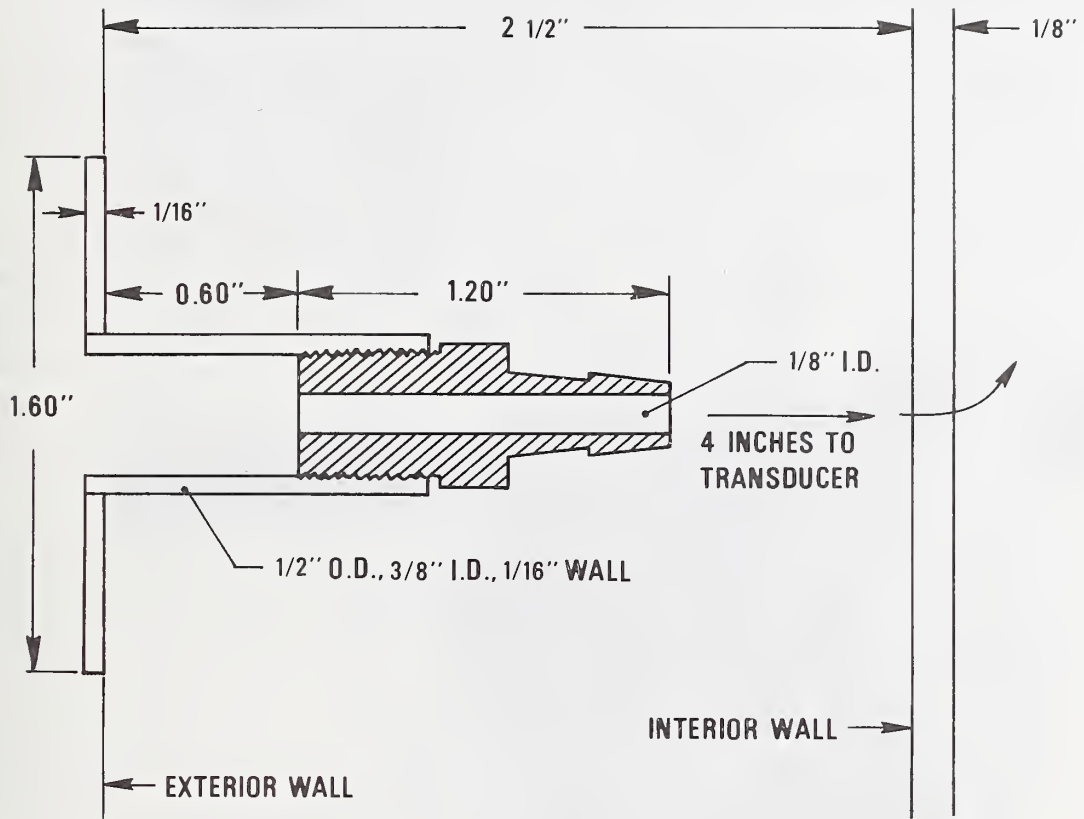


Fig. 3.3 - Details of Pressure Tap



Fig. 3.4 - Transducer - Valve Assembly

(4.8-mm) I.D. flexible tubing. The probe, shown in Figure 3.5, registers true ambient pressure for all wind directions in the horizontal and accommodates vertical angles of attack up to ± 10 degrees.

Dynamic calibration of the tap-tube-transducer arrangement shown in Figures 3.2 and 3.3 indicated a flat response to 40 Hz. Nominal output was ± 10 volts at the full-scale range of ± 0.1 psi (± 689 N/m²). A switch-selectable filter on the output stage of the transducer demodulator could be set at 5, 10, 200 or 1000 Hz. For most of the pressure recordings obtained in this study the outputs were filtered at 10 Hz. Twenty-seven pressure transducers were used in the study.

Although the pressure taps were designed to operate under conditions of wind-driven rain, problems were encountered with the accumulation of water in the ceiling taps. Porous drain plugs at the bottoms of these taps had a tendency to clog during periods of heavy rainfall with the result that water entered the active line to the pressure transducers. This required that the ceiling taps be blown out periodically. The meniscus formed in the active line caused a pronounced shift in the transducer offset and it was therefore obvious when a clogging condition had occurred.

Transducer offsets were recorded at the beginning of each record and full-scale outputs were checked against a secondary pressure standard once each week on average. Maximum error due to transducer drift, changes in sensitivity, recorder drift and A-D conversion is estimated to be of the order of ± 0.03 psf (1.4 N/m²).

3.3 Drag and Lift - Direct measurements of response to drag and lift forces were obtained from the force links briefly described in Section 2.3. Stiffness requirements for the force links and the relatively high input levels required by the data acquisition system complicated the instrumentation scheme for the force links. Foil straingages in a full-bridge configuration were used in conjunction with DC amplifiers to obtain output levels which were compatible with the input section of the data acquisition system. The gages were sealed with a protective rubber coating and were powered with a common 10 VDC supply. A shunt resistor on each bridge allowed the condition of the bridges to be monitored under load. The nominal sensitivities (without amplification) were 4.5 and 12.3 μ v/lbf (1.0 and 2.8 μ v/N) for the vertical and horizontal force links, respectively. Amplifiers with a nominal gain of X200 and an adjustable DC offset were used with the vertical force links, the amplifier outputs being nulled under calm conditions. The outputs of the horizontal force links were nulled with a trimming resistor prior to amplification (X100). Only four of the vertical force links were operated continuously as transducers during the study due to problems with drift in the amplifiers and offset suppression circuits. Problems encountered with the vertical force links are discussed in a subsequent section. The bridge-amplifier configuration for the horizontal force links proved to be far more stable, the offsets of the individual links measured under calm conditions being caused by warping of the mobile home superstructure with changes in temperature and humidity.



Fig. 3.5 - Ambient Pressure Probe

3.4 Acceleration - In addition to the preliminary acceleration measurements used to determine the mobile home natural frequencies, recordings of the transverse acceleration of the roof structure under windy conditions were obtained by mounting a single-component accelerometer on the bottom chord of a roof truss directly below tap R10 (See Figure 2.2). These recordings were used to obtain estimates of the structural damping. Damping is discussed in Section 5.5.

3.5 Data Acquisition - The data acquisition system used in this phase of the study consists of a computer-controlled multiplexer, sample-and-hold amplifier, 12-bit A-D converter and 7-track tape deck. Triggering level, sampling rate, amplifier gain and record length are selected during program entry, and initiation and termination of recording can also be accomplished by manual intervention. Channels are multiplexed at a rate of 20 kHz. The system also provides for a 14-track analog tape recorder to be operated under computer control. Master time is supplied to both the digital and analog systems by a time code generator. Details of the system have been previously described in the literature [6].

It was intended at the outset to record the outputs of all data channels (49 maximum) on digital tape and to record selected channels on analog tape as well so that higher sampling rates could, if necessary, be obtained at a later date. However, problems with the digital tape recorder resulted in most of the data being recorded in analog form and only a few records incorporating all data channels were recorded on digital tape near the end of the test schedule. Two 14-track analog recorders were used at other times to record a total of 26 channels of data simultaneously, one channel on each recorder being reserved for time code.

The maximum sampling rate is governed by the number of channels being recorded. For this study the limit was approximately 30 samples per channel per second. However, a rate of 24 samples per second was generally used, being reduced to 12 samples per second for records consisting only of wind speed data. Record lengths of 20 minutes were the usual case, but continuous analog recordings of up to 2 hours were obtained on certain occasions. It was standard procedure to also record open-scale stripchart records of wind speed and direction. A continuous closed-scale record of wind speed at the 10 m-level was also obtained during the course of this study. The data acquisition system is shown in Figure 3.6. The three cabinets on the left contain signal conditioning equipment and the analog tape recorder while those on the right contain the digital data acquisition system.

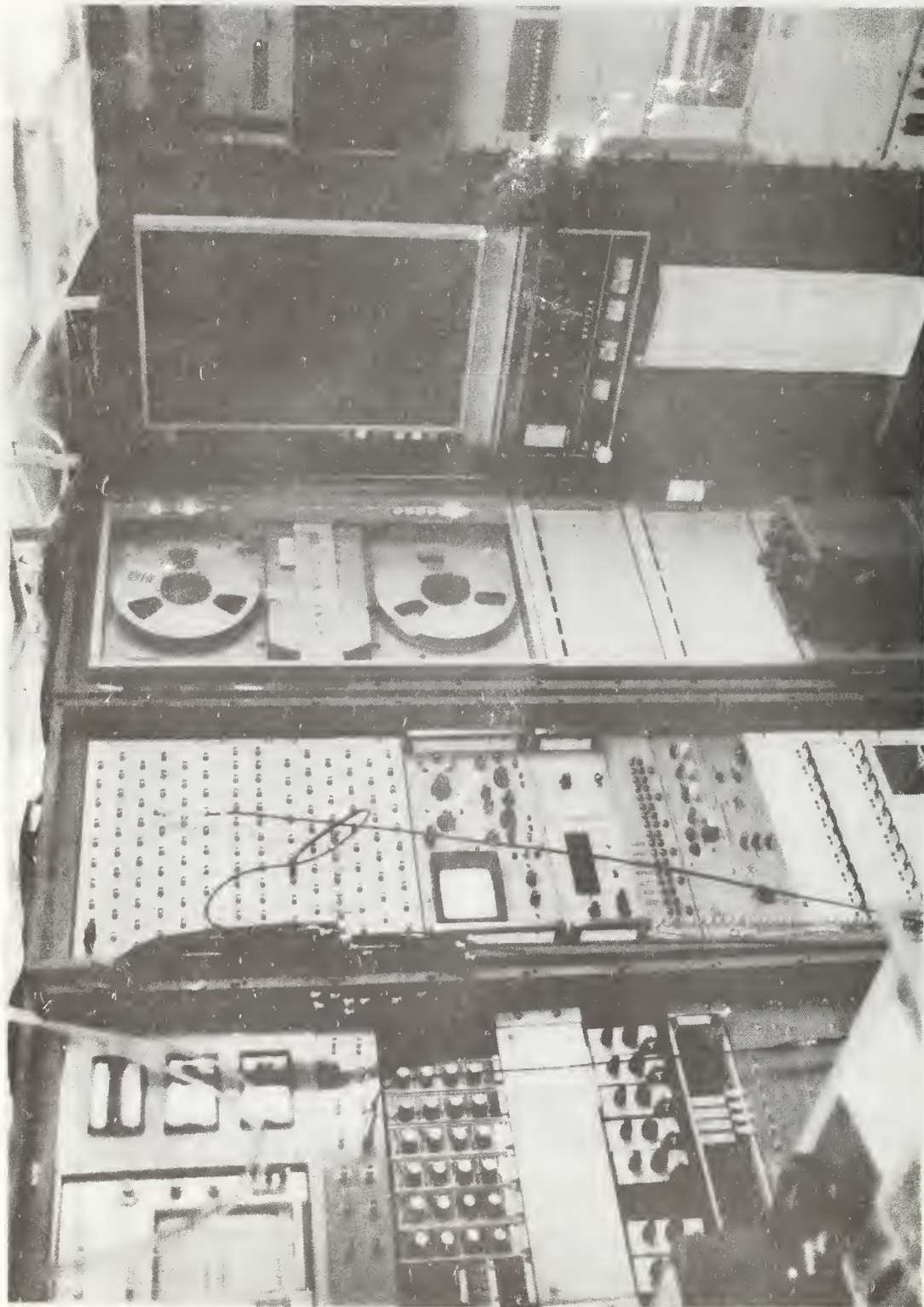


Fig. 3.6 - Data Acquisition System

4. DATA REDUCTION AND ANALYSIS

Approximately 45 hours of recordings were obtained during six months of operation at the test site and it was essential that the data be carefully screened for quality and content prior to committing time and funds for computer processing. The open-scale stripchart records of wind speed and direction proved to be extremely valuable in this screening process and the procedure was to visually estimate the maximum and mean speeds, and the mean direction. Also, a subjective index of stationarity (1 = poor to 5 = excellent) was assigned to each record. This information, combined with a table indicating the types of transducers, their locations and the orientation and configuration of the mobile home, greatly simplified the process of determining which records were to be analyzed.

4.1 A-D Conversion - As indicated previously, problems with the digital tape recorder required that a good portion of the data (approximately 70 percent) be recorded in analog form. The analog tapes were played back at the original record speed (3 3/4 ips) for A-D conversion and a 30 Hz lowpass filter was used on each channel to improve the signal-to-noise ratio. The A-D conversion was accomplished with the same digital system used in the data acquisition stage. A rate of 24 samples per second was standard, but certain records containing only wind speed data were sampled at a rate of 12 samples per second because of the mechanical filtering of the anemometers. In most cases a record length of 1000 seconds was used for the A-D conversion, but this was reduced to 500 seconds and in some cases 300 seconds where portions of the original record exhibited poor stationarity. Spot checks were made for tape dropouts during the A-D conversion process and several channels of data were rejected at this stage. However, some records were processed and later found to contain dropouts, this effect being quite obvious in the plots of the cumulative distribution functions.

Once the records had been converted to digital form, a routine procedure was used to carry out the data analysis. This involved the use of three computer programs developed at the NBS for the analysis of random data. These include PROGRAM 2 which formats sequential channel samples into sequential samples for a given channel; CDF which contains subroutines for data condensation, trend removal, calculation of mean and r.m.s. values, peak values associated with upcrossings, and probability distributions of peak values; and SUMP which combines multiple records into a single time series. A flow chart for the data acquisition and analysis process is given in Figure 4.1.

4.2 Mean and Standard Deviation - The mean and standard deviation were calculated for each record using all samples remaining in the series after lowpass digital filtering or condensation. Following this analysis of the entire series, the record was divided into three equal blocks and the block means and standard deviations determined. Finally, a new time series was formed by removing the block means and the standard deviation of the resulting series was determined. While the block means and standard deviations provided some insight

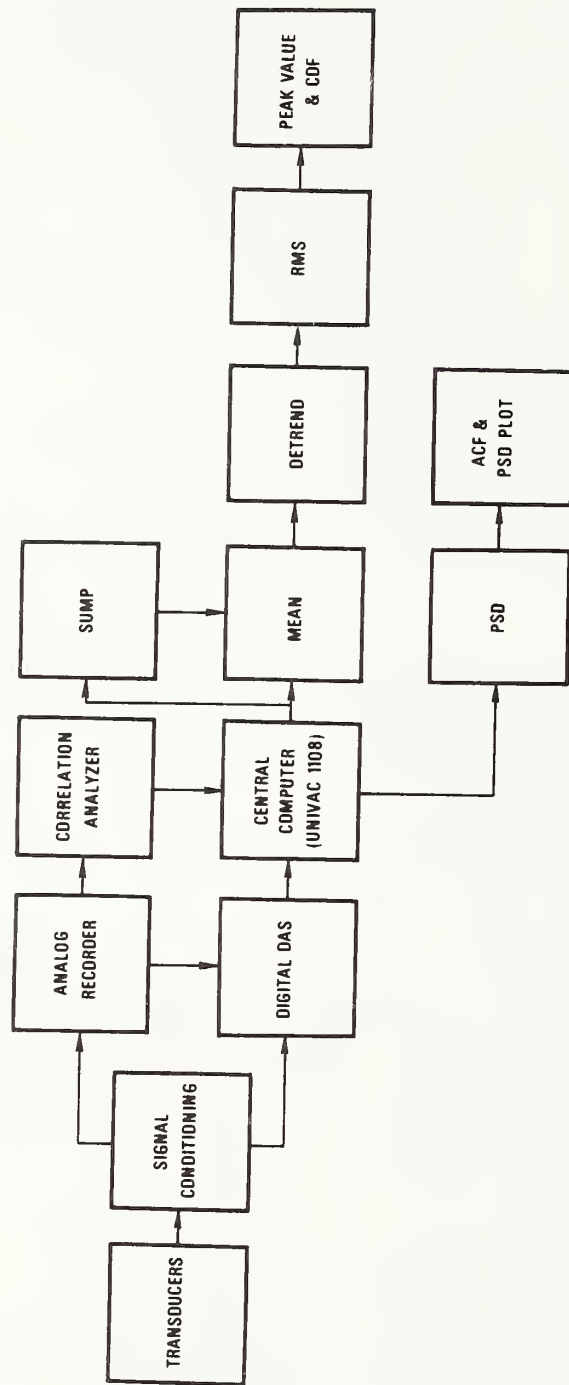


Fig. 4.1 - Data Acquisition and Analysis Flow Chart

as to the stationarity of the record and could have been used to obtain estimates of mean and fluctuating coefficients, most of the coefficients presented in this report are based on the total record length.

4.3 Peak Values - The average rate of occurrence of peaks, n_p , and upcrossings of the mean, n_o , were determined for each record. In addition, the maximum (or minimum) value of the signal associated with each upcrossing of the mean was determined. These values were then put in the form of a reduced or standardized variate (see Sec. 5.3) and plotted as cumulative distribution functions.

4.4 Spectral Analysis - While computer routines have been used in the past for the calculation of spectral density functions from digital data, the scheme used in this study was to determine the autocorrelation function directly from analog data and to then carry out a Fourier transformation using digital techniques. A combined correlation and probability analyzer was used to obtain a 400-point representation of the autocorrelation function. The analog records were reproduced at 16 times the record speed to simplify removal of the DC component with a highpass filter and approximately five entries of the record were used to obtain an estimate of the autocorrelation function. The 400-point function was then operated on using a window function described in Ref. 10 to obtain estimates of the spectral density function.

5. TEST RESULTS

Twenty-three records were selected for detailed analysis and certain characteristics of these records, including the test configurations and digital sampling rates, are presented in Table 1. The first twenty records were initially recorded in analog form and subsequently converted to digital form for analysis. The last three records were initially recorded in digital form.

5.1 Wind Speed - Mean wind speeds \bar{u}_{10} measured at the 10 m level with the standard 3-cup anemometer are listed in Table 1 along with the maximum speed observed in the record \hat{u}_{10} and the turbulence intensity $I = \sigma_u / \bar{u}_{10}$. Also listed in Table 1 are the mean wind direction $\bar{\beta}$ measured clockwise from true north and the relative mean wind direction $\bar{\theta}$ measured clockwise from the front end of the mobile home. As expected, most of the strong winds during the course of this study came from the west-northwest and a lesser number from the south-southwest (see Figure 2.3).

Details of the wind speed measurements obtained with the propeller anemometers at heights of 1.5, 3, 5, 10 and 18 m are presented in Table 2. With the exception of Records 5-1 and 10-5, mean wind speeds measured by the propeller anemometer at the 10 m level are consistently lower than the speeds measured at the same height with the 3-cup anemometer. This is to be expected as the propeller anemometers have a fixed orientation while the cup anemometer accommodates fluctuations and trends in the wind direction. The mean speeds measured by the propeller anemometer at the 10 m level average about 85 percent of the speeds measured by the cup anemometer for the first five records in Table 2 and about 98 percent for the other records. This anomaly cannot be explained by anemometer misalignment or errors in sensitivity. It seems likely that insufficient clearance between the anemometer body and the weather shroud on the propeller hub was the cause of this temporary problem since subsequent records taken at nearly the same wind directions show much better agreement between cup and propeller. No corrections were applied to the propeller anemometer data to account for departure from ideal response at higher frequencies. Dynamic response characteristics of these fixed-orientation anemometers have been established and reported in Ref. 11.

The mean velocity profiles are of interest in defining a reference wind speed for the pressure, drag and lift coefficients. Both a logarithmic law and a power law representation of the variation of mean wind speed with height above ground were compared with the measurements obtained in this study. The logarithmic law

$$\bar{u}_z = \frac{u_*}{k} \ln \frac{z - z_d}{z_0} \quad (1)$$

where \bar{u}_z = mean velocity at height z
 u_* = shear velocity

Table 1 - Test Configuration and Characteristics of Records

Record No.	Time GMT (day:hr:min)	Record Length (seconds)	$\bar{\beta}$ (degrees)	$\bar{\theta}$ (degrees)	\bar{u}_{10} (mph)	\bar{u}_{10} (mph)	\bar{I}_{10} (percent)	$\bar{u}_{3.3}$ (mph)	$\bar{q}_{3.3}$ (psf)	Mobile Home Skirts	Sampling Rate for Digital Analysis (Samples/sec)		
											Speed	Pressure	Force
1-5	033:12:21	1008	295	295	23.0	38.4	15.8	17.6	0.79	OFF	12/2*	12	-
2-7	033:08:49	922	298	298	31.2	53.9	18.4	24.1	1.49	"	12/2	12	-
4-4	042:16:59	898	287	287	23.3	34.0	15.5	18.4	0.87	"	12/2	-	-
4-5	042:19:33	1008	291	291	25.1	43.4	16.2	18.7	0.90	"	12/2	12	-
4-9	047:07:41	1008	194	194	19.5	34.5	22.1	16.0	0.66	"	12/2	12	-
5-1	054:23:38	931	301	301	16.3	27.6	18.1	13.5	0.47	"	12/2	-	-
5-3	055:15:33	1008	303	303	18.4	27.2	20.1	15.0	0.58	"	12/2	-	-
6-6	073:19:29	1008	288	258	31.7	49.9	16.2	25.3	1.68	ON	12/2	-	12/2**
8-2	074:03:53	302	296	266	21.6	30.5	14.8	17.3	0.77	"	24	-	24
8-5	077:00:12	302	301	271	24.0	42.0	19.5	19.7	0.99	"	24	-	24
9-1	077:01:36	504	301	271	21.5	38.2	18.0	17.7	0.80	"	24/2	24	24
9-2	077:02:17	504	302	272	21.3	34.4	21.0	17.5	0.78	OFF	24/2	24	24
9-3	077:03:09	504	303	273	21.0	31.9	20.3	17.1	0.75	"	24/2	24	24
10-4	081:08:31	504	200	92	16.2	31.9	18.2	13.0	0.43	ON	24/4	24	-
10-5	081:09:09	483	195	87	15.2	36.9	24.5	12.6	0.41	"	24/2	24	-
10-6	081:11:44	504	211	271	16.3	28.1	25.9	12.9	0.43	"	24/2	24	-
10-7	081:12:19	504	205	265	17.0	27.8	22.6	13.9	0.49	"	24/4	24	-
12-5	088:08:47	504	294	354	27.6	39.9	13.1	22.6	1.31	"	24	24	-
13-1	088:08:47	1008	294	354	26.7	38.6	15.6	21.9	1.23	"	12/2	-	12/2
15-1	117:14:50	1008	291	266	21.7	32.1	18.6	17.0	0.74	"	12/2	24	12/2
23-4	102:21:38	302	307	282	25.0	38.1	16.4	21.2	1.15	ON	24/4	24	24
29-2	118:20:50	501	305	280	19.8	30.9	19.4	16.1	0.66	OFF	24/4	24	24
35-1	140:18:17	501	289	264	27.6	39.3	16.1	20.7	1.10	"	24/4	24	24

*Denotes 12 samples/sec. initially and digital filtering by averaging every 2 successive samples.

** Analysis of combined drag forces based on 12 samples/sec.

Table 2 - Wind Characteristics From 1.5 to 18 Meters
as Measured by Propeller Anemometers

Record No.	\bar{u}_h (mph)				\hat{u}_h (mph)				I_h (percent)				α			
	h				h				h							
	1.5	3	5	10	18	1.5	3	5	10	18	1.5	3		5	10	18
1-5	15.4	17.2	19.3	19.4	23.4	27.8	30.0	33.0	31.6	36.7	22.8	22.1	22.6	20.0	16.2	0.17
2-7	21.1	23.5	26.5	26.8	31.4	43.2	49.8	51.1	49.1	54.6	25.3	24.7	24.8	22.1	19.0	0.18
4-4	16.1	18.0	20.2	20.4	24.7	32.4	36.1	38.8	34.7	35.6	25.3	23.3	23.0	19.7	15.1	0.18
4-5	16.6	17.9	20.3	20.7	25.6	35.3	36.4	39.0	39.3	43.4	24.7	23.5	24.1	22.2	17.3	0.18
4-9	13.6	16.0	17.9	16.3	18.8	29.9	31.8	38.8	32.5	33.7	27.7	26.4	26.7	27.4	23.9	0.19
5-1	-	13.2	-	16.7	-	-	23.7	-	27.6	-	-	22.2	-	18.9	-	0.19
5-3	-	-	-	18.3	-	-	-	-	28.7	-	-	-	-	23.2	-	-
6-6	-	-	26.7	31.0	34.7	-	-	47.2	50.6	48.6	-	-	20.3	17.4	14.8	0.18
10-4	-	12.6	-	16.0	-	-	21.8	-	29.3	-	-	25.1	-	19.7	-	-
10-5	-	12.3	-	15.5	-	-	25.3	-	30.1	-	-	27.1	-	24.5	-	0.19
10-6	-	12.6	-	16.2	-	-	28.4	-	31.6	-	-	34.3	-	28.3	-	-
10-7	12.2	13.4	14.1	17.0	18.0	21.7	29.9	29.1	27.3	28.3	32.2	32.5	29.7	24.2	25.3	0.17
13-1	-	17.8	21.6	25.7	29.5	-	37.9	37.6	38.8	40.9	-	23.3	19.7	17.8	14.3	0.17
15-1	14.1	14.1	17.2	20.8	24.0	28.6	27.8	31.6	32.8	35.4	26.4	28.8	25.0	20.9	16.8	0.19
23-4	17.8	19.7	21.6	24.3	27.0	33.4	37.0	37.0	39.4	40.6	23.3	23.8	22.6	18.7	17.8	0.17
29-2	14.8	15.8	17.1	19.4	21.1	30.4	29.4	30.3	32.2	35.5	25.0	25.3	24.7	20.3	19.3	0.16
35-1	18.1	20.3	22.5	26.0	28.9	33.6	35.0	35.2	39.3	39.6	23.7	23.1	21.4	18.2	14.9	0.19

$k =$ a constant (usually taken to be 0.4)

$z_d =$ zero-plane displacement

$z_o =$ surface roughness length,

can be derived from dimensional analysis and has been shown to be an adequate expression of mean velocity profiles measured in neutrally stratified flows over flat terrain of uniform roughness [12, 13]. However, the empirical power law

$$\bar{u}_z = \bar{u}_h \left(\frac{z}{h} \right)^\alpha \quad (2)$$

where $\bar{u}_h =$ mean velocity at some reference height h

$\alpha =$ exponent which depends upon the surface roughness,

is widely used in codes and standards dealing with wind loading [14, 15]. In practice, both descriptions of the mean velocity profile involve a subjective assessment of surface roughness. The power law was found to best fit the wind speed measurements obtained in this study and it has, therefore, been used in the presentation of test results as well as in the formulation of recommended design loads in Section 6.

Typical mean velocity profiles are shown in Figure 5.1. Estimates of α obtained from these and similar plots ranged from 0.17 to 0.21 and averaged 0.18. The plot of α versus wind direction in Figure 5.2 indicates little change in surface roughness with direction.

Wind speeds at the reference height of 3.3 m (the height of the roof-wall intersection of the mobile home) were obtained from the mean velocity profiles or were calculated using the mean speeds at 10 m and values of α interpolated from Figure 5.2. Values of the mean wind speed $\bar{u}_{3.3}$ at the reference height of 3.3 m and the corresponding mean dynamic pressure, $\bar{q}_{3.3} = 1/2 \rho \bar{u}_{3.3}^2$, are listed in Table 1.

5.2 Time Histories and Spectra of Wind Speed and Pressure - The time histories of wind speed and pressure plotted in Figure 5.3 represent a typical 1-minute segment of record No. 10-4 for which the wind direction was approximately normal (face-on) to the right side of the mobile home. The pressures are plotted in terms of non-dimensional pressure coefficients (to be discussed in the following section) and provide some insight regarding the variation of pressure with respect to time and location of the pressure tap. Pressure tap designations are given in Figure 2.2. It should be noted that the location of the meteorological mast relative to the center of the mobile home for this particular record was approximately 60 ft (18 m) upwind and 80 ft (24 m) transverse to the wind direction. Thus, while there appears to be a very strong correlation between wind speed fluctuations at 10 m and 3 m, the correlation between the wind speed fluctuations at 3 m and the pressure fluctuations on the windward face (tap 79) is weak. The superior frequency response of the propeller anemometer compared with the standard 3-cup anemometer is obvious. Comparing the time histories for taps 79 and R11 suggests a fairly strong correlation between the two and

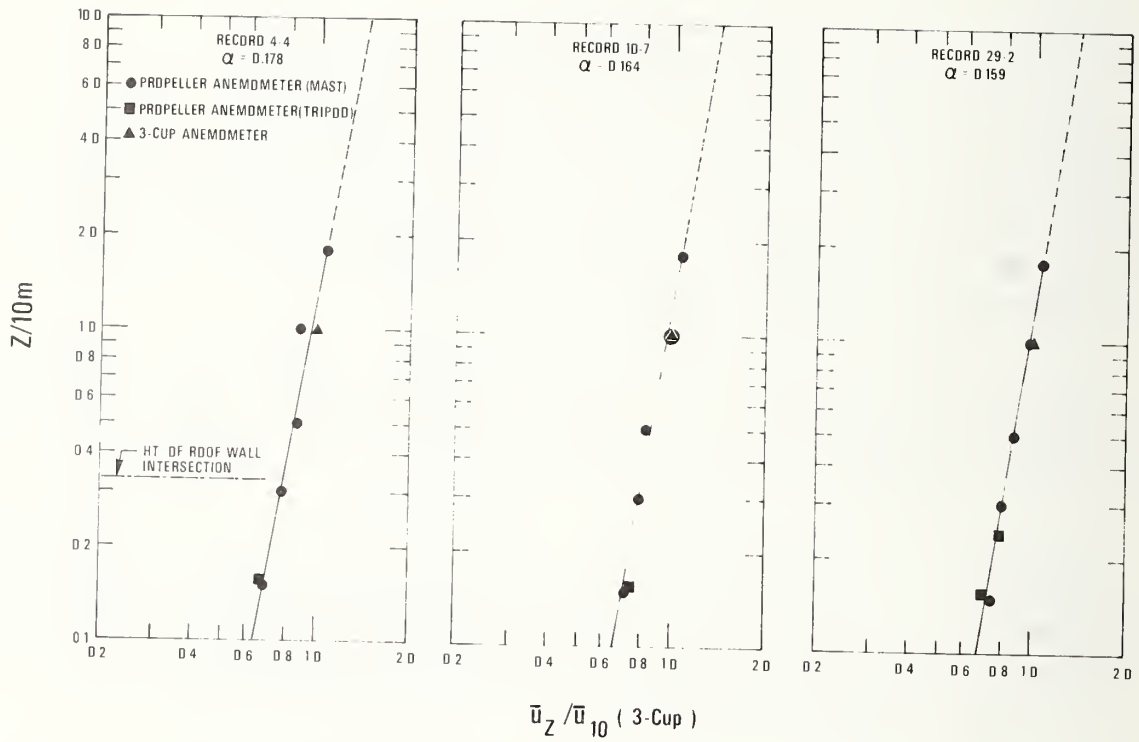


Fig. 5.1 - Typical Mean Velocity Profiles - Power Law Representation

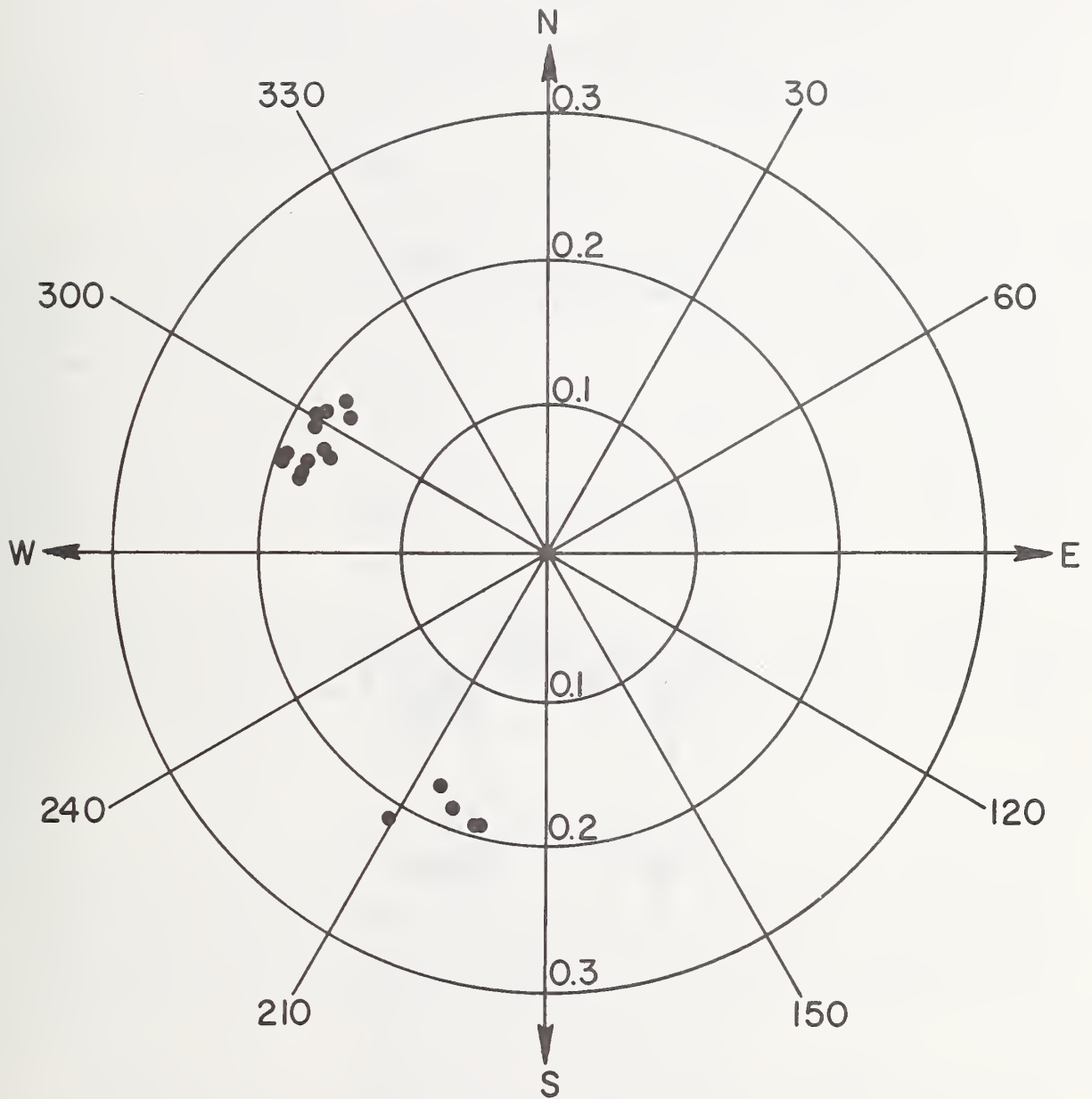


Fig. 5.2 - Estimates of Mean Wind Speed Profile Index α for Various Wind Directions

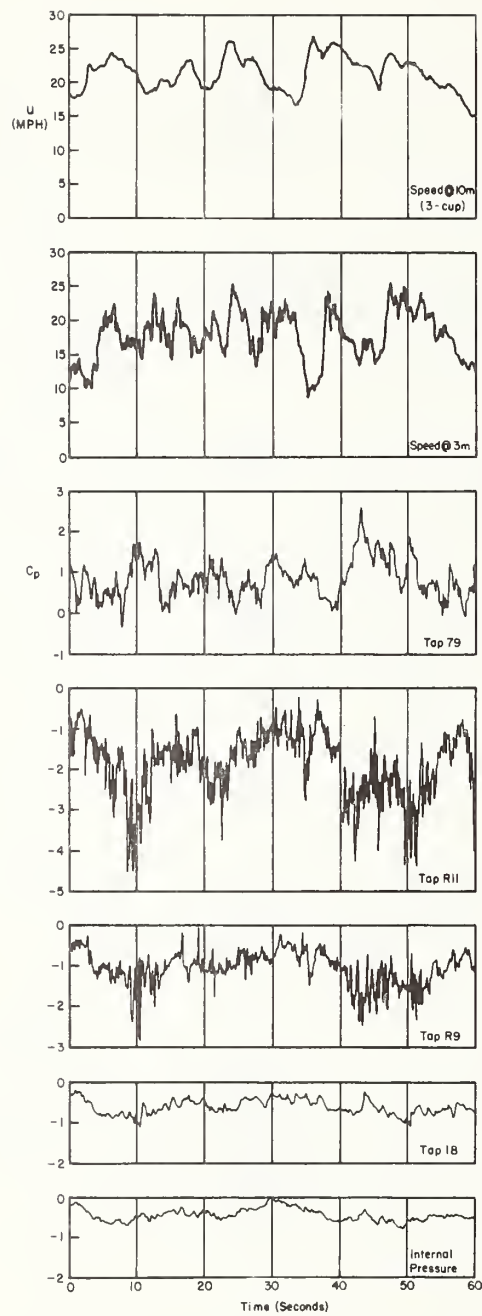


Fig. 5.3 - Typical Time Histories of Wind Speed and Pressure, Record No. 10-4

indicates a dramatic change in both the mean and fluctuating components of the surface pressure as the flow passes over the windward edge of the roof and actually becomes detached or separated from the roof surface. This separation is highly intermittent and is influenced by the turbulence and relative direction of the oncoming wind, the geometry of the roof in the region of separated flow, and to some extent by the ratio of width to depth of the mobile home. The effect of flow separation is a negative mean pressure with intense negative-going fluctuations which occur at frequencies considerably higher than those observed on the windward wall.

The time histories for taps R11 and R9 are also well correlated. However, the intensities of both the mean and fluctuating components at R9 are substantially less owing to the reattachment of the flow a short distance downwind of the separation point. A further reduction in mean and fluctuating components of the pressure is observed at the leeward side and in the mobile home interior (tap 18 and internal pressure), and while they appear to correlate poorly with the other pressures and with the wind speed, there is a fair degree of correlation between the two. This is to be expected since the internal pressure is related to the permeability of the mobile home and the major portion of the exterior surface area is subject to pressure fluctuations occurring in the wake created by the mobile home.

While the time histories of wind speed and pressures are informative, a clearer picture of their fluctuating components can be obtained from the spectral density function $S(n)$ which indicates the manner in which the harmonic content of a signal is distributed over the frequency range. The spectral density function has the property

$$\sigma_x^2 = \int_0^{\infty} S(n) \, dn \quad (3)$$

in which σ_x^2 is the variance of the variable $x(t)$, and n is the frequency. The spectral functions presented in Figures 5.4(a) to 5.4(f) are plotted in terms of a dimensionless ordinate $nS(n)/\sigma^2$ and an abscissa which is the log of the frequency n . Thus the ratio of the area associated with any frequency increment Δn to the total area under the curve represents that fraction of the total variance related to Δn .

Comparing the spectrum of the wind speed fluctuations at 3 m (Figure 5.4(a)) with that of the pressure fluctuations on the windward wall (Figure 5.4(b)), the peaks in the low-frequency range occur at approximately the same frequency and there is little contribution to the variance from frequencies above 1 Hz. This suggests a quasi-static relationship between speed and pressure fluctuations in the case of the windward wall. As the flow passes over the roof the contribution of higher frequencies becomes significant as is clearly indicated by the spectrum for tap R11 shown in Figure 5.4(c). On the leeward portion of the roof where the flow tends to become reattached the high-frequency components are still significant, but the low-frequency peak is beginning to emerge again as is shown

REC. NO. 10-4
SENSOR V-3M

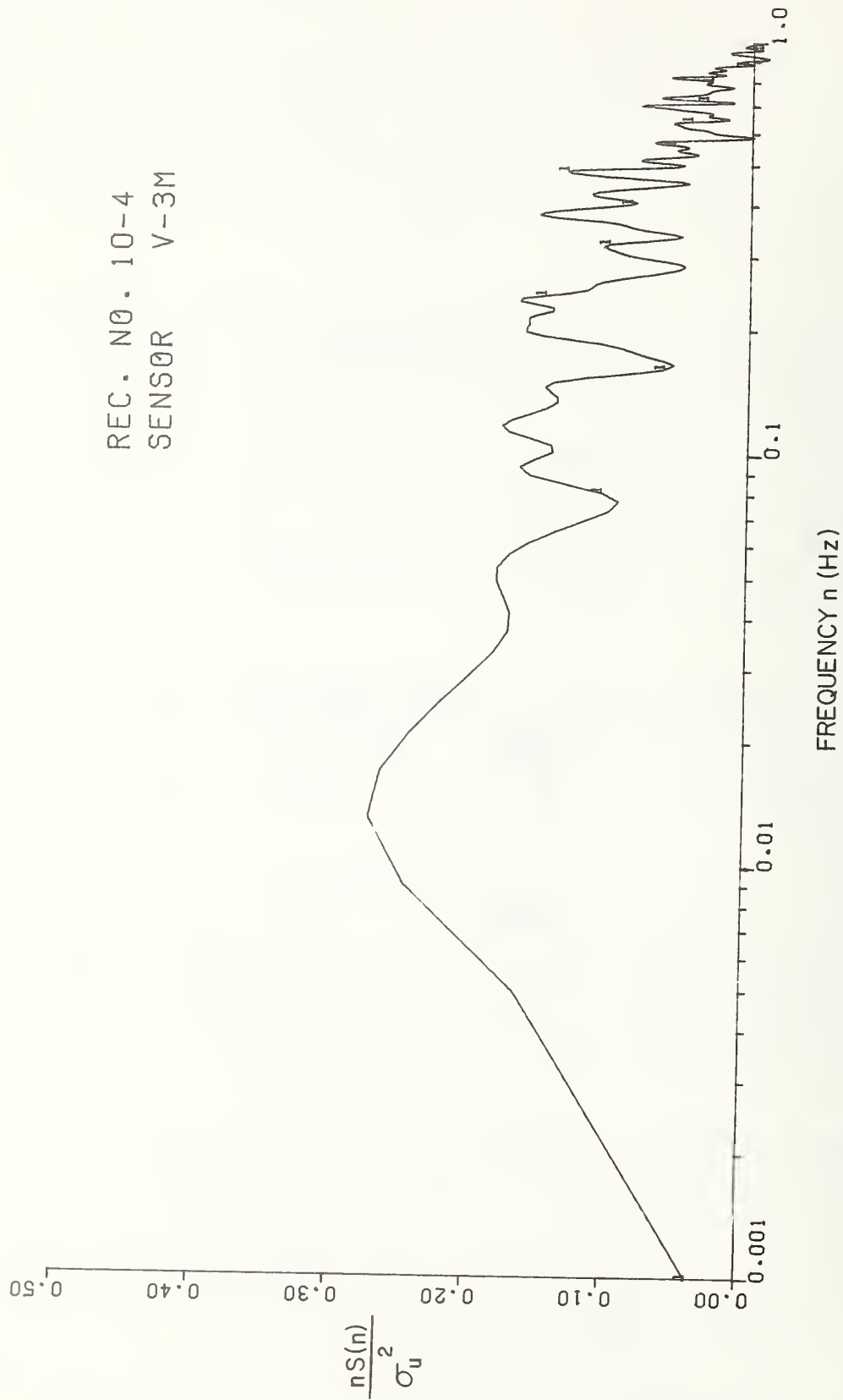


Fig. 5.4(a) - Spectrum of Wind Speed at 3 Meters

REC. NO. 10-4
SENSOR TAP 79

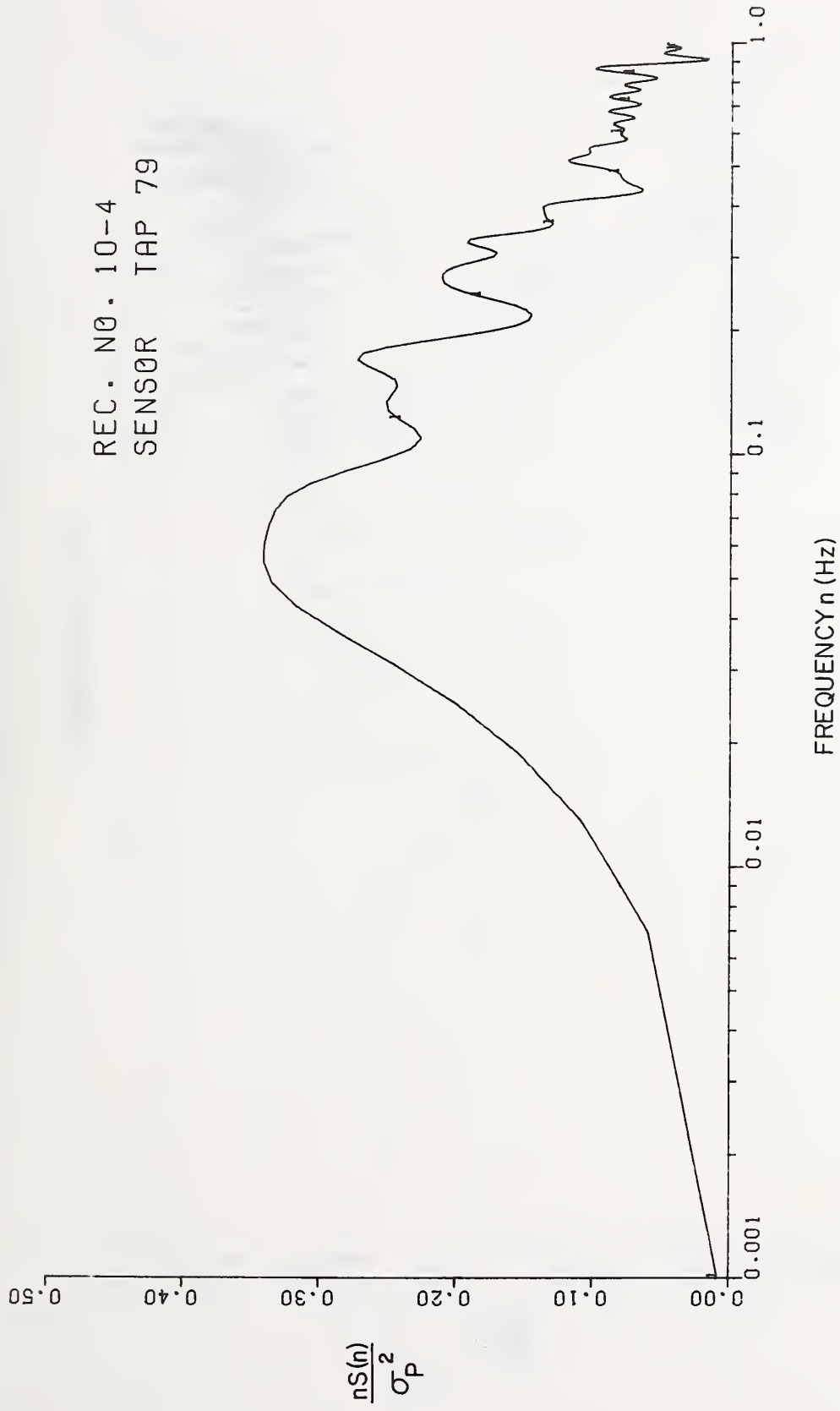


Fig. 5.4(b) - Spectrum of Wind Pressure at Tap No. 79

REC. NO. 10-4
SENSOR R11

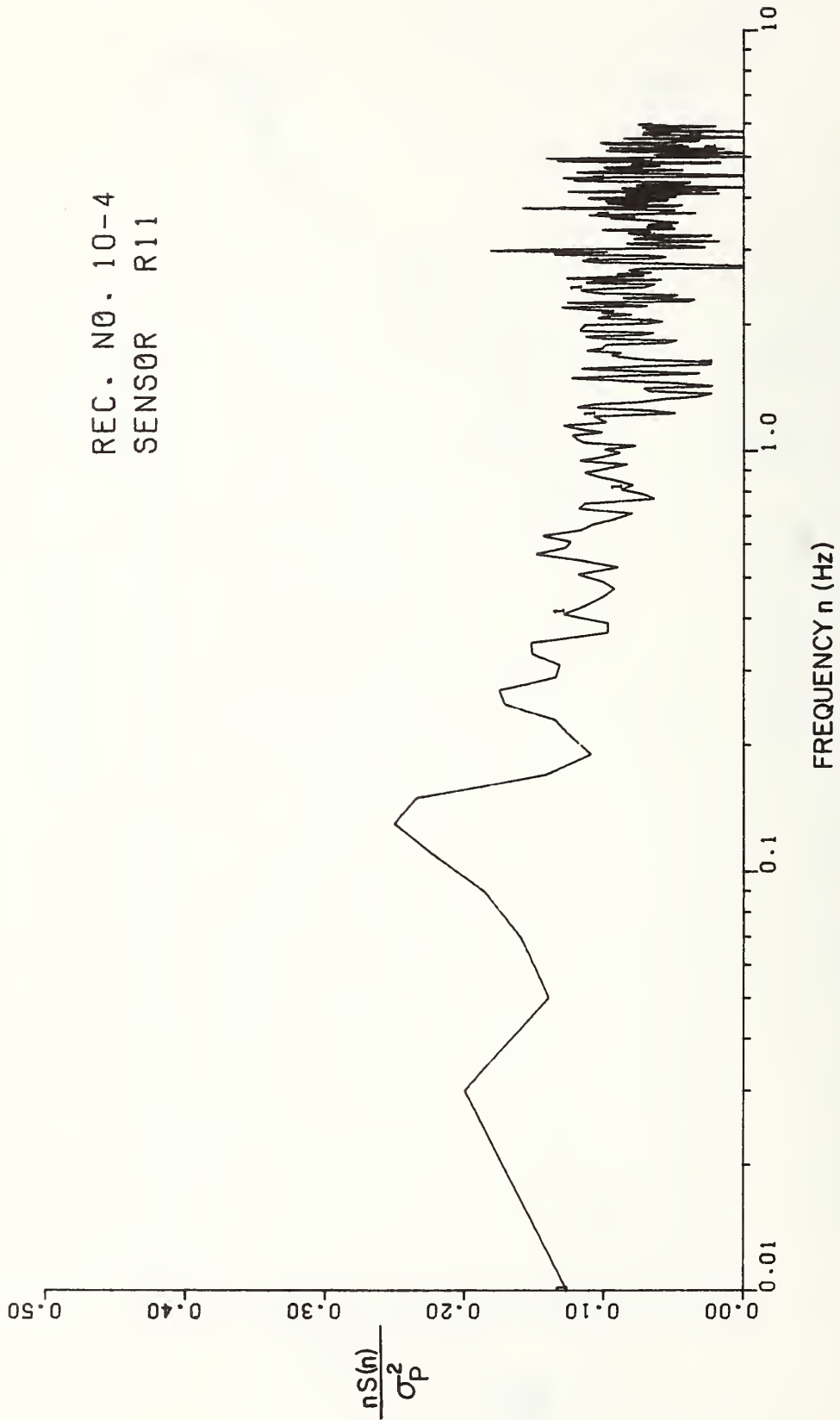


Fig. 5.4(c) - Spectrum of Wind Pressure at Tap No. R11

REC. NO. 10-4
SENSOR R9

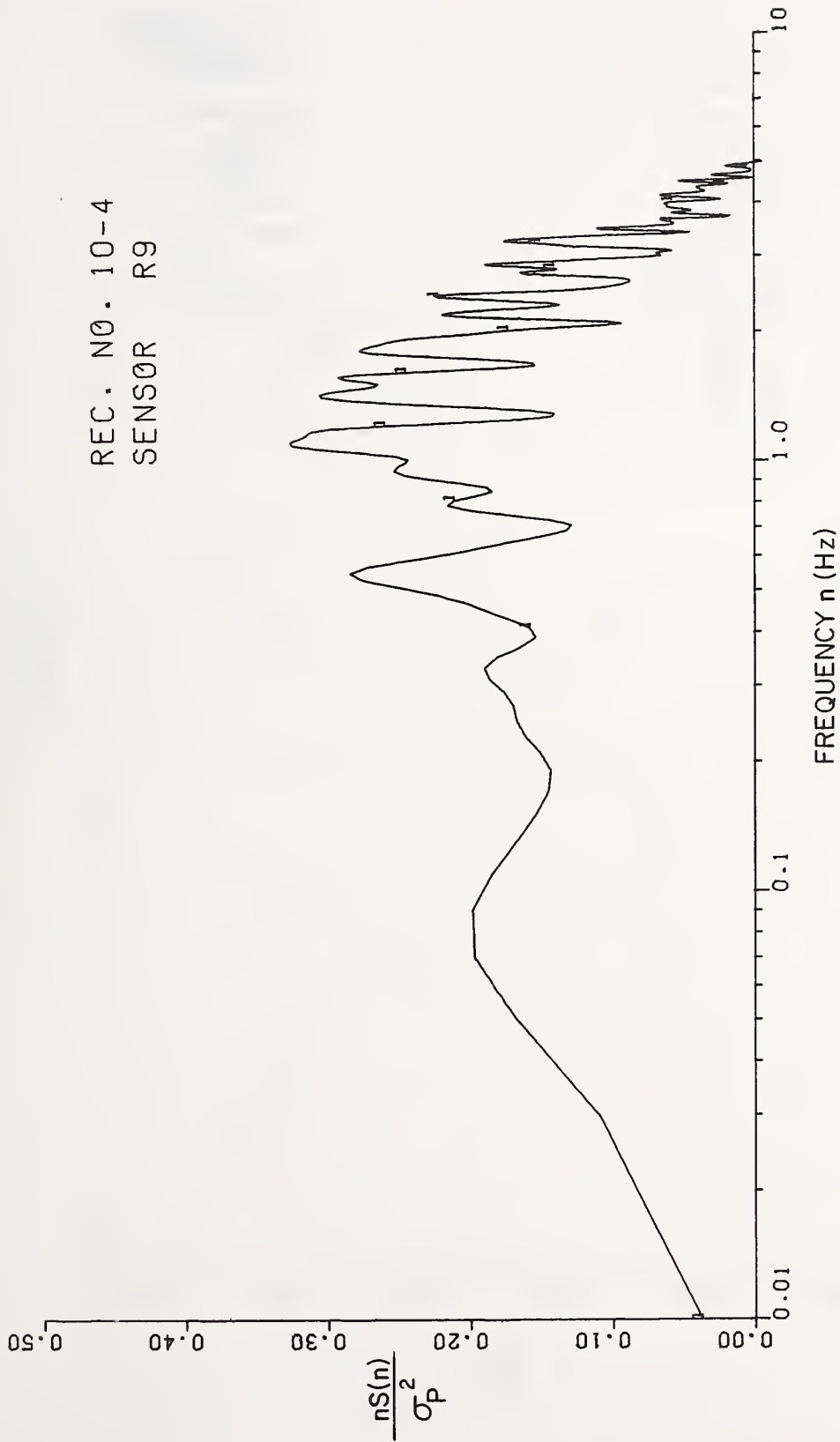


Fig. 5.4(d) - Spectrum of Wind Pressure at Tap No. R9

REC. NO. 10-4
SENSOR TAP 18

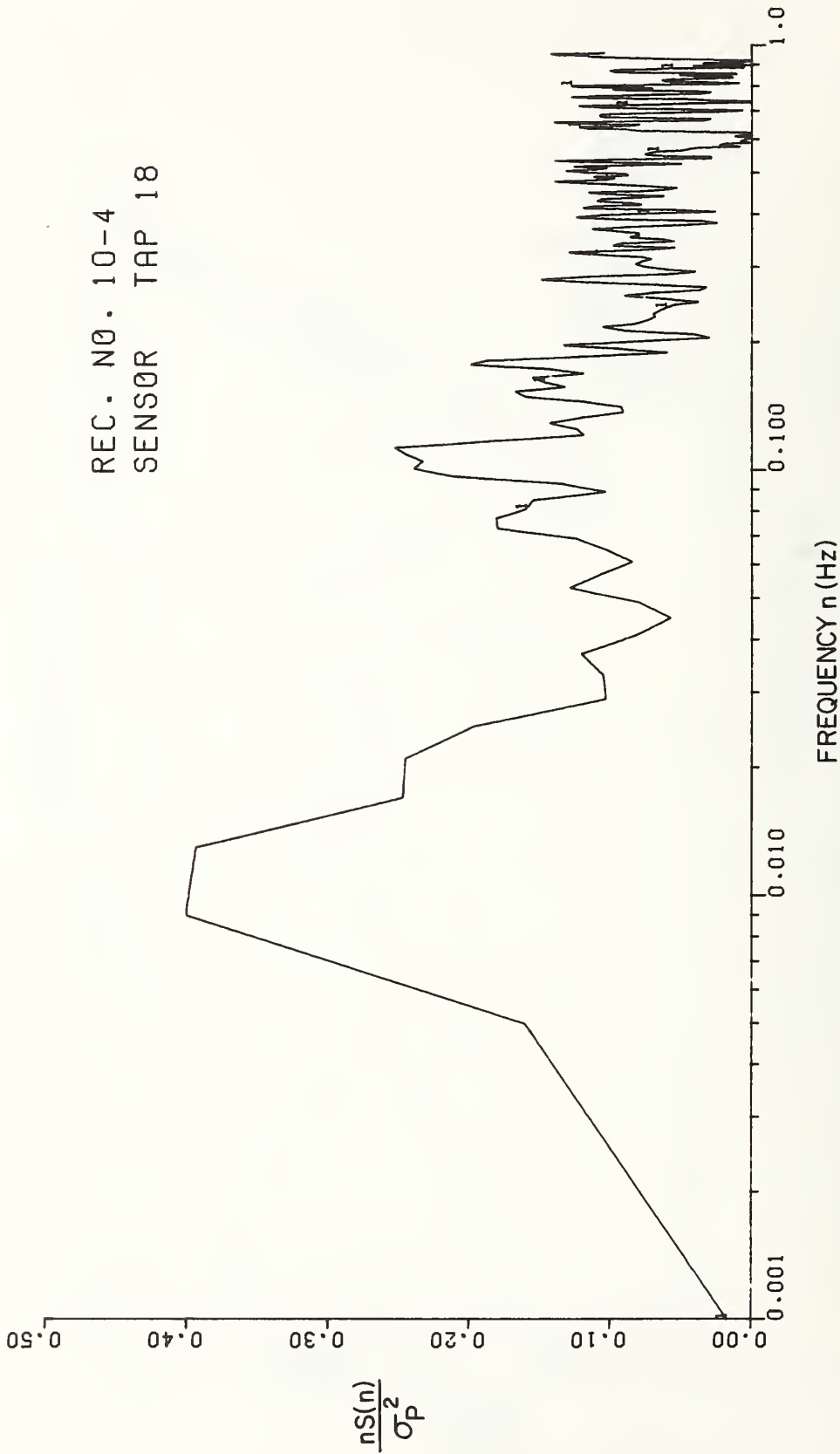


Fig. 5.4(e) - Spectrum of Wind Pressure at Tap No. 18

REC. NO. 10-4
SENSOR INT PR

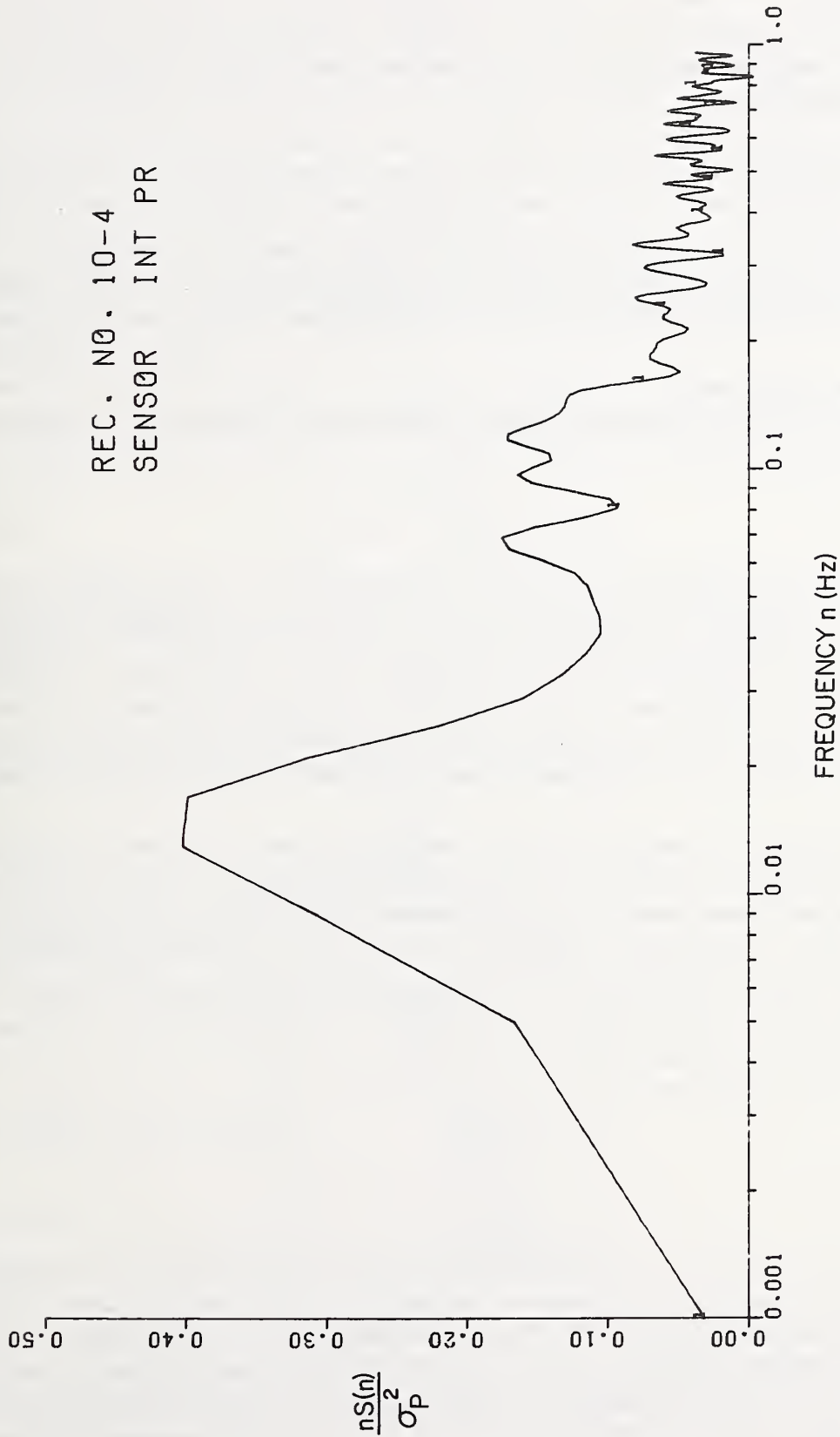


Fig. 5.4(f) - Spectrum of Wind Pressure Inside Mobile Home

in Figure 5.4(d). The spectra for the leeward side and for the internal pressure, Figure 5.4(e) and 5.4(f) respectively, indicate a dominant low-frequency peak which again coincides with that of the wind speed spectrum. Contributions from the higher frequencies are proportionately less.

The observations described above are in general agreement with the measurements obtained by Eaton and Mayne [8] on a two-story house and illustrate the dramatic changes in the characteristics of pressure signals that occur in regions of separated flow. The consequences of intense pressure fluctuations at high frequencies can be serious when construction materials are involved that do not perform well under repeated loading.

5.3 Pressure Coefficients - It is usual in experimental studies such as this to express pressures in terms of some dynamic reference pressure and a dimensionless pressure coefficient defined as

$$C_p = \frac{p - p_o}{1/2 \rho u^2} \quad (4)$$

where p is the local pressure on the surface of the building, p_o is the freestream ambient or atmospheric pressure, ρ is the mass density of air, and u is a reference wind speed, usually taken at some point in the undisturbed wind field. For the case of building aerodynamics, specified design wind speeds and surface pressures are usually associated with short time periods (2 to 3 seconds) and represent maximum values likely to occur. The reference height for the wind speed usually corresponds to the height of the building.

In this study the pressure records were analyzed in terms of mean and fluctuating components as outlined in Section 4.1. The reference wind speed was based on measurements obtained from the instrumented mast and tripod-mounted anemometers, interpolated to a height of 10.8 ft (3.3 m) which corresponds to the height of the roof-wall intersection of the mobile home. The averaging time for mean pressure and mean speed was equal to the record length (300 to 1000 seconds) and both mean and fluctuating pressure coefficients were determined in accordance with the definitions

$$C_p = \frac{\bar{p}}{1/2 \rho \bar{u}_{3.3}^2} \quad (5)$$

and

$$C_{p\sigma} = \frac{\sigma_p}{1/2 \rho \bar{u}_{3.3}^2} \quad (6)$$

in which \bar{p} will be understood to indicate the mean pressure over the record length relative to freestream ambient pressure ($p - p_o$), σ_p is the standard deviation of the pressure fluctuations (rms level with respect to the mean), and $\bar{u}_{3.3}$ is the mean wind speed over the record length at the reference height of 10.8 ft (3.3 m). The maximum (or minimum) pressure in the record can then be expressed as

$$\hat{p} = 1/2 \rho \bar{u}_{3.3}^2 (C_p + g C_{p\sigma}) \quad (7)$$

where g is the number of standard deviations by which the maximum (or minimum) pressure departs from the mean pressure over the record length. The definitions of the mean, standard deviation and the peak factor g for a random variable $x(t)$ are shown graphically in Figure 5.5.

It is not sufficient to simply determine the maximum departure from the mean in a given record. As will be demonstrated in Section 6.3, the average rate of fluctuation and the probability distribution of the fluctuation amplitudes will also be required when specifying design pressures.

For a stationary, narrow-band, gaussian process with zero mean it can be shown [16] that the probability that any peak in the record is greater than some value, a , is

$$P(x > a) = e^{-a^2/2\sigma_x^2} \quad (8)$$

It can also be shown that for a narrow-band gaussian process with most of the energy centered at some frequency n_0 , the average rate of upcrossings of the value $x = a$ can be expressed as

$$n_a = n_0 e^{-a^2/2\sigma_x^2} \quad (9)$$

It follows from Eq. 8 that for sufficiently large values of n_0 ,

$$P(x > a) = \frac{n_a}{n_0} \quad (10)$$

Note that the Rayleigh probability distribution function (Eq. 8) is a special case of the Weibull distribution function

$$P(x > a) = e^{-\left(\frac{a}{c}\right)^k} \quad (11)$$

where $k = 2$ and $c = \sqrt{2} \sigma_x$. When plotted on $\ln(-\ln)$ versus \ln coordinates, Eq. 11 should exhibit a linear relationship since

$$\ln[-\ln P(x > a)] = k(\ln a - \ln c) \quad (12)$$

Although a narrow-band gaussian process has been assumed in the above, the relationship indicated by Eq. 10 has been used in the analysis of various records obtained in this study, many of which are wide-band random and highly intermittent. The procedure used in the analysis of pressure measurements was to determine the maximum (or minimum) value p' of the pressure signal following each upcrossing of the mean and to define X as a reduced or standardized variate as follows:

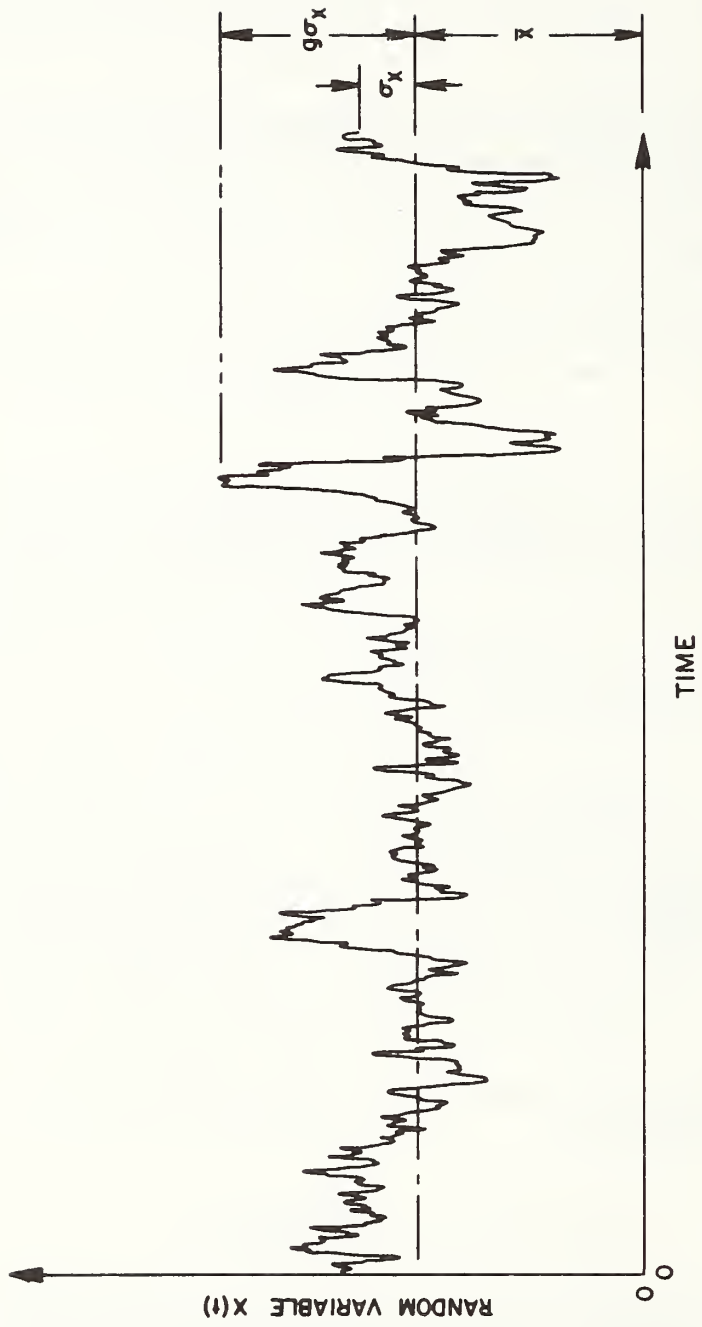


Fig. 5.5 - Definition Sketch of Mean, Standard Deviation and Peak Factor

$$X = \frac{p' - \bar{p}}{\sigma_p} \quad (13)$$

The probability distribution of X was then determined from Eq. 10 using a class interval of $0.25 \sigma_p$. In addition to the maximum (or minimum) values of the variable, the rate of occurrence of peaks in the record, n_p , was also determined. Typical values for C_p , $C_{p\sigma}$, g , n_o and n_p are given in Table 3. Typical plots of probability distributions are shown in Figures 5.6 and 5.7. Values of the Weibull parameters k and c (slope and intercept) resulting from these plots are listed in Table 3. Mean pressure coefficients obtained from recordings for which the wind direction was approximately face-on to the sides of the mobile home are plotted for the skirted and unskirted configurations in Figures 5.8 and 5.9, respectively.

The procedure just described was also used in the analysis of combined records which were generated using the SUMP program mentioned in Section 4.1. In this program weighting factors, w , are selected for each data channel, n , such that

$$\sum_{n=1}^N w_n = 1 \quad (14)$$

and the summed channels thus represent a spatial average of N concurrent time histories. In the case of an array of pressure transducers with each transducer representing adjacent surface areas of approximately equal size and shape, the weights for each data channel would be identical. For irregular transducer spacing the choice of weights is somewhat subjective, but in either case it is implied that all pressure fluctuations sensed at a point by a transducer act with equal intensity over the entire surface area assigned to the transducer. That is to say, the coherence is assumed to be unity between all points in the area for the entire range of frequencies in the signal. Thus, for a given set of flow conditions, the amount by which the contribution of a pressure fluctuation is over-estimated will increase with the size of the assigned surface area and with the reciprocal of the duration of the fluctuations. The weight factors used in this analysis were all equal and results for selected combined pressure time histories are given in Table 4.

The test results presented in Tables 3 and 4 provide some insight concerning the spatial extent of extreme pressure fluctuations on the exterior surface of the mobile home. Of particular interest are the largest instantaneous loads imposed on tributary surface areas supported by structural elements such as wall studs and roof trusses and on assemblies such as doors and windows. The degree to which these loads can be approximated by pressures measured at discrete points without regard to the coherence of the pressure signals will, of course, depend upon the size and shape of the tributary area as mentioned above and upon the nature of the pressure fluctuations typified by the time histories shown in Figure 5.3.

Table 3 - Single-Point Pressure Coefficients

Record No.	Pressure Tap No.	C_p	$C_{p\sigma}$	g	n_o	n_p	c	k
1-5	36	-0.08	0.37	4.94	0.92	1.77		
	39	0.51	0.31	6.09	0.58	1.44		
	43	0.65	0.37	8.97	0.58	1.36		
	R4	-2.32	1.15	4.10	1.19	1.85		
2-7	30	0.73	0.39	5.90	0.59	1.38		
	36	0.19	0.32	6.21	1.05	1.85		
	39	0.67	0.33	10.33	0.48	1.30		
	43	0.75	0.39	4.05	0.57	1.30		
4-5	76	-0.50	0.29	8.18	0.26	1.24		
	84	-1.29	0.36	3.46	0.18	1.40		
	85	-1.34	0.37	3.56	0.20	1.39		
	R4	-2.86	1.42	2.79	1.09	1.83		
4-9	76	-0.50	0.49	7.81	0.43	1.38		
	84	-0.28	0.20	5.91	0.42	1.39		
	85	-0.30	0.21	5.27	0.42	1.43		
	R4	-0.54	0.31	7.18	0.60	1.63		
9-1	R2	-2.42	1.43	*	1.38	3.11		
	R2	-2.42	1.39	*	1.47	2.97		
10-4	18	-0.43	0.19	-3.37	0.35	1.28	0.53	0.86
	77	0.54	0.37	3.78	0.52	2.01		
	79	0.67	0.48	5.74	0.51	1.99	0.45	0.71
	83	0.65	0.41	5.02	0.61	1.82		
R8	R8	-0.65	0.35	-7.56	1.12	2.66		
	R9	-0.73	0.31	-7.13	1.18	2.99	0.86	0.87
R10	R10	-0.90	0.40	-5.99	1.22	2.98		
	R11	-1.52	0.71	-4.65	1.49	3.04	0.72	0.86
Internal	Internal	-0.32	0.15	3.32	0.35	1.29	0.20	0.54

Table 3 - Single-Point Pressure Coefficients
(continued)

Record No.	Pressure Tap No.	C_p	$C_{p\sigma}$	ξ	n_o	n_p	c	k	
10-5	57	-0.80	0.47	-8.74	0.96	2.77	0.67	0.77	
	61	-0.84	0.50	-7.89	0.90	2.59	0.65	0.74	
	63	-0.92	0.59	-6.58	0.95	2.41			
	64	-0.90	0.58	-6.98	0.86	2.38	0.72	0.79	
	69	-1.01	0.60	-5.07	0.53	2.30			
	70	-1.17	0.72	-5.38	0.55	2.28			
	71	-1.45	0.85	-4.23	0.47	2.10	0.55	0.71	
	72	1.58	1.13	*	0.59	2.22			
	Internal		-0.27	0.22	2.34	0.27	2.98	0.20	0.55
	10-6	57	-1.03	1.05	-14.78	0.53	2.32		
61		-1.02	0.85	-7.66	0.47	1.87			
63		-1.03	0.80	-5.13	0.52	2.13			
64		-1.01	0.83	-4.89	0.46	1.85			
69		-0.87	0.71	-5.76	0.35	1.69			
70		-0.81	0.67	-5.73	0.40	1.80			
71		-0.73	0.56	-7.34	0.59	2.32			
72		-0.75	0.72	-8.22	0.68	2.14			
Internal		-0.17	0.20	4.72	0.40	2.19	0.58	0.81	
10-7		R8	-2.47	1.28	*	2.21	4.10		
	R9	-1.44	0.96	13.47	1.41	3.24	0.55	0.82	
	R10	-0.95	0.51	9.42	1.25	3.29	0.70	0.87	
	R11	-0.65	0.35	5.76	1.13	2.98	0.77	0.81	
	70	-0.32	0.10	-3.82	0.40	2.74	0.63	0.94	
12-5	72	-0.28	0.10	-3.71	0.42	2.66	0.56	0.92	
	R2	-2.56	2.21	*	2.76	-			

Table 3 - Single-Point Pressure Coefficients
(continued)

Record No.	Pressure Tap No.	C _p	C _{pσ}	g	n _o	n _p	c	k	
12-5 (cont.)	R3	-0.88	0.32	-5.47	1.62	3.22	1.03	1.15	
	R4	-0.49	0.23	-6.25	1.92	3.34	0.95	1.02	
	R5	-0.40	0.21	-6.34	1.93	3.64	0.95	1.00	
	R6	-0.47	0.50	*	2.18	2.64			
	R8	-0.33	0.15	-11.68	1.10	2.99	0.58	0.84	
	R9	-0.27	0.12	-5.70	0.98	3.04	0.48	0.72	
	R10	-0.20	0.10	-4.90	1.15	3.27			
	R11	-0.21	0.11	-5.95	1.15	3.21			
	Floor	-0.22	0.09	2.50	0.34	3.49	0.22	0.53	
	15-1	36	0.39	0.36	4.44	1.00	2.83		
		37	0.66	0.38	4.29	0.54	2.00		
38		0.79	0.35	4.32	0.45	2.00			
39		0.70	0.31	4.32	0.47	2.21			
73		-0.52	0.29	-10.30	0.47	2.34			
75		-0.60	0.30	-3.79	0.23	2.37			
78		-0.43	0.28	-5.85	0.49	1.99			
79		-0.47	0.25	-4.03	0.36	2.22	0.57	0.92	
80		-0.38	0.24	-4.13	0.26	2.42			
81		-0.37	0.24	-4.37	0.25	2.50			
82		-0.58	0.29	-10.09	0.46	2.09			
23-4	83	-0.55	0.27	-5.10	0.33	2.10	0.52	0.81	
	84	-0.48	0.26	-4.95	0.36	2.44			
	85	-0.48	0.25	-5.30	0.38	2.77			
	3	0.60	0.42	4.00	0.84	2.43			
	4	0.63	0.42	4.75	0.69	2.01			

Table 3 - Single-Point Pressure Coefficients
(continued)

Record No.	Pressure Tap No.	C_p	$C_{p\sigma}$	g	n_o	n_p	c	k
23-4 (cont.)	5	0.45	0.40	5.33	0.78	2.11		
	14	0.64	0.39	4.11	0.57	1.94		
	15	0.76	0.39	4.18	0.47	1.75		
	16	0.69	0.33	4.10	0.52	1.89		
	29	0.37	0.33	4.36	0.94	2.79		
	30	0.71	0.36	4.37	0.55	2.04	0.78	0.81
	31	0.66	0.34	4.42	0.51	1.92		
	32	0.64	0.29	4.61	0.49	2.18		
	49	0.64	0.38	4.39	0.68	2.10		
	50	0.74	0.39	4.33	0.50	1.80		
	51	0.64	0.35	4.57	0.46	1.98		
	52	0.73	0.35	4.64	0.57	1.85		
	54	0.52	0.37	5.09	0.82	2.30		
	74	-0.56	0.29	-3.84	0.34	1.75	0.46	0.75
	79	-0.59	0.22	-4.28	0.44	1.93		
	R1	-2.43	0.93	-3.69	1.66	4.15		
	R2	-2.21	0.91	-4.08	1.40	3.62	0.68	0.77
	R3	-1.24	0.50	-9.34	1.53	3.35		
	R4	-1.76	0.71	-5.87	1.09	3.00	0.70	0.85
	R5	-2.17	0.96	-3.94	1.06	3.33	0.71	0.77
	R6	-1.35	0.55	-6.59	1.40	3.10	0.77	0.83
	R8	-2.50	1.87	*	1.48	1.77		
	R9	-1.55	0.66	-6.10	1.20	3.01	1.00	0.99
	R10	-1.25	0.53	-5.94	1.30	2.88		
	R11	-0.91	0.42	-7.64	1.23	2.71	0.79	0.79

Table 3 - Single-Point Pressure Coefficients
(continued)

Record No.	Pressure Tap No.	C_p	$C_{p\sigma}$	g	n_o	n_p	c	k	
29-2	23	0.40	0.33	5.52	0.83	2.57			
	24	0.75	0.39	4.05	0.40	1.80			
	26	0.62	0.38	4.30	0.51	1.88			
	27	0.78	0.38	3.73	0.32	1.54			
	28	0.81	0.36	3.95	0.35	1.99			
	29	0.35	0.34	5.82	0.79	2.51			
	30	0.71	0.38	4.13	0.46	1.86			
	31	0.79	0.36	4.24	0.36	1.81			
	32	0.70	0.31	4.45	0.47	2.25			
	33	0.60	0.37	4.61	0.59	2.09			
	34	0.80	0.38	3.97	0.39	1.63	0.80	0.79	
	35	0.81	0.34	4.40	0.38	1.89			
	36	0.32	0.32	6.43	0.76	2.56			
	37	0.74	0.37	4.16	0.38	1.78			
	38	0.81	0.36	4.22	0.33	1.76			
	39	0.70	0.30	4.84	0.48	2.32			
	R2	-2.22	0.97	*	1.33	3.12			
	R3	-1.12	0.56	-5.49	1.13	2.86			
	R4	-1.69	0.78	-3.09	0.87	2.36	0.58	0.78	
	R5	-2.06	0.99	-2.64	0.80	2.28	0.57	0.91	
	R6	-1.28	0.61	-4.77	1.14	2.63			
	35-1	11	0.75	0.41	5.12	0.56	1.83		
		33	0.59	0.37	4.94	0.60	2.04		
		34	0.80	0.39	5.71	0.42	1.77		
		35	0.77	0.36	4.50	0.39	1.80		

Table 3 - Single-Point Pressure Coefficients
(continued)

Record No.	Pressure Tap No.	C_p	$C_{p\sigma}$	g	n_o	n_p	c	k
35-1 (cont.)	36	0.32	0.34	6.50	0.91	2.64		
	37	0.55	0.20	4.42	0.66	3.00		
	38	0.79	0.38	4.79	0.40	1.76		
	39	0.69	0.33	4.35	0.52	2.27		
	41	0.87	0.54	*	0.47	1.72		
	46	0.77	0.42	4.91	0.42	1.78		
	50	0.73	0.46	4.70	0.41	1.53		
	54	0.71	0.44	4.66	0.58	1.74		
	78	-0.65	0.25	-6.63	0.56	1.94		
	79	-0.61	0.23	-4.42	0.36	1.54		
	80	-0.61	0.23	-4.04	0.23	1.79		
	81	-0.64	0.23	-4.14	0.24	1.82		
	R1	-2.03	0.95	-4.69	1.75	3.79	0.61	0.89
	R2	-1.89	0.90	-5.08	1.41	3.48	0.79	0.94
	R3	-1.16	0.50	-6.49	1.57	3.21	0.82	0.94
	R4	-1.60	0.70	-5.98	1.13	2.85	0.95	1.08
	R5	-1.89	0.96	-4.76	1.17	3.17	0.62	0.74
	R8	-2.61	1.92	-2.13	1.16	1.93		
	R9	-1.56	0.60	*	1.09	2.11		
	R10	-1.29	0.56	-2.28	1.22	2.64		
	R11	-0.93	0.43	-3.73	1.19	2.82		
	Floor	-0.53	0.23	2.03	0.45	3.55	0.24	0.61
	Internal	-0.55	0.22	7.00	0.41	2.60	0.16	0.52

* Peak values exceeded range of recorder.

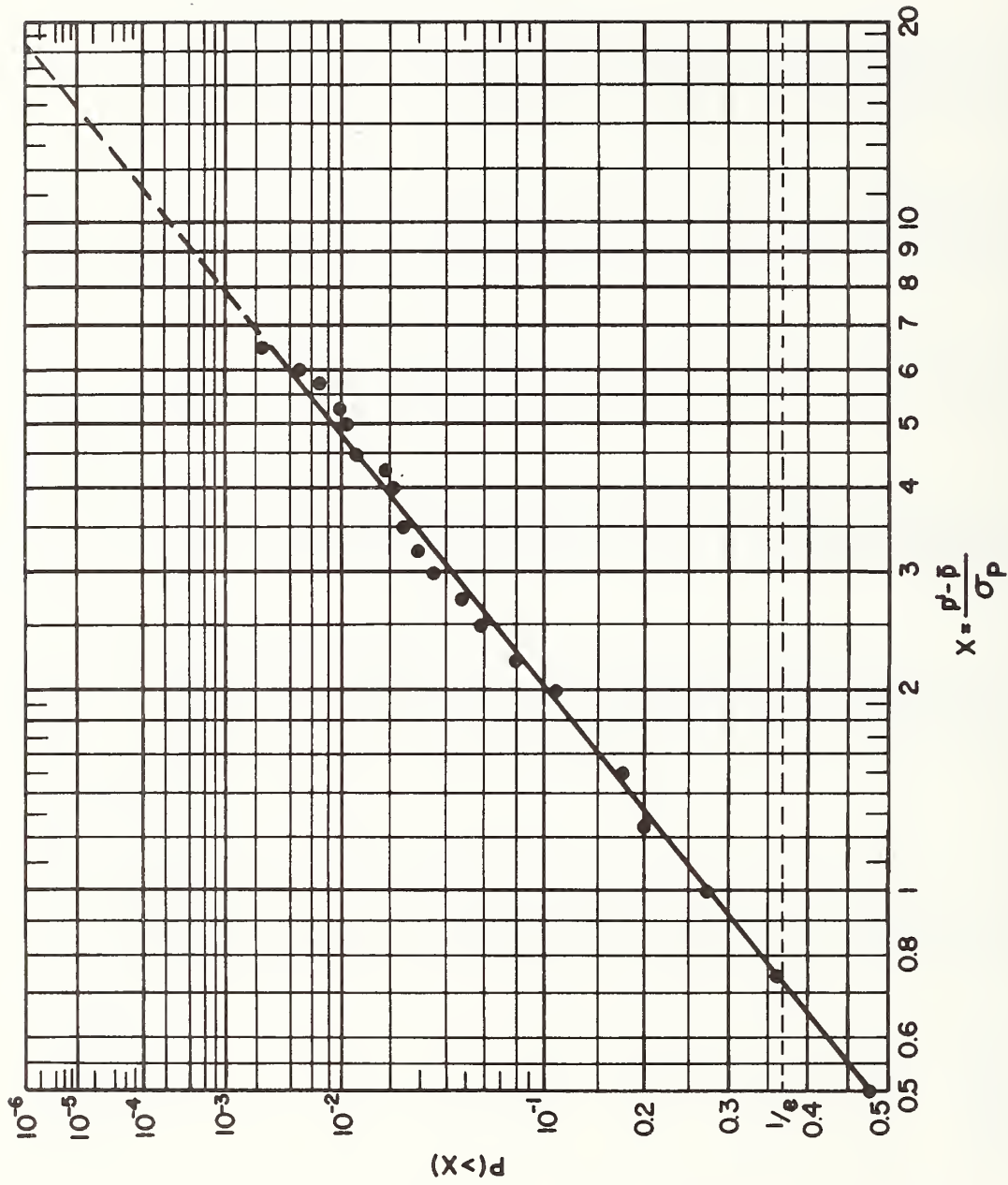


Fig. 5.6 - Probability Distribution of Peak Values, Record No. 10-5, Tap 64

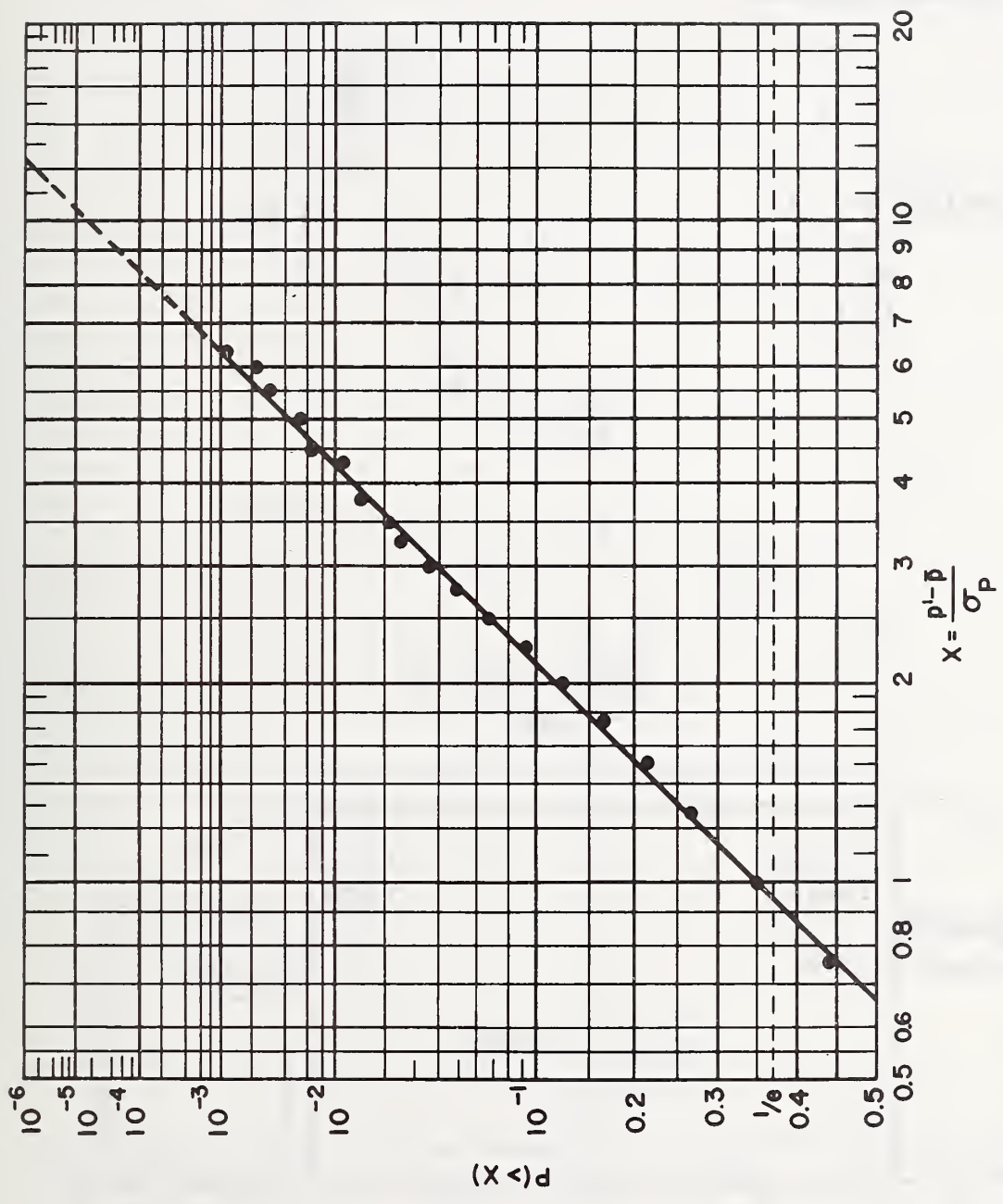


Fig. 5.7 - Probability Distribution of Peak Values, Record No. 12-5, Tap R4

SKIRTING INSTALLED

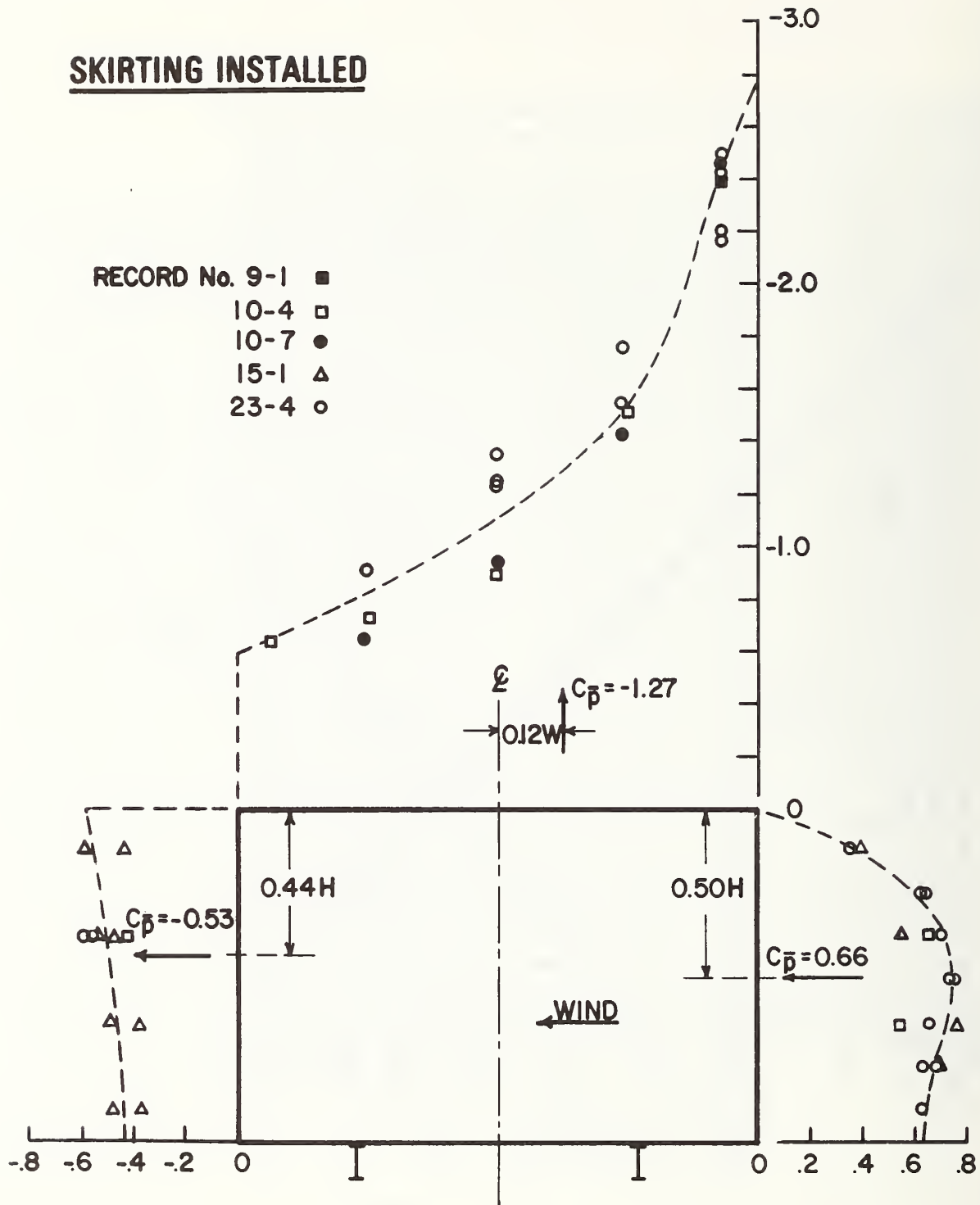


Fig. 5.8 - Distribution of Mean Pressure Coefficients, Skirting Installed

SKIRTING REMOVED

RECORD No. 9-2 □
 29-2 △
 35-1 ○

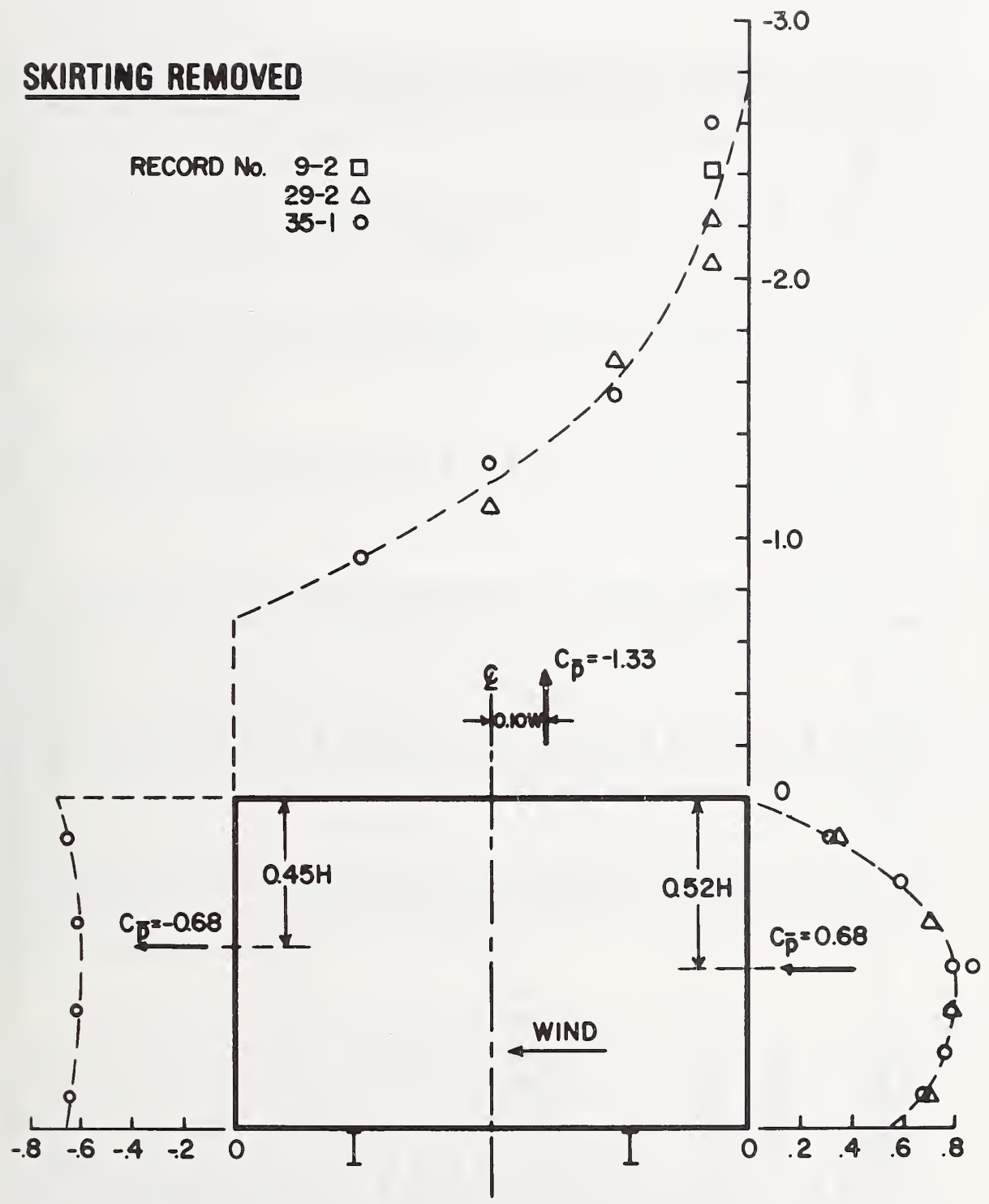


Fig. 5.9 - Distribution of Mean Pressure Coefficients, Skirting Removed

Table 4 - Multiple-Point Pressure Coefficients

Record No.	Pressure Tap Combination	C _p	g	n _o	n _p	c	k
10-4	R8 to R11	-0.95	-4.93	0.81	3.12	0.50	0.72
10-5	71,72	-1.57	-4.23	0.50	2.43		
10-6	57,61,63,64,69,70	-0.94	-5.07	0.37	2.31	0.35	0.58
	57,61,63,64	-1.03	-8.52	0.29	2.05	0.42	0.72
12-5	57,61,64,69,70,71,72	-0.89	-8.54	0.22	2.26	0.33	0.57
	R2,R3	-1.71	-1.75	2.83	3.85		
	R2 to R6	-0.94	-2.53	3.04	4.48		
23-4	R8 to R11	-0.25	-6.25	0.67	2.96	0.26	0.56
	29 to 32	0.60	3.97	0.44	2.05	0.80	0.83
	4,15,30,50,52,54	0.68	3.72	0.58	2.20	0.45	0.68
	3,4,5,14,15,16,29,30,31,32	0.61	4.71	0.46	1.93	0.52	0.71
	49,50,51,52,54	0.65	4.18	0.43	1.90	0.62	0.77
	R1,R2,R5	-2.27	-4.31	0.99	3.67	0.47	0.74
	R2,R4,R5	-2.05	-4.58	0.98	3.42	0.52	0.79
	R2 to R5	-1.84	-4.81	0.82	3.36	0.48	0.73
29-2	R8 to R11	-1.55	-3.43	1.22	3.35	1.18	1.74
	30,31,34,37,38	0.82	3.99	0.22	1.46	1.02	0.93
	27,30,31,33,34,35,37,38,41	0.81	4.03	0.20	1.38	1.12	0.99
	26 to 44	0.74	4.21	0.23	1.51	1.01	0.93
	R1,R2,R5	-1.99	-2.64	1.02	3.35	0.64	1.11
	R3,R4,R6	-1.37	-4.41	0.68	2.68	0.41	0.72
35-1	R1 to R6	-1.68	-3.49	0.79	3.16	0.39	0.79
	R1,R2	-1.96	-4.66	1.27	3.59	0.52	0.82
	R1,R2,R5	-1.94	-4.76	1.04	3.42	0.42	0.73
	R1 to R5	-1.71	-4.81	0.82	3.37	0.36	0.68

With regard to the windward wall, the following reductions in the r.m.s. pressure coefficients and the peak pressure fluctuations were determined by comparing results of the multiple-point analysis (see Table 4) with average values based on the single-point results presented in Table 3.

Record No.	Tap Combination	Area (ft ²)	C _{pσ} (percent reduction)	gC _{pσ} (percent reduction)
23-4	29 to 32	10	6	16
	4,15,30,50,52,54	120	32	44
	49,50,51,52,54	30	11	18
29-2	30,31,34,37,38	13	0	3
	27,30,31,33,34,35,37,38,41	24	3	5
	26 to 44	50	8	9

The areas listed above are somewhat subjective, it being assumed that continuous strips or zones can be represented by the pressure taps located within those strips or zones as, for example, in the case of the second combination for Record No. 23-4 where the area represents a continuous strip 60 ft (18.3 m) long and 2 ft (0.61 m) wide. It is clear that only when the transducer array becomes line-like in shape and is of appreciable length do the individual pressure measurements significantly overestimate the maximum loads acting on tributary areas. In the case of Record No. 29-2, individual measurements overestimate the r.m.s. pressure coefficient and the maximum load fluctuation on the 50-ft² (4.6-m²) area of regular shape by less than 10 percent. Since the pressure fluctuations on the windward wall are due primarily to the longitudinal component of the incident turbulence, strongly coherent pressure fluctuations are to be expected over tributary areas whose dimensions are small compared to the scale of the turbulence.

For the case of end walls with the wind approximately normal to the axis of the mobile home, flow separation occurs at the windward corner and the nature of the pressure fluctuations is more complex than is the case for a windward wall. Referring to Record Nos. 10-5 and 10-6, the following reductions were determined for the indicated tributary areas.

Record No.	Tap Combination	Area (ft ²)	C _{pσ} (percent reduction)	gC _{pσ} (percent reduction)
10-5	71,72	5	11	-
	57,61,63,64,69,70	16	12	32
10-6	57,61,63,64	11	8	7
	57,61,64,69,70,71,72	19	17	12

While the true maximum pressure fluctuation for the first tap combination of Record No. 10-5 cannot be determined because the range of the recorder was exceeded, it is obvious that the reductions in both the r.m.s coefficients and the maximum loads are more pronounced for streamwise surfaces than for surfaces normal to the flow. However, the region of extreme negative mean and fluctuating pressures (tap 72, Record No. 10-5) is of very limited extent and the coefficients based on combined records (Table 4) are sufficient for calculating loads acting over the entire end wall. As pointed out previously, the relative wind direction significantly influences the magnitude of surface pressures in regions of separated flow. In the case of Record Nos. 10-5 and 10-6, it appears that the flow over the end walls is fully separated with the possibility of reattachment occurring just at the trailing edge of the end wall for Record No. 10-6.

Referring to Figures 5.8 and 5.9, the magnitude of the mean or steady component of the pressure acting on the roof changes very rapidly near the leading edge. This is also true of the fluctuating component as can be seen from the results presented in Table 3. Compared with average values of the single-point results in Table 3, the following reductions are obtained for the r.m.s. pressure coefficients and the peak pressure fluctuations when based on combined records (see Table 4).

Record No.	Tap Combination	Area (ft ²)	$C_{p\sigma}$ (percent reduction)	$gC_{p\sigma}$ (percent reduction)
10-4	R8 to R11	16	26	34
12-5	R2,R3	20	28	-
	R2 to R6	50	53	-
	R8 to R11	16	8	22
23-4	R1,R2,R5	30	12	3
	R2,R4,R5	30	13	11
	R2 to R5	40	18	23
	R8 to R11	16	35	33
29-2	R1,R2,R5	30	29	-
	R3,R4,R6	30	12	9
	R1 to R6	60	29	-
35-1	R1, R2	20	6	10
	R1,R2,R5	30	13	14
	R1 to R5	50	18	24

As expected, estimates of both the r.m.s. pressure coefficients and the peak fluctuations obtained from combined records are significantly less than the averaged values obtained from the single-point analysis. This is particularly true where the tributary area includes pressure taps located along the leading edge as well as taps near the middle of the roof. On the other hand, those combinations that include taps located only along

the leading edge or only well back from the leading edge exhibit substantially smaller reductions for combined records. Flow over the roof clearly involves two regions: (1) a narrow strip along the leading edge where extremely low mean pressures and strong negative-going fluctuations occur and (2) the remainder of the roof where the mean pressure increases and the amplitudes of the pressure fluctuations decrease toward the trailing edge. Because local failures of the roof membrane can lead to complete failure of the roof system, special attention must be given to the membrane and fasteners along the perimeter of the roof.

5.4 Drag and Lift Coefficients - Data reduction and analysis techniques previously described for pressure measurements were also applied to the time histories of drag and lift reactions. Both single and combined records were reduced to mean and fluctuating components and distributions of the fluctuation amplitudes were described in terms of the Weibull coefficients discussed in Section 5.3.

As mentioned in Section 3.3, warping of the mobile home superstructure with changes in temperature and humidity caused shifts in the output signals of the instrumented force links that were difficult to distinguish from wind effects. Also, rotation of the mobile home and support frame to alter the relative wind direction introduced signal offsets that could only be evaluated under relatively calm wind conditions. This was not a serious problem in evaluating total drag response since all four horizontal force links were operated continuously during the study. For the vertical force or lift measurements, however, these induced offsets could not always be evaluated or eliminated since difficulties with stability in some of the data channels did not allow the simultaneous measurement of forces in all eight force links. The mean or steady components could thus be estimated with confidence only for those cases where the mobile home was not rotated between initial and final readings obtained under calm conditions. These problems with the evaluation of force-link offsets did not affect the evaluation of the fluctuating components of lift and drag response, however. In the following discussion, the numbering system in Figure 2.5 is used to identify the force links.

A typical spectral density function for the drag force fluctuations measured at the forward foundation assembly is shown in Figure 5.10. The same coordinates as described in Section 5.2 have been used with force replacing pressure as the time-dependent variable. Most of the contribution to the total measured variance is associated with frequencies of less than 0.6 Hz with a spectral peak at approximately 0.03 Hz. There is another peak centered at 3.6 Hz which represents the contribution of the resonant response of the forward portion of the mobile home. As pointed out in the discussion of pressure fluctuations, the area associated with a frequency increment Δn is proportional to that fraction of the variance contributed by frequencies over the same increment. For the plotted spectrum the resonant component amounts to less than 3 percent of the total variance and the assumption of a quasi-static response to wind fluctuations is reasonable. At higher wind speeds the

REC. NO. 8-2
SENSOR FL9

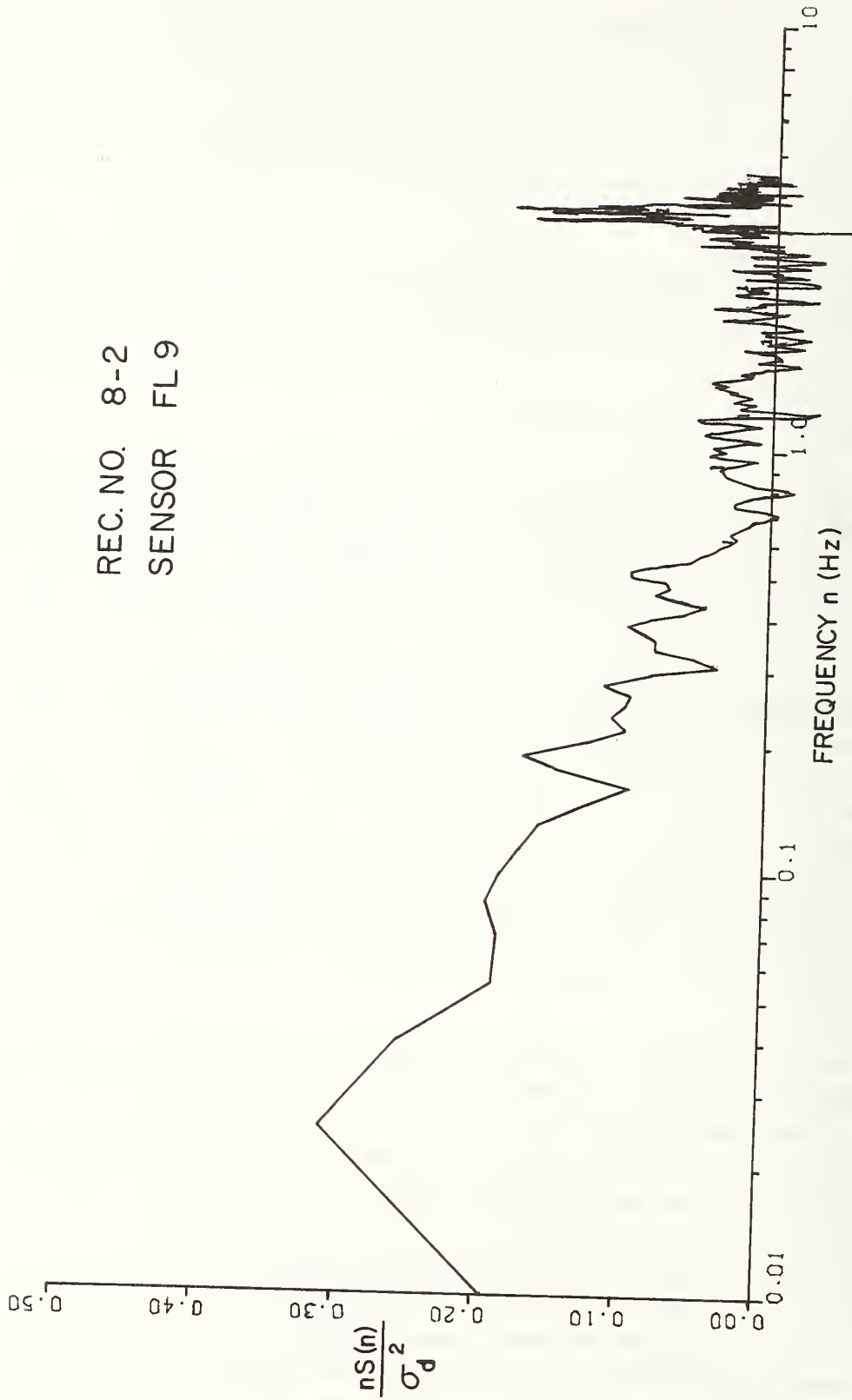


Fig. 5.10 - Spectrum of Drag Load, Record No. 8-2, Force Link No. 9

area of the low-frequency portion of the spectrum will be preserved, but the frequencies will increase in direct proportion to the mean speed. For a basic wind speed of 90 mph (40.2 m/s) (see Section 6.1) the corresponding speed at the reference height of 10.8 ft (3.3 m) and averaged over the same record length of 300 seconds as was used for Rec. No. 8-2 would be approximately 63 mph (28.2 m/s). Since the reference wind speed (see Table 1) was 17.3 mph (7.7 m/s), the frequencies would be multiplied by a factor of 3.6. Thus, for the assumed basic wind speed of 90 mph, the energy-containing frequency range would still be well below the first-mode natural frequency of 3.6 Hz and the resonant component of response would not be significant.

As with the pressure coefficients, the drag and lift coefficients are defined in terms of a dynamic pressure at the reference height $h = 3.3$ m and have the form

$$C_d = \frac{\overline{F}_d}{1/2 \rho \overline{u}_{3.3}^2 A} \quad (15)$$

and

$$C_{d\sigma} = \frac{\sigma_d}{1/2 \rho \overline{u}_{3.3}^2 A} \quad (16)$$

where \overline{F}_d and σ_d denote the mean and standard deviation of the drag force and A is the projection on a vertical plane of the mobile home area served by a given horizontal force link. Similar notation and expressions apply to the lift forces. It should be noted here that the projected areas for drag forces reflect the presence or absence of skirting at the bottom of the mobile home.

Drag coefficients based on individual and combined time histories are presented in Tables 5 and 6, respectively, for records obtained with the wind direction approximately normal to the longitudinal axis of the mobile home. Also included for certain records are the Weibull coefficients determined from plots of the probability distribution functions. Lift coefficients are presented in Table 7.

The mean drag coefficients, C_d , for the combined records listed in Table 6 exhibit considerable scatter. However, the test results do suggest a larger mean drag coefficient for the unskirted configuration and this is in agreement with the mean pressure coefficients plotted in Figures 5.8 and 5.9. Neglecting end effects, these plots suggest that the mean drag coefficient for the unskirted configuration is approximately 1.2 times that for the skirted configuration. This same ratio for the averages of the mean drag coefficients of Table 6 is 1.24. Removal of the skirting results in a larger aspect ratio and a larger drag coefficient is, therefore, to be expected.

Drag and lift coefficients have been measured by Harris [17] using 1:16 scale models of mobile homes placed in a wind tunnel having a uniform flow with low intensity of turbulence. For the unskirted configuration, mean drag coefficients of 1.22 and 1.23 were

Table 5 - Individual Drag Coefficients

Record No.	Force Link No.	C_d	$C_{d\sigma}$	ξ	n_o	n_p	c	k
6-6	9	0.85	0.29	6.88	0.25	0.83	0.40	0.56
	10	0.93	0.12	4.75	0.21	0.71	0.64	0.83
	11	0.94	0.22	7.18	0.19	0.65	0.44	0.62
	12	0.97	0.29	5.61	0.17	0.61	0.79	0.86
8-2	9	1.03	0.23	3.33	0.41	2.11	0.42	0.73
	10	1.13	0.11	3.92	0.46	3.53		
	11	0.94	0.13	3.74	0.54	3.21		
	12	0.79	0.16	4.21	0.39	3.24		
8-5	9	0.93	0.41	10.18	0.27	1.71		
	10	1.05	0.19	4.95	0.35	2.80		
	11	0.80	0.29	5.35	0.35	2.44		
	12	0.67	0.36	5.34	0.23	2.43		
9-1	9	1.27	0.54	9.20	0.24	1.62	0.20	0.54
	10	1.14	0.20	5.53	0.40	2.78	0.18	0.55
	11	0.95	0.25	4.52	0.33	2.54	0.23	0.55
	12	0.93	0.33	4.56	0.32	2.71	0.22	0.53
9-2	9	1.59	0.36	4.74	0.59	2.10	0.35	0.66
	10	1.48	0.18	4.12	0.58	3.20	0.13	0.46
	11	1.08	0.27	6.30	0.45	2.65	0.34	0.71
	12	1.05	0.37	7.53	0.41	2.56	0.26	0.61
9-3	9	1.46	0.41	4.32	0.38	1.94		
	10	1.43	0.18	4.26	0.26	3.12		
	11	0.85	0.24	4.40	0.41	2.86		
	12	1.05	0.32	4.02	0.36	2.86		
15-1	9	0.94	0.35	5.47	0.14	0.65		
	10	0.70	0.14	5.06	0.14	0.56		

Table 5 - Individual Drag Coefficients
(continued)

Record No.	Force Link No.	C_d	$C_{d\sigma}$	g	n_o	n_p	c	k
15-1 (cont.)	11	1.08	0.15	3.94	0.18	0.57		
	12	0.89	0.21	4.57	0.16	0.56		
23-4	9	0.96	0.30	4.42	0.45	2.42	0.57	0.74
	10	0.67	0.14	3.86	0.46	2.94	0.46	0.67
	11	1.13	0.18	4.29	0.47	3.11	0.36	0.65
	12	0.66	0.27	5.57	0.43	2.65	0.37	0.67
29-2	9	1.50	0.43	3.93	0.31	1.87	0.21	0.54
	10	0.62	0.19	3.57	0.42	3.25	0.22	0.58
	11	1.18	0.20	3.71	0.60	3.38	0.18	0.58
	12	0.83	0.23	3.90	0.56	3.04	0.23	0.64
35-1	9	0.81	0.38	5.90	0.44	1.87		
	10	0.98	0.17	4.53	0.34	2.51		
	11	1.29	0.24	4.29	0.39	2.49		
	12	0.90	0.35	4.53	0.30	2.25		

Table 6 - Combined Drag Coefficients

Record No.	Force Link Combination	C_D	$C_{D\sigma}$	g	n_o	n_p	c	k
6-6	9,10,11,12	0.92	0.19	5.96	0.28	1.44	0.42	0.65
8-2	"	1.03	0.16	3.54	0.22	2.74	0.40	0.68
8-5	"	0.86	0.29	6.09	0.21	2.70		
9-1	"	1.07	0.28	7.09	0.26	2.40	0.10	0.37
9-2	"	1.29	0.27	5.24	0.36	2.71	0.28	0.57
23-4	"	0.85	0.19	3.41	0.27	2.59	0.38	0.54
29-2	"	1.06	0.24	3.71	0.35	2.83	0.21	0.55

Table 7 - Lift Coefficients

Record No.	Force Link Combination	$\overline{C_{l\sigma}}$	$C_{l\sigma}$	g	n_o	n_p	c	k
8-2	1,2	0.83	0.21	3.54	0.48	2.93	0.47	0.70
	5,6	0.89	0.22	3.87	0.30	3.15	0.41	0.64
8-5	1,2,5,6	0.86	0.19	3.79	0.38	3.00	0.30	0.59
	1,2		0.33	4.78	0.42	2.81	0.25	0.68
	5,6		0.28	15.20	0.33	2.98	0.27	0.64
9-1	1,2,5,6		0.28	9.71	0.31	2.79	0.28	0.76
	1,2	1.03	0.38	5.69	0.40	2.92	0.20	0.52
	5,6	0.91	0.27	4.81	0.27	2.65	0.39	0.62
9-2	1,2,5,6	0.97	0.29	5.30	0.35	2.73	0.20	0.50
	1,2		0.26	4.45	0.71	3.75	0.32	0.70
	5,6		0.18	4.63	0.48	2.94	0.64	0.76
23-4	1,2,5,6		0.19	4.69	0.68	3.30	0.26	0.59
	1,2		0.19	6.32	0.61	3.10	0.50	0.71
29-2	5,6		0.19	3.90	0.42	3.28	0.64	0.76
	1,2,5,6		0.17	5.04	0.44	3.04	0.65	0.77
	1,2		0.21	4.40	0.67	3.36	0.37	0.69
	5,6		0.18	4.45	0.32	3.20	0.46	0.67
	1,2,5,6		0.16	4.30	0.54	3.30	0.31	0.65

obtained for prototype lengths of 50 and 60 ft (15.24 and 18.29 m), respectively, with the wind normal to the longitudinal axis of the model. The width of the model corresponded to a prototype width of 10 ft (3.05 m). With skirting installed, a mean drag coefficient of 1.31 was obtained for the 50-ft prototype length. However, since the surface area on which these coefficients are based does not include the area of the skirting, the actual drag coefficient for the skirted configuration would be approximately 1.05. Thus the trends observed in the wind tunnel with uniform flow are in line with the full-scale measurements of drag forces in the atmospheric boundary layer.

Harris also measured lift forces and calculated lift coefficients for several relative wind directions. For the model of a 50-ft prototype without skirting, a maximum lift coefficient of 0.62 was obtained with the wind at 45 degrees to the longitudinal axis. With the wind normal to the longitudinal axis, the lift coefficient was 0.13. With skirting installed, the lift coefficients for these same relative wind directions were 0.89 and 0.78. Although surface pressures are not discussed in Ref. 17, the lift coefficients for wind normal to the longitudinal axis of the model suggest a change of $0.13 - 0.78 = -0.65$ in the average pressure coefficient on the underside of the model with removal of the skirting.

The mean lift coefficients in full scale could be determined with some confidence for only two records as is indicated in Table 7, skirting being attached in both cases and the mean lift coefficient averaging 0.92. Referring again to the mean pressure coefficients plotted in Figures 5.8 and 5.9 and noting the floor pressure coefficients listed in Table 3, mean lift coefficients of 1.05 and 0.80 are obtained for the skirted and unskirted configurations, respectively. These are only rough estimates, it being assumed that the pressures acting on the underside of the mobile home (measured at the centerline) are uniform across the width of the home and that end effects are negligible. The change in the mean pressure coefficient on the underside of the mobile home (see Table 3) with removal of the skirting is $0.22 - 0.53 = -0.31$, approximately half that observed in the model studies conducted by Harris. While skirting apparently has a pronounced effect on the mean lift coefficient in uniform flows, this is not the case in the atmospheric boundary layer.

5.5 Structural Damping - Recordings of accelerations under strong wind conditions afforded an opportunity to obtain estimates of the combined structural damping of the mobile home superstructure and the foundation system. Two methods were used in the analysis; the random decrement or "randomdec" technique [18, 19], and the autocorrelation technique. The details of the analysis and the test results have been reported by Yang [20] and only a summary of the procedure and typical results are presented herein. In the randomdec technique, estimates of the damping ratio are obtained from the decay of a signature resulting from the averaging of a large number of segments of the acceleration time history, the initial point of the segments corresponding to consecutive crossings (with both positive or negative slope) of some specified amplitude. The main advantages of the randomdec technique over the commonly-

used autocorrelation technique are a fixed amplitude of signature and a signature which has the same dimensions as the original time history since no multiplications are involved. The fixed amplitude feature stabilizes the form of the signature for nonlinear variations of damping with amplitude and simple summations replace summations of time-lagged products.

A typical randomdec signature is shown in Figure 5.11(a) and is based on the acceleration time history obtained with skirting installed on the mobile home and with the accelerometer mounted as described in Section 3.4. The mean wind speed at the reference height of 3.3 m was 22.5 mph (10.1 m/s) and the relative wind direction ranged from 265 to 270 degrees. Thus, the wind was blowing nearly face-on to the left side of the mobile home and the mobile home superstructure was responding in the horizontal bending and racking modes. The autocorrelation function and the spectral density function for the same acceleration time history are shown in Figures 5.11(b) and (c), respectively. With reference to Figure 5.11(c), the predominant peak in the spectrum is centered at approximately 4.3 Hz with a second well-defined peak at approximately 9 Hz. There is no significant contribution above 15 Hz.

The sampling rate for the randomdec analysis was 66.7 samples per second and the record length was approximately 300 seconds. An amplitude of 1.50σ was selected for which there occurred 766 segments in the record and the cut-off frequency was 7.8 Hz. The results of the analysis are given in Table 8.

The damping ratio estimates obtained by the randomdec technique are more consistent than those obtained from the autocorrelation function which is to be expected because of its "fixed amplitude" feature. The autocorrelation function, on the other hand, incorporates the entire time history and is therefore more sensitive to nonlinear damping and cross products of modes.

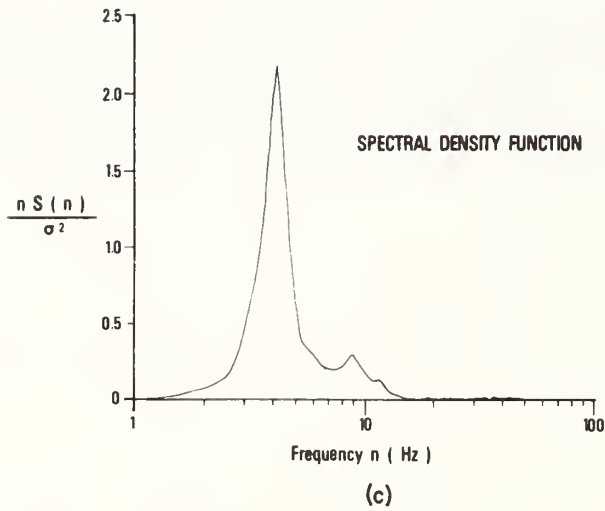
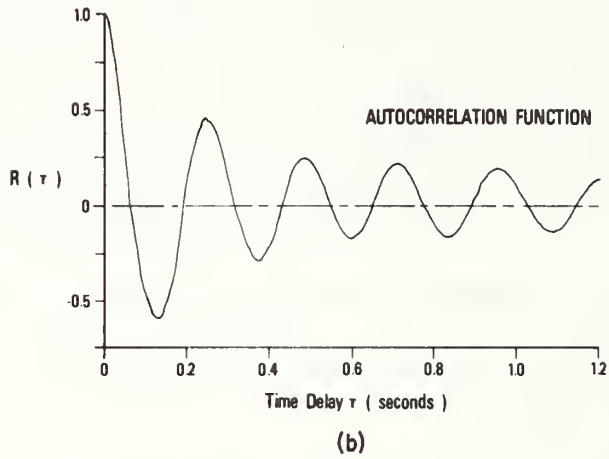
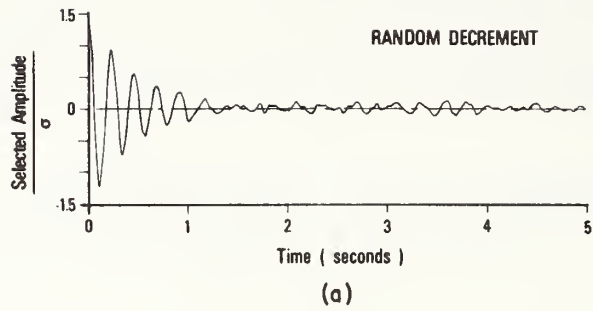


Fig. 5.11 - Analysis of Acceleration Time History

Table 8 - Damping Ratios

<u>Frequency</u>	<u>Random Decrement</u>	<u>Autocorrelation</u>
Average of 3 periods	4.4 Hz	4.3 Hz
<u>Damping Ratio</u>		
First and second peak	.079	.115
First and third peak	.080	.093
Second and third peak	.081	.071
Average	.080	.093

6. RECOMMENDED DESIGN WIND LOADS

This chapter describes the criteria, assumptions and procedures used to establish appropriate static loads for the design of mobile homes and their anchoring systems to resist wind forces. These design loads are largely based on the test results presented and discussed in Section 5 and represent the average maximum loads likely to occur for the stated conditions.

6.1 Basic Wind Speeds - Section 280.305 of the current version of the federal Mobile Home Construction and Safety Standards (December, 1975) specifies design wind loads for a "Standard Wind Zone" and a "Hurricane Wind Zone." Approximately, these zones are defined by the 80 mph isotach for a 50-year mean recurrence interval as presented in Ref. 14. Implicit in the specified design loads for the two zones are basic wind speeds of 70 and 90 mph (31 and 40 m/s) based on the "fastest mile of wind" at 30 ft (9.15 m) above ground in open terrain. Thus, there are substantial portions of each zone for which the basic wind speeds are exceeded by the "map" values of Ref. 14. The wind speed distributions specified in Ref. 14 are currently under review and the zone designations and basic wind speeds of 70 and 90 mph will continue to be used in the interim. However, it is important to note that these wind speeds imply a mean recurrence interval of approximately 30 years for portions of the two zones.

6.2 Design Wind Speeds - In calculating dimensionless pressure, drag and lift coefficients in Section 5, the mean wind speed at a fixed reference height was used to determine a freestream dynamic pressure. This reference height is usually taken as the height of the building or structure for convenience in specifying pressure and force coefficients for buildings of various aspect ratios. For a minimum clearance of 1 ft (0.31 m) between the ground surface and the mobile home underframe as specified in Ref. 21, a suitable reference height would be 9.5 ft (2.90 m). All other conditions being equal, the mean wind speed at this height will be less than that at the 30 ft reference height used in Ref. 14, the reduction depending upon the average terrain roughness at the site. Using the power law representation of the mean velocity profile and selecting an exponent of 0.17 as being representative of a moderately open exposure, the following relationship between wind speed at the standard reference height of 30 ft (9.15 m) and at the reference height of 9.5 ft (2.90 m) is obtained.

$$\begin{aligned} \frac{\bar{u}_{9.5}}{\bar{u}_{30}} &= \left(\frac{9.5}{30}\right)^{0.17} \\ &= 0.82 \end{aligned} \quad (17)$$

The choice of averaging time is somewhat arbitrary, but it should be long enough to reflect

the effects of low-frequency components of turbulence generated by the terrain roughness and short enough so that a reasonably stationary time history free of significant trends will be obtained. Experience has shown that averaging times of from 15 to 30 minutes generally satisfy these requirements and a time interval of 1000 seconds will be used here.

To relate the fastest mile speeds to speeds averaged over 1000 seconds, reference is made to data obtained by Durst [22] in strong winds over flat, unobstructed terrain. A plot based on Durst's results and which gives the ratio of the average probable maximum wind speed to the mean hourly speed for a terrain roughness in line with the exponent of 0.17 has been presented by Vellozzi and Cohen [23] and is reproduced in Figure 6.1. Fastest mile speeds of 70 and 90 mph correspond to averaging times of 51 and 40 seconds, respectively. The corresponding speed ratios for an averaging time of 1000 seconds are

$$\frac{\bar{u}_{(1000)}}{\bar{u}_{(40)}} = 0.80 \quad (18)$$

and

$$\frac{\bar{u}_{(1000)}}{\bar{u}_{(51)}} = 0.82 \quad (19)$$

Taking 0.81 as an average ratio, the design wind speed at the reference height of $h = 9.5$ ft (2.90 m) and averaged over a period of 1000 seconds is related to the fastest mile basic wind speed by the following expression.

$$\begin{aligned} \bar{u}_h &= (0.82)(0.81) u_{FM} \quad (20) \\ &= 0.66 u_{FM} \end{aligned}$$

The corresponding mean dynamic reference pressure for standard atmospheric conditions is

$$\begin{aligned} \bar{q}_h &= 1/2 \rho \bar{u}_h^2 \quad (21) \\ &= 0.0011 u_{FM}^2 \end{aligned}$$

with \bar{q}_h expressed in psf and u_{FM} in mph.

6.3 Selection of Peak Factors - To obtain pressures or forces for design purposes, reference is made to the dimensionless coefficients discussed in Section 5. For the record lengths used in this study, the coefficients based on the means and standard deviations can be assumed to be independent of averaging time and the determination of design values thus involves the selection of appropriate peak factors, g . Taking surface pressure as an example, the design value is

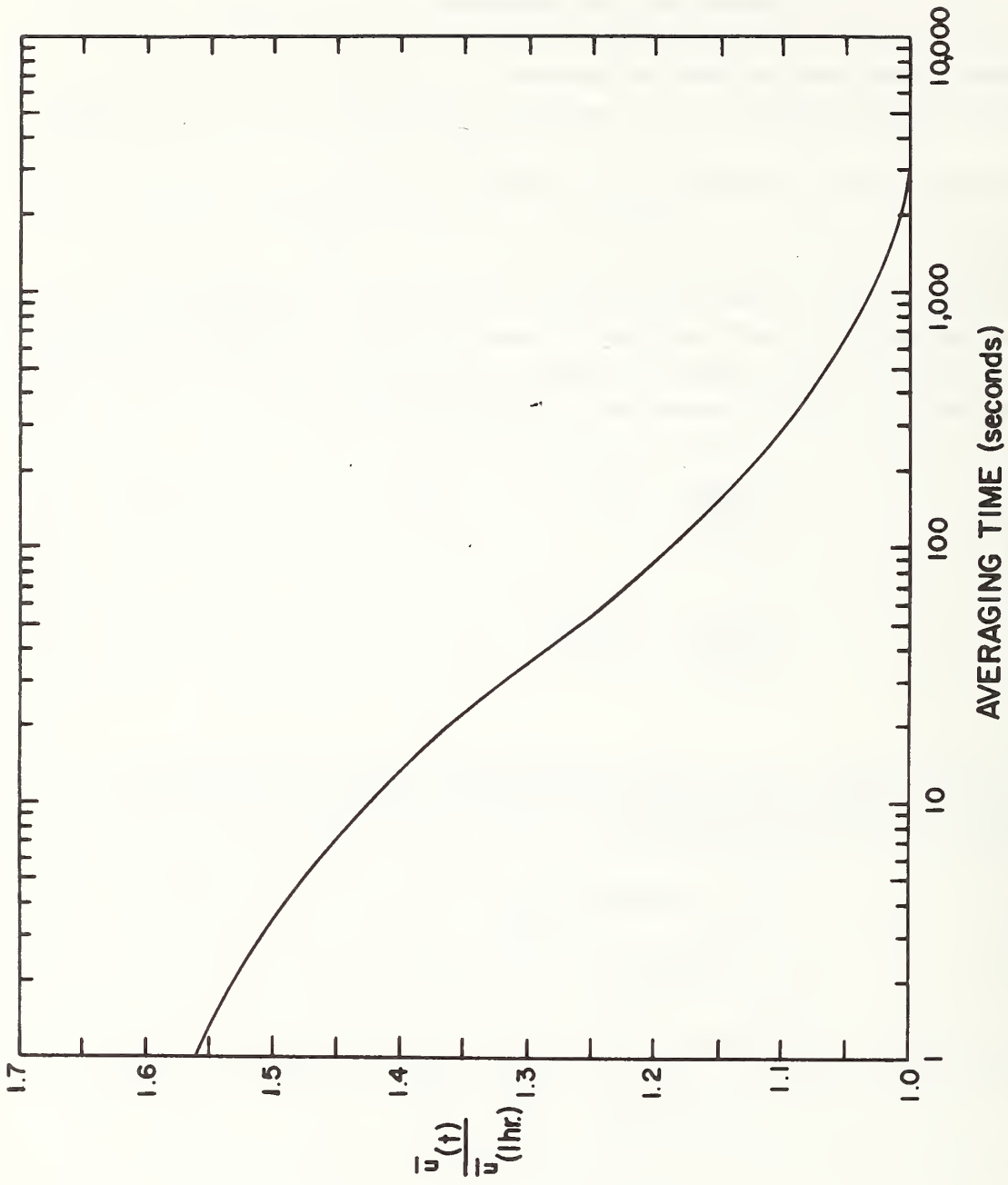


Fig. 6.1 - Variation of Maximum Wind Speed With Averaging Time

$$\hat{p} = q_h C_p \quad (22)$$

$$= q_h (C_p + g C_{p_g})$$

with g corresponding to the average maximum value of the peak factor occurring in a time interval of 1000 seconds. From similarity arguments it can be readily shown that the probability of the peak factor exceeding some value, X , is

$$P(>X) = \frac{\bar{u}_{3.3}}{660 n_o u_{FM}} \quad (23)$$

where $\bar{u}_{3.3}$ is the measured mean reference wind speed and n_o is the average upcrossing rate obtained from the analysis of peak values. Having established $P(>X)$, the value of g is obtained from the plot of the probability distribution function. It is assumed in Eq. 23 that the upcrossing rate scales directly with the reference wind speed, i.e.,

$$\left(\frac{n_o}{u_h/1}\right) = \left(\frac{n_o}{u_h/2}\right) \quad (24)$$

This only requires that the characteristic length scales for the two wind speeds be equal and that the flow process be independent of the Reynolds number. Experimental results obtained from studies on bluff bodies in both model and full scale support these assumptions.

To illustrate the effect of averaging time on the average maximum fluctuating component of pressure or load, peak factors have been calculated for two values of the ratio $\bar{u}_{3.3}/n_o$ and for averaging times ranging from 3 seconds to 1 hr. A basic wind speed of 90 mph was assumed and the Weibull coefficients $c = 0.7$ and $k = 0.8$ were used to obtain the values of g . The results are plotted in Figure 6.2 as a ratio of $g_{(t)} \bar{u}_{(t)}^{-2}$ to $g_{(1000)} \bar{u}_{(1000)}^{-2}$ which represents the change in the peak value of the fluctuating component with averaging time. The values of the ratio u/n_o and the Weibull coefficients are typical of the values obtained in this study. It is seen from Figure 6.2 that the maximum change is less than 10 percent for averaging times ranging from 100 to 1000 seconds.

6.4 Internal and External Pressures - Having established a procedure for selecting the peak factor, the pressure coefficients presented in Tables 3 and 4 can be used to obtain the average maximum (or minimum) pressure coefficients associated with a time interval of 1000 seconds. In calculating the pressures tabulated in this section and the drag and lift forces presented in the following section, the dynamic reference pressure defined by Eq. 21 has been used. Single-point and multiple-point pressure coefficients (see Sec. 5.3) are listed in Tables 9 and 10, respectively, for basic wind speeds of 70 and 90 mph. Note that the peak factors increase slightly with wind speed because of the larger number of upcrossings occurring in a given time interval. The peak departures from the mean have been estimated for the critical cases, i.e., positive-going values for

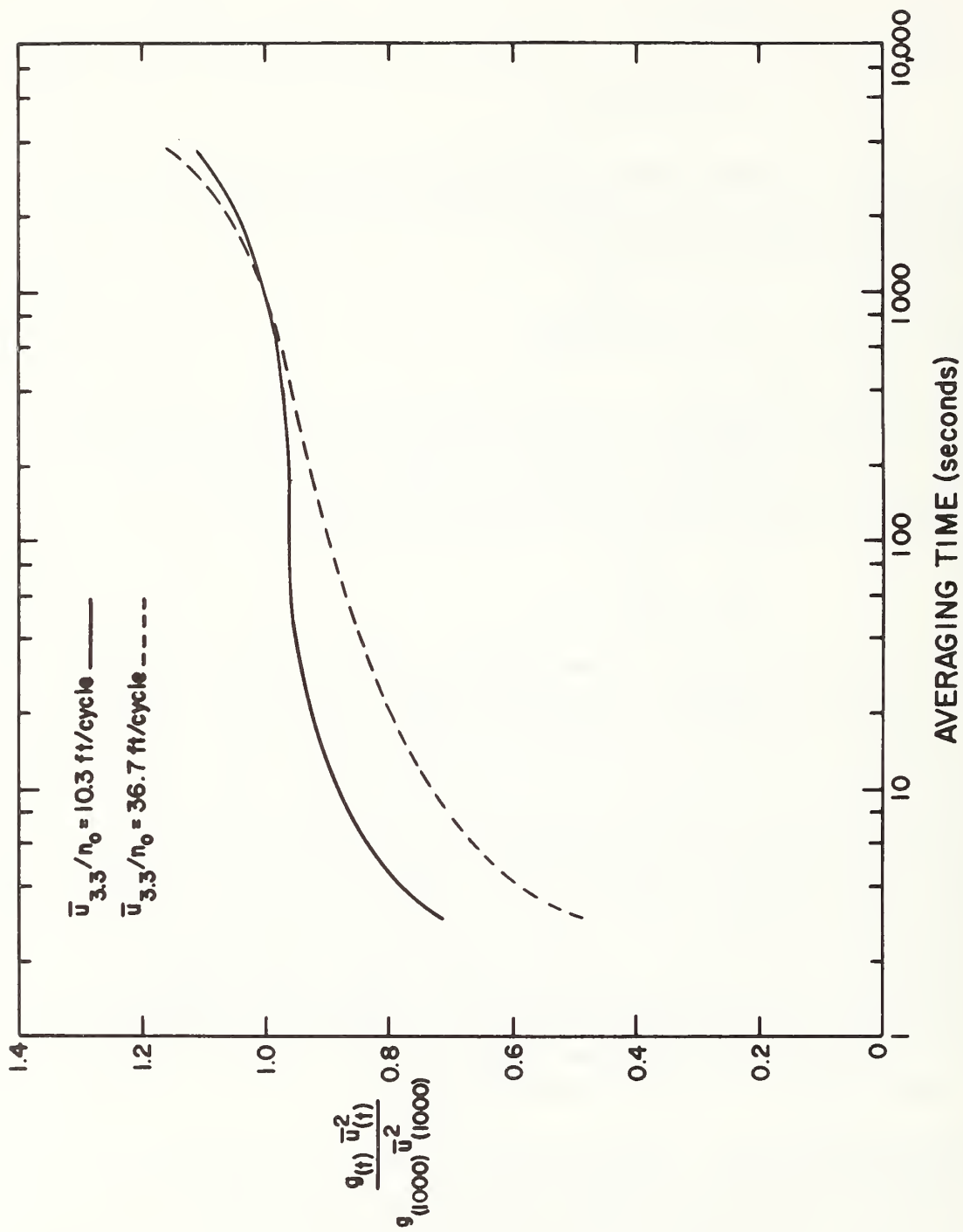


Fig. 6.2 - Variation of Peak Factor With Averaging Time

Table 9 - Average Maximum Single-Point Pressure Coefficients

Record No.	Pressure Tap No.	$u_{FM} = 70$ mph			$u_{FM} = 90$ mph		
		$P(>X) \times 10^3$	g	C_p	$P(>X) \times 10^3$	g	C_p
10-4	18	0.80	-5.3	-1.44	0.63	-5.4	-1.46
	79	0.55	7.7	4.37	0.43	8.1	4.56
	R11	0.19	-8.8	-7.77	0.15	-9.2	-8.05
10-5	Internal	0.80	8.0	0.88	0.63	8.4	0.94
	57	0.28	-10.5	-5.74	0.22	-10.9	-5.92
	61	0.30	-11.1	-6.39	0.24	-11.7	-6.69
	64	0.32	-9.5	-6.41	0.25	-10.0	-6.70
	71	0.58	-9.2	-9.27	0.45	-9.7	-9.70
10-6	Internal	1.01	6.6	1.18	0.79	7.2	1.31
	Internal	0.70	6.7	1.17	0.54	7.0	1.23
10-7	R9	0.21	-7.3	-8.45	0.17	-7.8	-8.93
12-5	70	1.2	-4.8	-0.80	0.95	-5.0	-0.82
	72	1.2	-4.5	-0.73	0.91	-4.7	-0.75
15-1	Floor	1.4	7.5	0.46	1.12	8.0	0.50
	79	1.0	-4.7	-1.65	0.80	-5.0	-1.72
23-4	83	1.1	-5.6	-2.06	0.87	-5.9	-2.14
	30	0.83	8.8	3.88	0.65	9.1	3.99
	74	1.35	-5.9	-2.27	1.05	-6.1	-2.33
29-2	R2	0.33	-10.2	-11.5	0.26	-10.7	-11.9
	R5	0.43	-10.1	-11.9	0.34	-10.5	-12.3
	R9	0.38	-8.1	-6.90	0.30	-8.4	-7.09
35-1	34	0.89	9.6	4.45	0.70	10.0	4.60
	R1	0.26	-6.6	-8.30	0.20	-6.9	-8.59
	R2	0.32	-7.3	-8.46	0.25	-7.6	-8.73

Table 9 - Average Maximum Single-Point Pressure Coefficients
(continued)

Record No.	Pressure Tap No.	$u_{FM} = 70 \text{ mph}$			$u_{FM} = 90 \text{ mph}$		
		$P(>X) \times 10^3$	g	C_p	$P(>X) \times 10^3$	g	C_p
35-1 (cont.)	R3	0.29	-7.7	-5.01	0.22	-8.0	-5.16
	R4	0.40	-6.4	-6.08	0.31	-6.7	-6.29
	R5	0.38	-10.0	-11.5	0.30	-10.4	-11.9
	Floor	1.00	5.7	0.78	0.77	6.1	0.87
	Internal	1.09	6.2	0.81	0.85	6.6	0.90

Table 10 - Average Maximum Multiple-Point Pressure Coefficients

Record No.	Pressure Tap Combination	$u_{FM} = 70$ mph			$u_{FM} = 90$ mph		
		$P(>X)$ $\times 10^3$	g	C_p	$P(>X)$ $\times 10^3$	g	C_p
10-4	R8 to R11	0.35	-8.6	-3.96	0.27	-9.1	-4.14
10-5	57,61,63,64,69,70	0.74	-10.9	-6.50	0.57	-11.4	-6.75
10-6	57,61,63,64	0.96	-6.3	-6.20	0.75	-6.6	-6.44
12-5	57,61,64,69,70,71,72	1.27	-9.1	-6.81	0.99	-9.8	-7.26
23-4	R8 to R11	0.73	-8.9	-1.23	0.57	-9.5	-1.30
	29 to 32	1.04	8.3	3.17	0.80	8.7	3.30
	4,15,30,50,52,54	0.79	8.3	2.84	0.62	8.7	3.02
	3,4,5,14,15,16,29,30,31,32	1.00	8.8	3.07	0.78	9.5	3.27
	49,50,51,52,54	1.07	7.6	3.16	0.83	7.9	3.26
	R1,R2,R5	0.46	-7.5	-8.42	0.36	-7.9	-8.75
	R2,R4,R5	0.47	-7.0	-7.37	0.36	-7.3	-7.60
	R2 to R5	0.56	-7.8	-6.91	0.44	-8.1	-7.11
	R8 to R11	0.38	-3.8	-4.13	0.29	-3.9	-4.20
29-2	30,31,34,37,38	1.58	7.5	3.75	1.23	7.8	3.86
	27,30,31,33,34,35,37,38,41	1.74	7.4	3.62	1.36	7.7	3.74
	26 to 44	1.52	7.6	3.40	1.18	8.0	3.54
	R1,R2,R5	0.34	-4.2	-4.80	0.27	-4.3	-4.87
	R3,R4,R6	0.51	-6.9	-5.37	0.40	-7.2	-5.55
	R1 to R6	0.44	-5.2	-4.70	0.34	-5.4	-4.81
35-1	R1,R2	0.35	-6.5	-7.62	0.27	-6.8	-7.88
	R1,R2,R5	0.43	-7.1	-7.76	0.33	-7.3	-7.93
	R1 to R5	0.55	-7.1	-7.47	0.42	-7.4	-6.67

windward faces and negative-going values for the roof and leeward faces. Internal pressures and pressures acting on the underside of the floor system are based on peak positive departures from the mean.

The pressure coefficients listed in Tables 9 and 10 have been averaged where more than one record is available for relative wind directions which are approximately equal. The resulting coefficients are listed in Table 11 along with the corresponding maximum or minimum pressures for basic wind speeds of 70 and 90 mph (31 and 40 m/s).

Also listed in Table 11 are the combined pressures for the roof, roof overhangs, walls and floor. Combined pressures for tributary areas of the roof represent the average maximum distributed loads acting on areas typical of those supported by individual roof trusses. The combined pressures listed for the perimeter of the roof represent the average maximum loads acting over a perimeter strip approximately 2 ft (0.6 m) wide, this width being based on the shape of the mean pressure distributions as plotted in Figures 5.8 and 5.9. For the case of walls, the pressures represent worst-case net loadings for tributary areas typical of doors, windows and wall elements supported by individual wall studs. These combined pressures, adjusted to account for code-specified working stresses as discussed in Section 6.6, are the basis for the recommended design wind loads. An example which illustrates the procedure used to determine design loads is presented in Appendix A.

6.5 Maximum Drag and Lift Coefficients - Estimates of peak factors and maximum drag coefficients for individual and combined records are listed in Tables 12 and 13, respectively. The procedure for obtaining these coefficients is identical with that used in the previous section for pressure coefficients. Although the combined records suggest a larger drag coefficient for the unskirted configuration, the variation in the values listed in Table 13 is too large to reach any definite conclusions.

There is no obvious explanation for the very flat slope of the Weibull distribution for the combined force link outputs of Record No. 9-1. The distributions for the individual force links result in much smaller peak factors as is indicated in Table 12 and the results of the combined analysis for Record No. 9-1 must, therefore, be discounted.

Averaging the maximum drag coefficients for all records except No. 9-1 of Table 13, the following values are obtained for the overall drag coefficients and for the equivalent static loads which are to be taken as acting on the area obtained by projecting the area of the mobile home onto a vertical plane normal to the wind direction.

Basic Wind Speed (mph)	\hat{C}_d	\hat{p} (psf)
70	2.69	14.5
90	2.74	24.5

Table 11 - Average Maximum Combined Pressures

ITEM	$u_{FM} = 70$ mph		$u_{FM} = 90$ mph		Combined Pressures (psf)	
	C_p	\hat{p} (psf)	C_p	\hat{p} (psf)	$u_{FM} = 70$ mph	
					$u_{FM} = 90$ mph	
ROOF						
Tributary areas	-4.30	-23.2	-4.45	-40.1	-23.2 - 5.4 = -28.6	-40.1 - 9.8 = -49.9
Perimeter of roof	-7.35	-39.7	-7.50	-66.8	-39.7 - 5.4 = -45.1	-66.8 - 9.8 = -76.6
Overhangs (net uplift)					-39.7 - 17.0 = -56.7	-66.8 - 29.4 = -96.2
WALLS						
Sides (windward)	3.15	17.0	3.30	29.4	17.0 + 1.9 = 18.9	29.4 + 3.1 = 32.5
" (leeward)	-1.85	-10.0	-1.90	-16.9	-10.0 - 5.4 = -15.4	-16.9 - 9.8 = -26.7
Ends (windward)	3.15	17.0	3.30	29.4	17.0 + 1.9 = 18.9	29.4 + 3.1 = 32.5
" (leeward)	-6.50	-35.1	-6.80	-60.5	-35.1 - 5.4 = -40.5	-60.5 - 9.8 = -70.3
FLOOR	1.00	5.4	1.00	8.9	5.4 + 1.9 = 7.3	8.9 + 3.1 = 12.0
INTERNAL						
Maximum	1.00	5.4	1.10	9.8		
Minimum	-0.35	-1.9	-0.35	-3.1		

Table 12 - Average Maximum Drag Coefficients (Individual)

Record No.	Force Link No.	u _{FM} = 70 mph			u _{FM} = 90 mph		
		P(>X) x 10 ³	g	C _d	P(>X) x 10 ³	g	C _d
6-6	9	2.19	9.6	3.63	1.70	10.2	3.81
	10	2.61	5.4	1.58	2.03	5.6	1.60
	11	2.88	7.8	2.66	2.24	8.3	2.77
	12	3.22	6.0	2.71	2.51	6.2	2.77
8-2	9	0.91	6.1	2.43	0.71	6.4	2.50
	9	1.60	6.2	4.61	1.24	6.5	4.78
9-1	10	0.96	6.3	2.40	0.75	6.8	2.50
	11	1.16	7.3	2.78	0.90	7.9	2.93
	12	1.20	7.8	3.50	0.93	8.4	3.70
	9	0.64	6.4	3.89	0.50	6.7	4.00
9-2	10	0.65	7.8	2.88	0.51	8.2	2.96
	11	0.84	5.2	2.48	0.66	5.4	2.54
	12	0.92	6.1	3.31	0.72	6.5	3.45
	9	1.02	6.5	2.91	0.79	6.9	3.03
23-4	10	1.00	8.3	1.83	0.78	8.9	1.92
	11	0.98	7.2	2.43	0.76	7.7	2.52
	12	1.07	6.2	2.33	0.83	6.7	2.47
	9	1.12	7.2	4.59	0.87	7.8	4.85
29-2	10	0.83	6.6	1.87	0.65	7.0	1.95
	11	0.58	4.2	2.02	0.45	4.4	2.06
	12	0.62	4.7	1.91	0.48	4.9	1.96

Table 13 - Average Maximum Drag Coefficients (Combined)

Record No.	Force Link Combination	$u_{FM} = 70 \text{ mph}$			$u_{FM} = 90 \text{ mph}$		
		$P(>X)$ $\times 10^3$	g	C_d	$P(>X)$ $\times 10^3$	g	C_d
6-6	9 to 12	1.96	7.0	2.25	1.52	7.2	2.29
8-2	"	1.70	5.7	1.94	1.32	5.9	1.97
9-1	"	1.47	16.0	5.55	1.15	17.2	5.89
9-2	"	1.05	7.9	3.42	0.82	8.2	3.50
23-4	"	1.70	11.1	2.96	1.32	11.3	3.00
29-2	"	1.00	7.5	2.86	0.77	7.9	2.96

Because the ends of the mobile home are cantilevered from the foundation assemblies, the dynamic response at the front and rear assemblies can be expected to be larger than for the intermediate assemblies. This is in agreement with the results for individual force links presented in Table 12. The following values were obtained by averaging the peak drag coefficients for force link Nos. 9 and 12.

Basic Wind Speed (mph)	C_d^{\wedge}	\hat{p} (psf)
70	3.21	17.3
90	3.30	29.4

Estimates of peak factors and average maximum lift coefficients are presented in Table 14. With the exception of Record Nos. 8-2 and 9-1, a mean lift coefficient of 0.90 has been assumed in estimating the peak value. As with the estimates of drag coefficients, the lift coefficients for Record No. 9-1 are questionable. Discounting this record, the following average maximum lift coefficients and equivalent static loads are considered to be representative of the load conditions for the individual foundation assemblies, no distinction being made between skirted and unskirted configurations.

Basic Wind Speed (mph)	C_l^{\wedge}	\hat{p} (psf)
70	2.40	13.0
90	2.50	22.3

For the case of extreme uplift, it is assumed that failure of the windward skirting can occur or that the area under an unskirted mobile home can become blocked with debris during a severe storm, thus subjecting the underside of the mobile home to positive pressure. The intensity of this positive or uplift pressure will, of course, depend upon the size of opening in the windward skirting or the degree of debris blockage, but it is reasonable to assume that pressures at least as large as the mean pressure on the windward face at ground level can develop. Figure 5.8 suggests a mean pressure coefficient of 0.6. When added to the average maximum uplift loads determined above, the extreme uplift loads for basic wind speeds of 70 and 90 mph are 16.2 and 27.6 psf (775 and 1320 N/m²), respectively.

6.6 Design Wind Loads - The surface pressures acting on localized areas (see Table 11) and the drag and lift loads determined in Sections 6.4 and 6.5 are tabulated as design loads for standard and hurricane wind zones in Table 15 with adjustments being made for working stresses as will be discussed later in this section. The areas over which the loads act are shown in Figure 6.3. These design loads, expressed in terms of wind pressure acting on projected surface areas, represent the average maximum values to be expected for the criteria and assumptions discussed in Sections 6.1 to 6.3.

Table 14 - Average Maximum Lift Coefficients

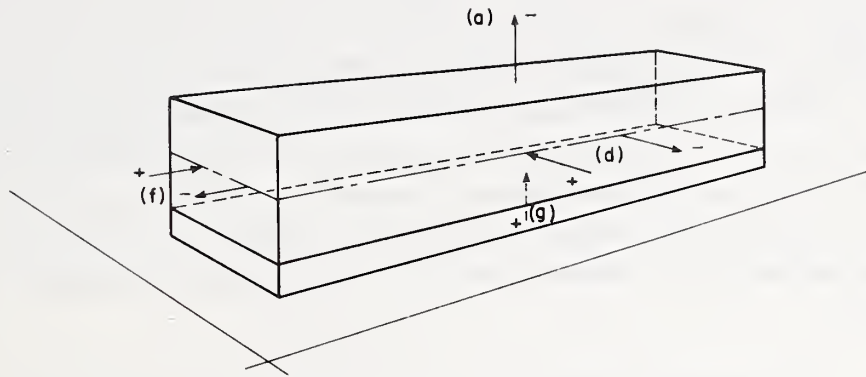
Record No.	Force Link Combination	u _{FM} = 70 mph			u _{FM} = 90 mph		
		P(>X) x 10 ³	g	C _l	P(>X) x 10 ³	g	C _l
8-2	1,2	0.78	7.3	2.36	0.61	7.7	2.45
	5,6	1.25	8.1	2.67	0.97	8.6	2.78
8-5	1,2,5,6	0.99	8.0	2.38	0.77	8.4	2.46
	1,2	1.02	4.2	2.29	0.79	4.5	2.39
	5,6	1.29	5.3	2.38	1.00	5.5	2.44
	1,2,5,6	1.38	3.4	1.85	1.07	3.5	1.88
9-1	1,2	0.96	7.9	4.03	0.75	8.3	4.18
	5,6	1.42	8.2	3.12	1.10	8.7	3.26
9-2	1,2,5,6	1.09	8.8	3.52	0.85	9.4	3.70
	1,2	0.53	5.9	2.43	0.42	6.2	2.51
23-4	5,6	0.79	8.0	2.34	0.61	8.3	2.39
	1,2,5,6	0.56	8.2	2.46	0.43	8.6	2.53
	1,2	0.75	8.1	2.44	0.59	8.5	2.52
	5,6	1.09	8.0	2.42	0.85	8.4	2.50
29-2	1,2,5,6	1.04	7.4	2.16	0.81	7.8	2.23
	1,2	0.52	6.9	2.35	0.41	7.2	2.41
	5,6	1.09	8.1	2.36	0.85	8.6	2.45
	1,2,5,6	0.65	6.6	1.96	0.50	7.0	2.02

Table 15 - Recommended Design Loads for Standard and Hurricane Wind Zones

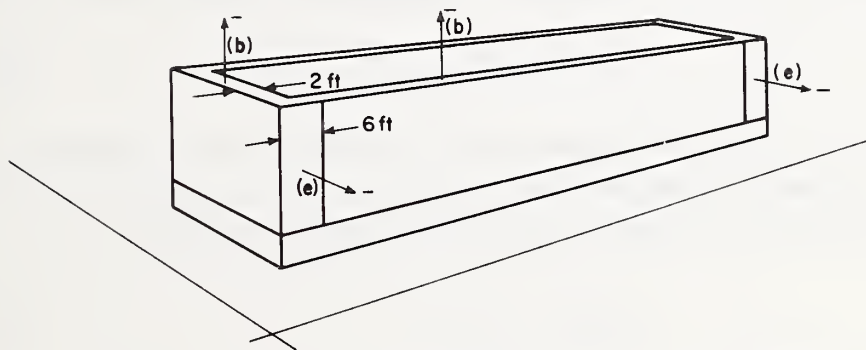
	<u>STANDARD</u>	<u>HURRICANE</u>
ROOF		
(a) Design of trusses, roof membrane and fasteners (except as noted below)	-23 (-18)	-40 (-30)
(b) Roof membrane and fasteners on strip 2 feet wide extending around perimeter of roof	-36	-61
(c) Overhangs (net uplift)	45	77
SIDE WALLS		
(d) Design of studs, doors, windows, exterior wall covering and fasteners (except as noted below)	15	26
(e) Exterior wall covering and fasteners at ends of sidewalls on vertical strips 6 feet wide	-12	-21
	-24	-40
END WALLS		
(f) Design of studs, windows, exterior wall covering and fasteners	15	26
FLOOR		
(g) Design of joists, floor panels and fasteners (occupancy load excluded)	-32 (-24)	-56 (-40)
	6	10
DRAG LOAD		
Load acting on horizontally projected area of structure and used for design of structural subsystems to resist racking	17 (15)	29 (24)
(h) End sections (1/4 length)	15	24
(j) Central section (1/2 length)		
UPLIFT LOAD(k)		
Load acting vertically upward on plan area of structure and used for design of structural subsystems to resist bending in vertical plane	16	28

Notes:

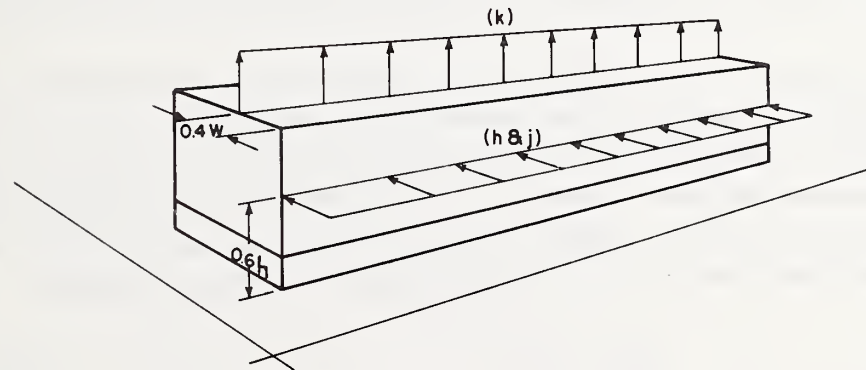
1. All pressures in pounds per square foot.
2. Negative sign indicates pressures acting outward.
3. Loads indicated by () are to be applied to double-wide units only.



ROOF, WALLS AND FLOOR



ROOF PERIMETER AND CORNERS OF WALLS



DRAG AND UPLIFT

Fig. 6.3 - Loading Diagrams for Recommended Design Loads Listed in Table 15

The loads presented in Table 15 are based on measurements obtained from a single-wide mobile home and cannot, in all cases, be directly applied with confidence to double-wide units. Roof geometry and the width-to-depth ratio of a double-wide unit can be expected to substantially reduce the loads acting on tributary roof areas and on end walls. In addition, the dynamic response of the cantilevered end sections will be attenuated because of the increased width. Therefore, certain design loads in Table 15 for double-wide units are based on the provisions of Ref. 14. This includes the provision for exterior wall covering and fasteners at the ends of side walls on vertical strips 6 ft (1.8 m) wide since no reliable measurements for this case were obtained in the full-scale study of the single-wide unit. Unless otherwise indicated, the tabulated loads are to be applied to both single- and double-wide mobile homes.

To account for the inherent randomness and uncertainties in the various design parameters, load and/or resistance factors are applied to some appropriate limit state equation

$$\phi R \geq \gamma_d D + \gamma_w W \quad (25)$$

in which ϕR , $\gamma_d D$ and $\gamma_w W$ are the factored ultimate resistance, dead load and wind load, respectively. Alternatively and equivalently, this equation may be reduced to the working stress design relationship that many building codes currently prescribe:

$$R_{\text{allow}} \geq D + W \quad (26)$$

in which R is an allowable stress or resistance. Since dead load generally constitutes a stabilizing force, it may be neglected in the limit state equation for wind-critical members.

The resistance factor ϕ or allowable stress depends upon the coefficient of variation of resistance V_R and some measure of the required design reliability. For wood construction, V_R ranges from 0.16 for tension and flexure to 0.28 for compression perpendicular to grain [24], with a representative value of about 0.2. The reliability may be measured by the safety index which is about 3 for typical steel and concrete construction [25]. This information is utilized to obtain the following working stress design equation:

$$R_{\text{UBC}} = 0.8 W \quad (27)$$

in which R_{UBC} is the resistance based on allowable stresses for wood specified by the Uniform Building Code [26] and W is the wind load determined using the methods outlined in this chapter. The wind loads listed in Table 15 have been reduced by the factor 0.8 and are intended to be used directly with the requirements (including allowed increases in working stresses for wind) of the various standards listed in Sec. 280.304 "Materials" of the federal Mobile Home Construction and Safety Standards [5].

The reduction factor of 0.8 has not been applied to the average maximum drag and lift loads determined in Section 6.5. To establish an appropriate working stress design equation for tie-down hardware, a representative value of the coefficient of variation of resistance, V_R , is required. The ultimate resistance of tie-down components can be expected to decrease with the repeated application of extreme loads and this should be accounted for in the experimental determination of V_R .

7. LOAD-DEFLECTION STUDIES

Upon completion of the first phase of the study concerned with pressure and force measurements (presented in Sections 2 through 6) a second phase, involving the measurement of deflections of the mobile home superstructure and the foundation system under known applied loads, was conducted. The primary purpose was to obtain estimates of stiffness in the racking and lateral bending modes and to measure the forces in certain components of the tie-down system. Finally, modes of failure were established under load conditions which were a reasonable approximation of actual wind loads.

Relevant to the load-deflection measurements and the observed failure modes are the following construction details of the specimen mobile home. Wall studs are 1 1/2 by 2 1/2 in (38 by 64 mm) actual dimension on 16-in (406-mm) centers and plates and headers are 1 by 3 nominal. The roof system consists of standard bowed trusses on 16-in centers, nailed into the top wall plate through the 1/2-in (13-mm) fiberboard ceiling. The roof membrane is 26 gauge galvanized steel sheet attached by staples to a header nailed into the ends of the roof trusses. With the exception of the hallway, which has been retrofitted with 5/16-in (8mm) gypsum board, interior paneling is 5/32-in (4-mm) plywood stapled to the wall studs. The floor system consists of 5/8-in (16-mm) particle board supported on 2 by 4 nominal joists. Bar joists on 48-in (1.22-m) centers and 10-in junior beams make up the underframe as is shown in Figure 2.4. Exterior cladding is 22 gauge aluminum sheet attached to let-in longitudinal nailing strips by screws on 8-in (203-mm) centers.

7.1 Experimental Setup - The load-deflection tests were conducted at the field test site using the same support frame and drag and lift instrumentation described in Section 2.3. Based upon the pressure and load measurements previously described and the fact that the overall response of the mobile home is quasi-static in nature, it was decided that drag loads could best be simulated by the application of equivalent static line loads applied to the "windward" wall. To apply these loads, the following scheme was used. Four equally-spaced booms were installed as shown in Figure 7.1, the outer ends being restrained by vertical cables attached to earth anchors and the inner ends bearing directly on the main support frame at points in line with the steel beam and column assemblies of the foundation system. Tension rods, connected to the booms and passing through the mobile home, were attached to a system of whiffletrees as shown in Figure 7.1. Tension was applied by hydraulic rams and the applied loads were measured at the centers of the whiffletrees by load cells installed on the ends of the tension rods. Two rams were placed back-to-back in the upper tension rods to accommodate deflections up to 10 inches (250 mm). Views of the booms and whiffletrees are shown in Figures 7.2 and 7.3. In addition to the lateral line loads applied to the "windward" wall, a vertical line load was applied to the "windward" edge of the roof system by means of hydraulic rams and pipe columns bearing on the left-hand longitudinal member of the main support frame. The load was distributed to the roof trusses through a system of eight whiffletrees, three of which are shown in Figure 7.4. Ideally, the uplift load should have been applied directly to the roof membrane by means of

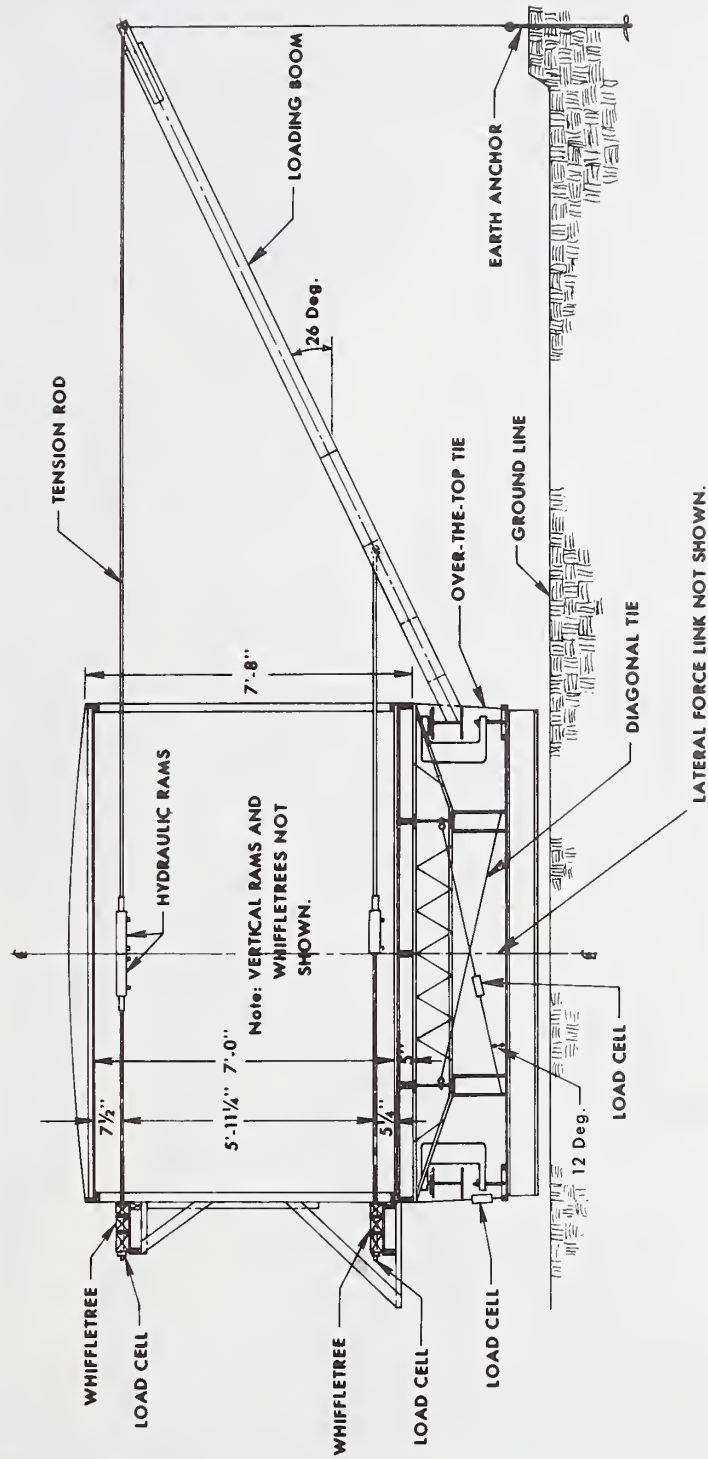


Fig. 7.1 - Loading Scheme for Load-Deflection Studies



Fig. 7.2 - View Showing Booms and Tension Rods



Fig. 7.3 - View Showing Whiffletrees on "Windward" Side



Fig. 7.4 - View of Whiffletree System for Applying Uplift Forces

air bags, but this would have required removal of the ceiling panels and some of the partition walls, thereby reducing the stiffness of the mobile home superstructure. In view of the fact that the roof membrane acts as a true membrane, being secured only at the perimeter to headers which are in turn nailed into the ends of the roof trusses, the uplift line load applied directly to the ends of the roof trusses was deemed to be an acceptable approximation of actual wind loading. No corresponding line load was applied to the "leeward" edge of the roof system as this would have required penetrating all of the partition walls with the wiffletrees. This omission was not considered to be significant because the intensities of both the mean and fluctuating pressures are much less on the leeward half of the roof.

The rams were controlled by a multiple-channel hydraulic load maintainer which allowed the load increments to be simultaneously applied to each wiffletree while maintaining a constant relative load intensity. The force links between the foundation system and the main support frame allowed a direct comparison between applied loads and reactions. Load cells were installed in the diagonal and over-the-top tie-downs at load point No. 3 (see Figures 7.1 and 7.5). Horizontal deflections were measured by means of displacement transducers mounted on supports along the leeward wall. These transducer supports were isolated from the mobile home and the main support frame and the measured deflections therefore included contributions from both the mobile home proper and the foundation system. Vertical displacements of the floor system were measured at selected points along the "windward" wall so that apparent horizontal deflections due to rotation of the mobile home could be accounted for. Two displacement transducers mounted on telescoping supports provided a measure of diagonal strain in a vertical plane at midlength of the mobile home.

The digital data acquisition system used in this phase of the study can multiplex up to 200 low-level signal inputs at a rate of 10 channels per second and averages each sample over a 16 msec period to improve the signal to noise ratio. Maximum error due to transducer drift, nonlinearity and A-D conversion was approximately ± 1 percent.

7.2 Load-Deflection Measurements and Failure Modes - All loads were applied in increments and deflections were in most cases recorded from 1 to 2 minutes after the load increment had been applied. The line loads were proportioned so as to approximate the pressure distributions suggested by Figure 5.8 and the load intensities were calculated for assumed basic wind speeds using the drag and lift coefficients presented in Section 6.5. In the following discussion, reference is made to Figure 7.5 which indicates the locations of the booms (load points 1 to 4) and the sections at which horizontal deflections were measured at the ceiling and floor planes (designated as 1T, 1B, 2T, etc.) Unless otherwise noted, horizontal deflections at the ceiling plane are relative to the floor plane and have been corrected for rotation of the floor system. The loads plotted against deflections at the floor plane correspond to the total shear per unit length, i.e., the sum of the top and bottom horizontal line loads. In addition to direct measurement of horizontal displacements, extension and contraction of the interior diagonals of a cross-section through the mobile home were measured at section 3 (see Figure 7.5). In the following discussion Diagonal "A"

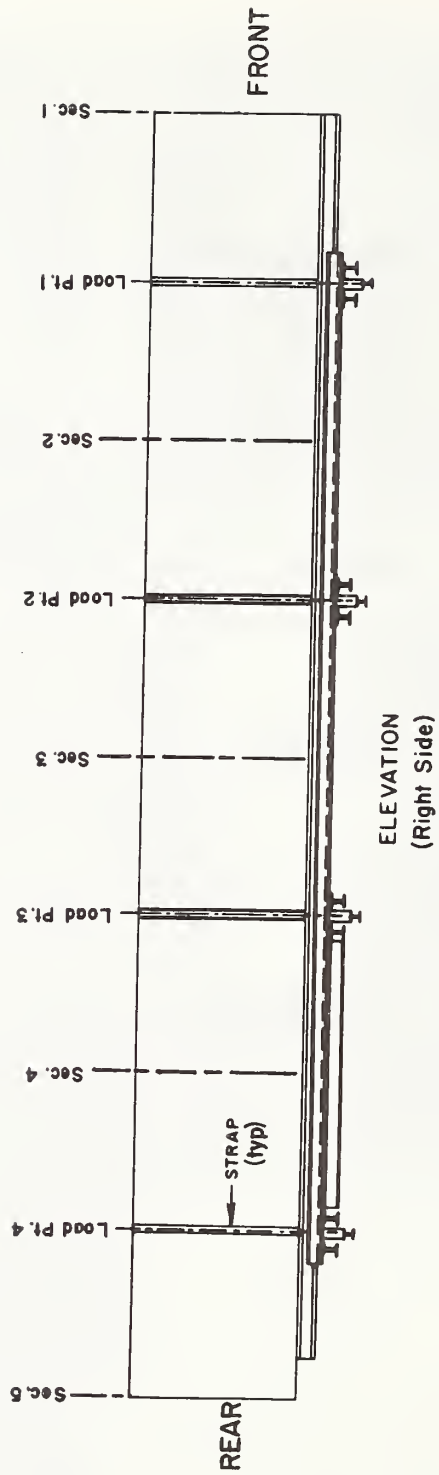


Fig. 7.5 - Locations of Load Points and Deflection Measurement Sections

refers to the line extending from the floor at the windward wall to the ceiling at the leeward wall and vice versa for Diagonal "B".

Load Case No. 1 - Line loads were applied to the windward wall only and only one boom-whiffletree combination was loaded at a given time. The measured absolute deflections for loads applied sequentially to load points 1 through 4 are plotted in Figure 7.6. Load intensities are listed on the figure and correspond approximately to the drag forces associated with a basic wind speed of 50 mph (22 m/s). The loads were applied in a single increment.

As expected, the forward portion of the mobile home superstructure exhibits less stiffness than do the central and rear portions where the transverse partition walls are located. It is also apparent from Figure 7.6 that the indicated stiffness of the foundation system at load point No. 4 is substantially less than at the other three load points. This is believed to be due to slack in the connections between the mobile home floor system and the underframe (bar joists and stringers) since the foundation assemblies were all identical in construction and all tie-down cables were given the same preload (approximately 100 lbf or 450 N) prior to testing. Also note that the main support frame does not transfer any horizontal loads to the ground and does not, therefore, contribute to horizontal deflections.

Load Case No. 2 - Line loads were applied to the windward wall at all load points simultaneously and, as with Load Case No. 1, corresponded to a basic wind speed of approximately 50 mph (22 m/s). The relative horizontal deflections are plotted in Figure 7.7. Note that although the load vs. deflection relationships at both the floor and ceiling planes are nonlinear, the foundation system responds directly to load while the superstructure requires an initial racking load of approximately 10 lbf/ft (15 N/m) before the "leeward" wall on which the deflections were measured becomes fully mobilized.

Load Case No. 3 - This load case included horizontal line loads acting on the windward wall to simulate drag and a vertical line load acting at the leading edge of the roof to simulate uplift. The maximum load attained during the test corresponds to a basic wind speed of approximately 70 mph (31 m/s). The horizontal loads and deflections are plotted in Figure 7.8. The vertical line loads for this load case were as follows.

<u>Increment Number</u>	<u>Load Intensity</u>
1	21 lbf/ft
2	44
3	63
4	82
5	105
6	120
7	106
8	61
9	21

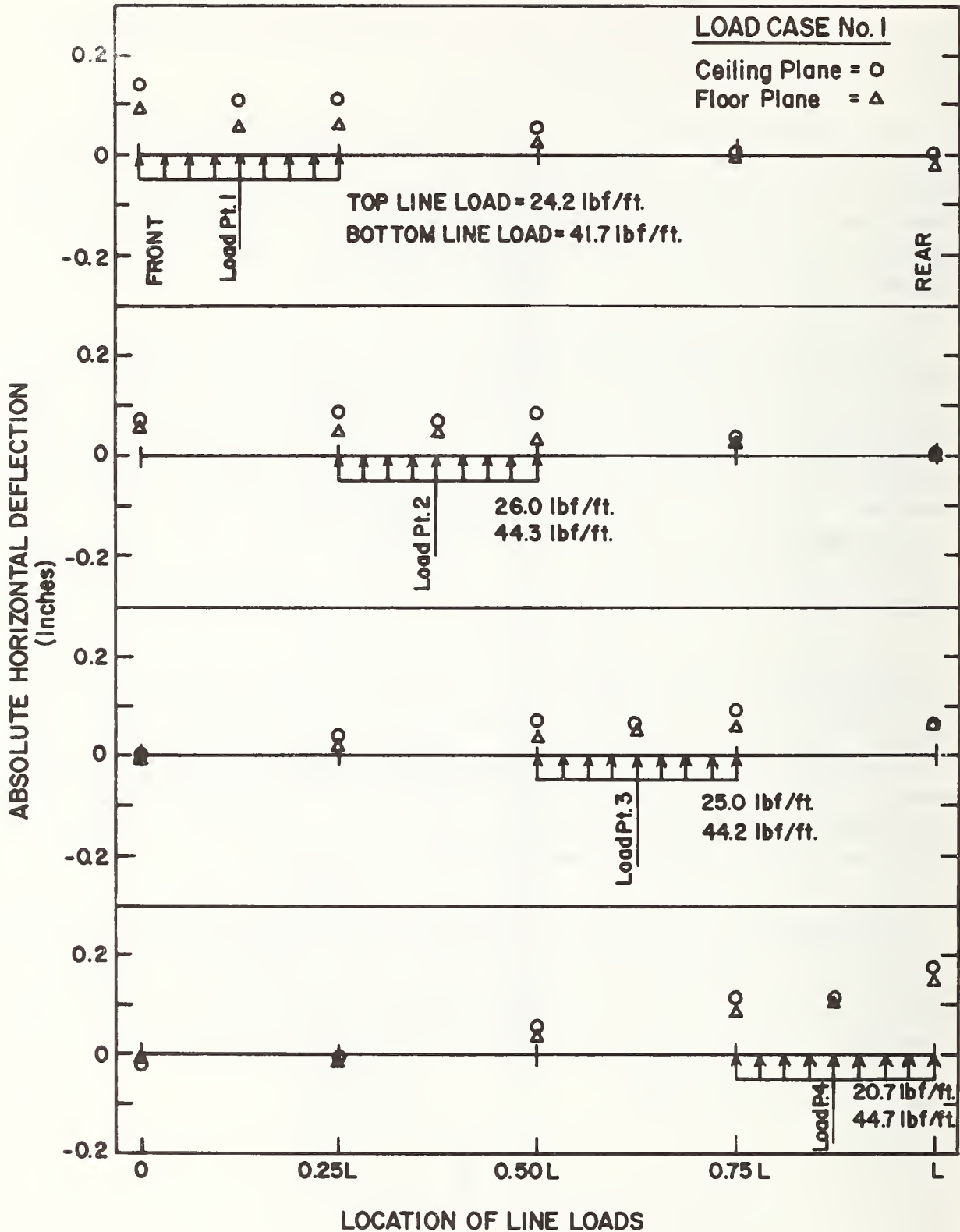


Fig. 7.6 - Load versus Deflection for Load Case No. 1

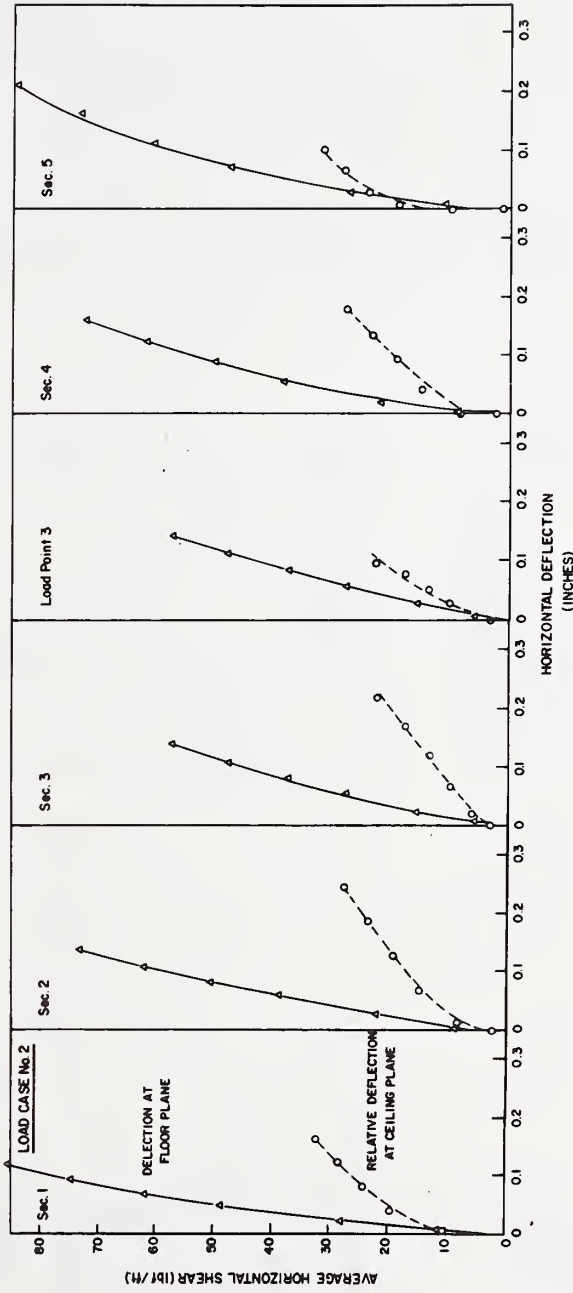


Fig. 7.7 - Load versus Deflection for Load Case No. 2

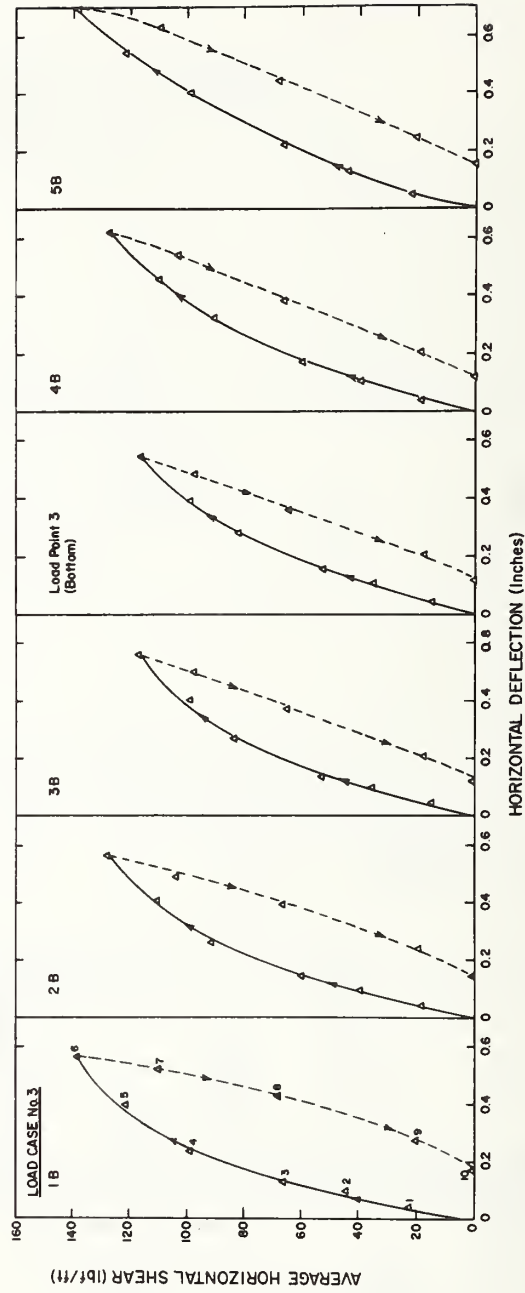
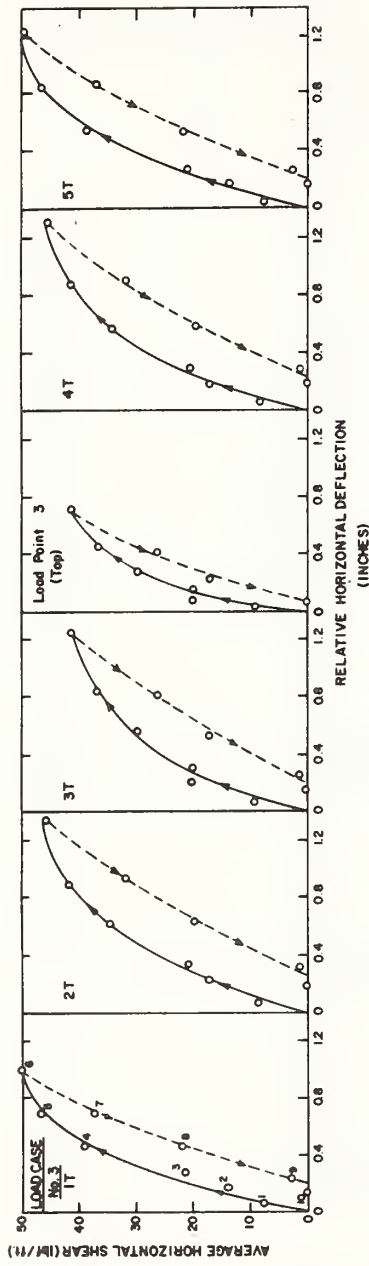


Fig. 7.8 - Load versus Deflection for Load Case No. 3

It is important to note that the deflections plotted for the ceiling plane in Figure 7.8, while being referenced to the floor plane, have not been corrected for rotation of the floor plane and thus do not reflect the true stiffness of the superstructure under the loads described above. The rotations for the load tests involving application of a vertical line load were in all cases large enough to preclude reliable corrections of the measured horizontal displacements at the ceiling plane. To obtain an estimate of the superstructure stiffness, reference is made to Figure 7.9 in which the diagonal displacements have been plotted against the intensity of the upper horizontal line load. Based on simple geometric relationships, the true relative horizontal displacements between the floor and ceiling planes are approximately 17 percent greater than the measured diagonal displacements.

Load Case No. 4 - This load combination was identical to Load Case No. 3 and was applied with the intention of establishing the ultimate load capacity of the mobile home superstructure under combined lift and drag loading. Also of interest was the failure mode of the mobile home underframe to which the diagonal ties were attached. However, the test had to be terminated at a load level corresponding to a basic wind speed of approximately 90 mph (40 m/s) because the alignment of the vertical rams could not be maintained under the large rotation and lateral deflections encountered. The test was repeated after the over-the-top tie-downs had been preloaded to approximately 650 lbf (2.9 kN). Initial failure of the superstructure occurred in the roof-to-wall connection on the windward side between load points 1 and 2 and was followed very shortly by an identical failure between load points 3 and 4 with the same loads applied. Load levels at the time of failure were as follows.

<u>Load Point</u>	<u>Load Intensity</u>
1 & 4 Top horizontal	95 lbf/ft
" Bottom "	164
2 & 3 Top "	73
Bottom "	143
Vertical	255

The region of initial failure with loads still applied is shown in Figure 7.10. In Figure 7.11 the roof membrane has been peeled back and the fascia strip removed to expose the header and wall plate. Separation of the header from the plate was approximately 2 in (50 mm) with the uplift loading of 255 lbf/ft (3.7 kN/m) applied. The failure was progressive and extended over the region between the load spreaders under the tie-down cables. Load-deflection data for the ceiling plane could not be plotted with accuracy because of the large rotations. As with load case No. 3, reference is made to the measured diagonal displacements for an estimate of stiffness of the central portion of the superstructure. The results for load case No. 4 are presented in Figure 7.12, the final increment of displacement being measured after failure of the roof-to-wall connection. Although the relative horizontal deflection at the ceiling plane for this load level averaged 0.8 in (20 mm), the partition walls and end walls showed no significant signs of distress.

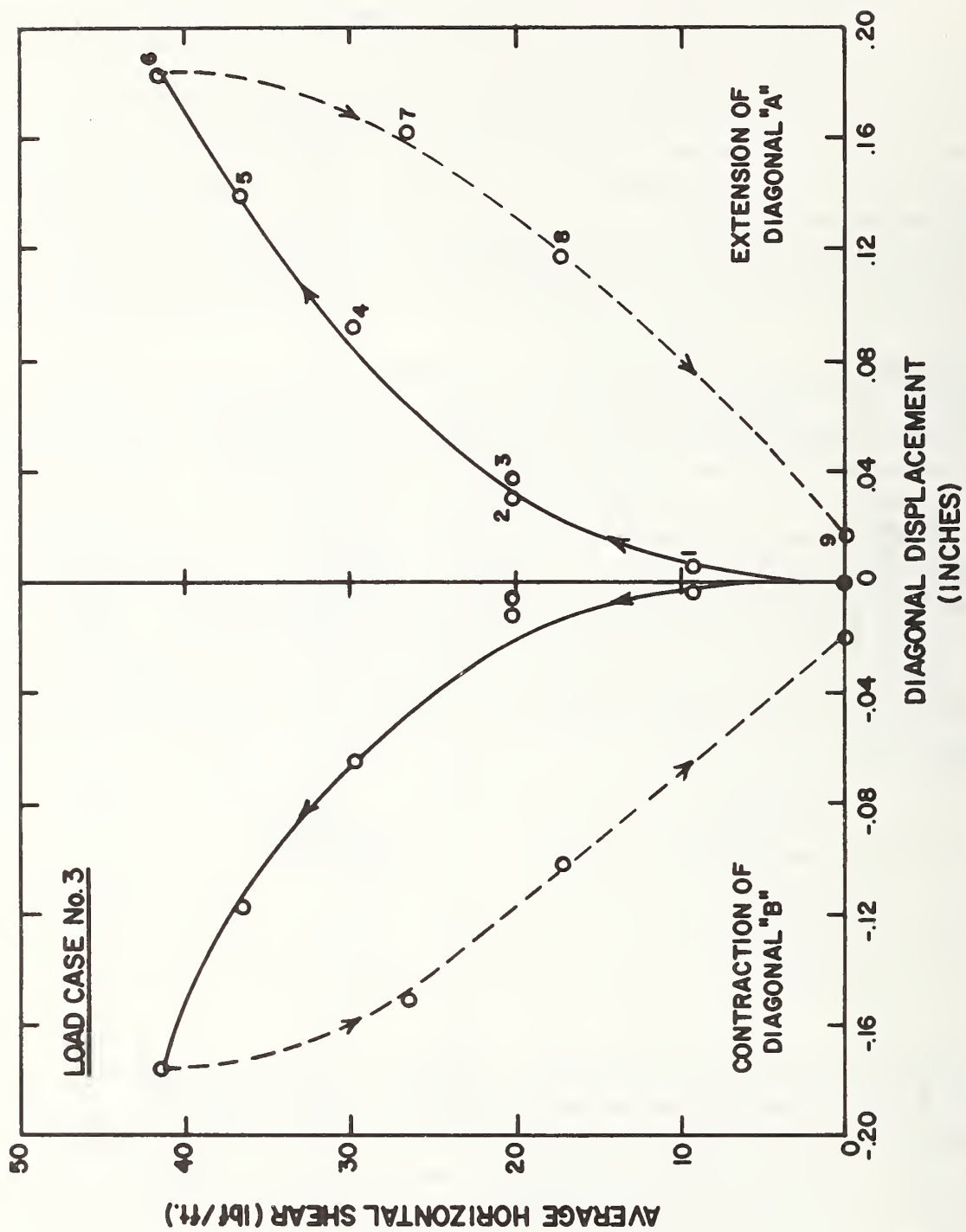


Fig. 7.9 - Load versus Diagonal Displacement for Load Case No. 3

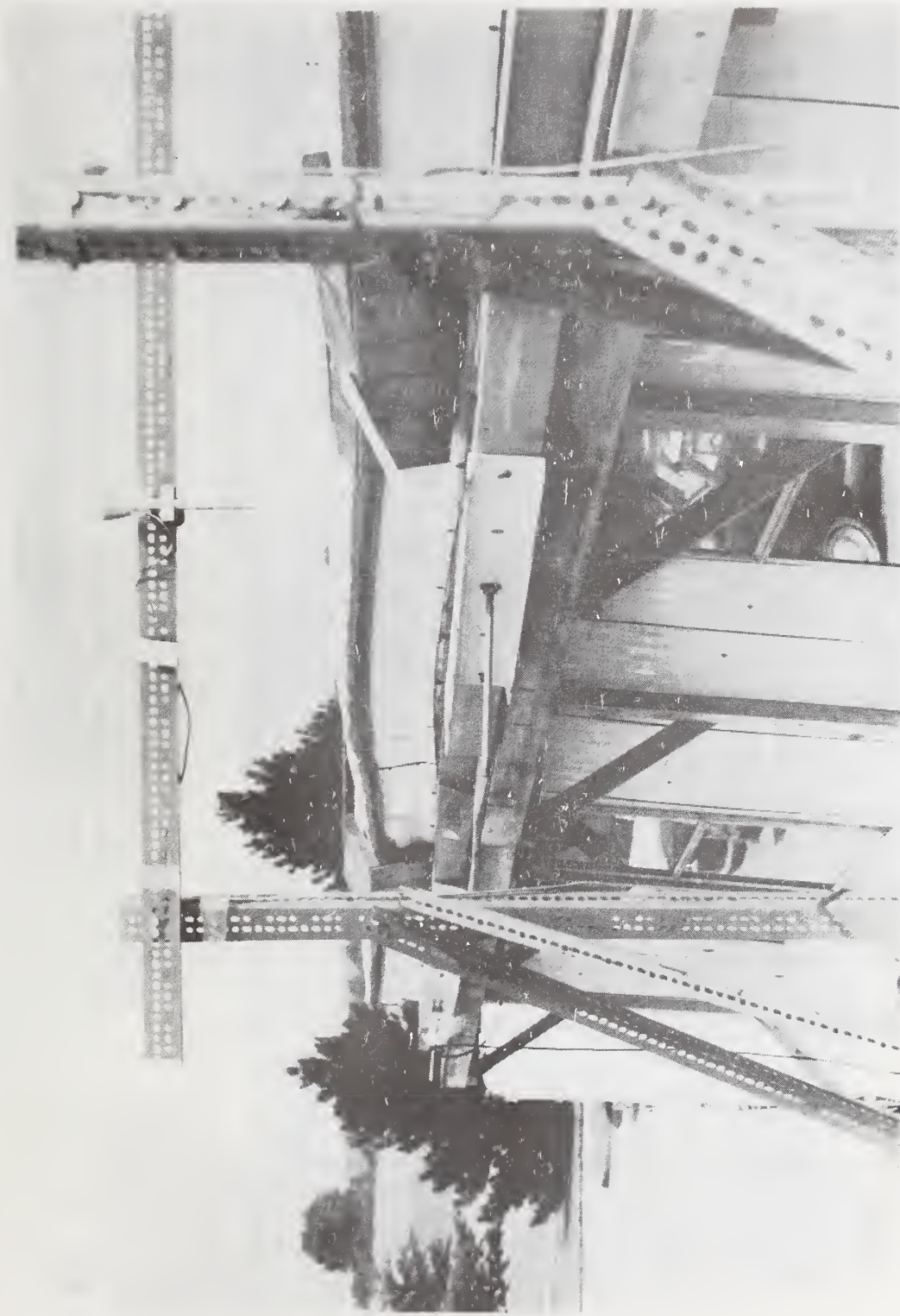


Fig. 7.10 - View of Failure in Roof-to-Wall Connection (load applied)

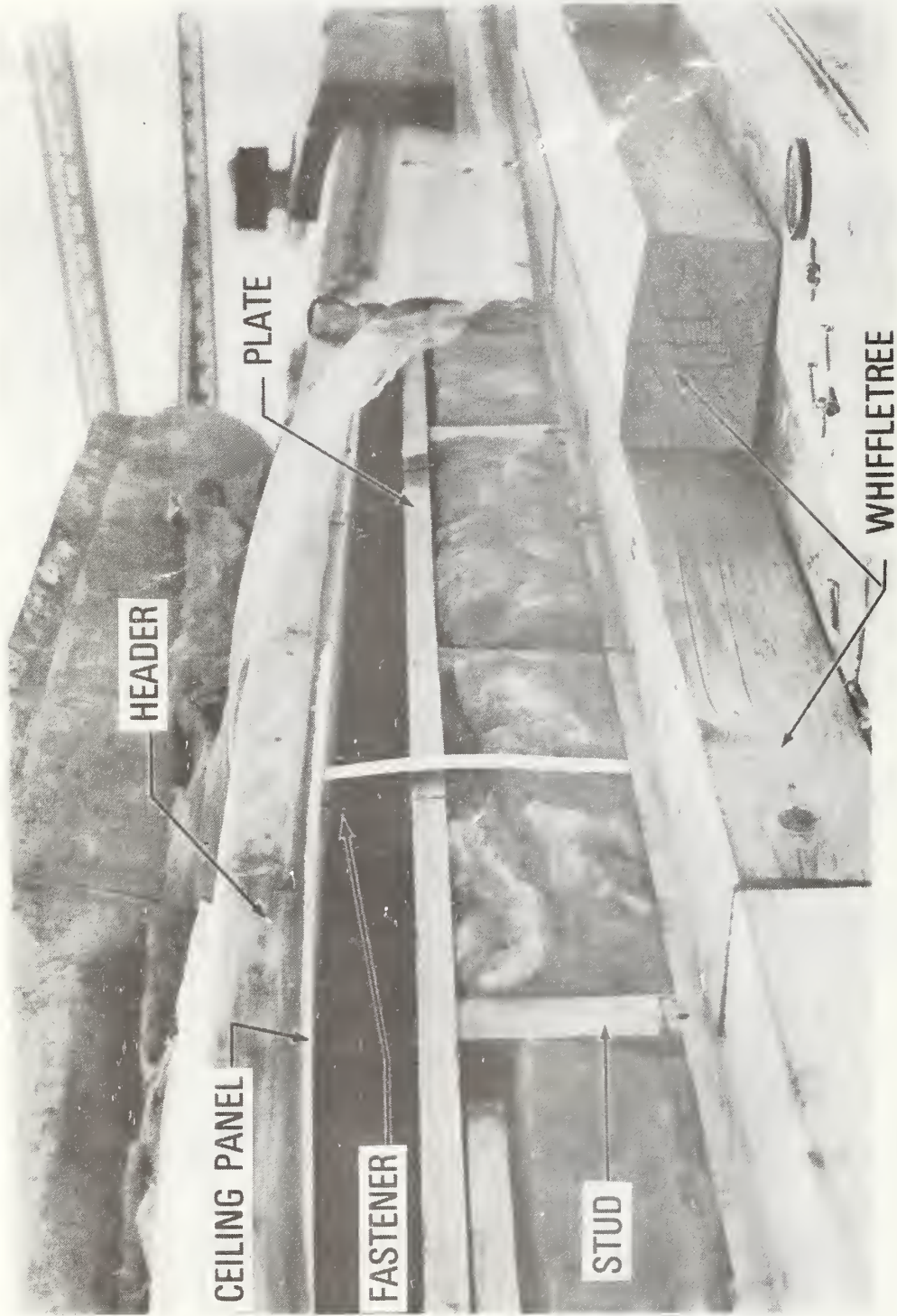


Fig. 7.11 - View of Top Plate and Header (facia strip and roof membrane removed)

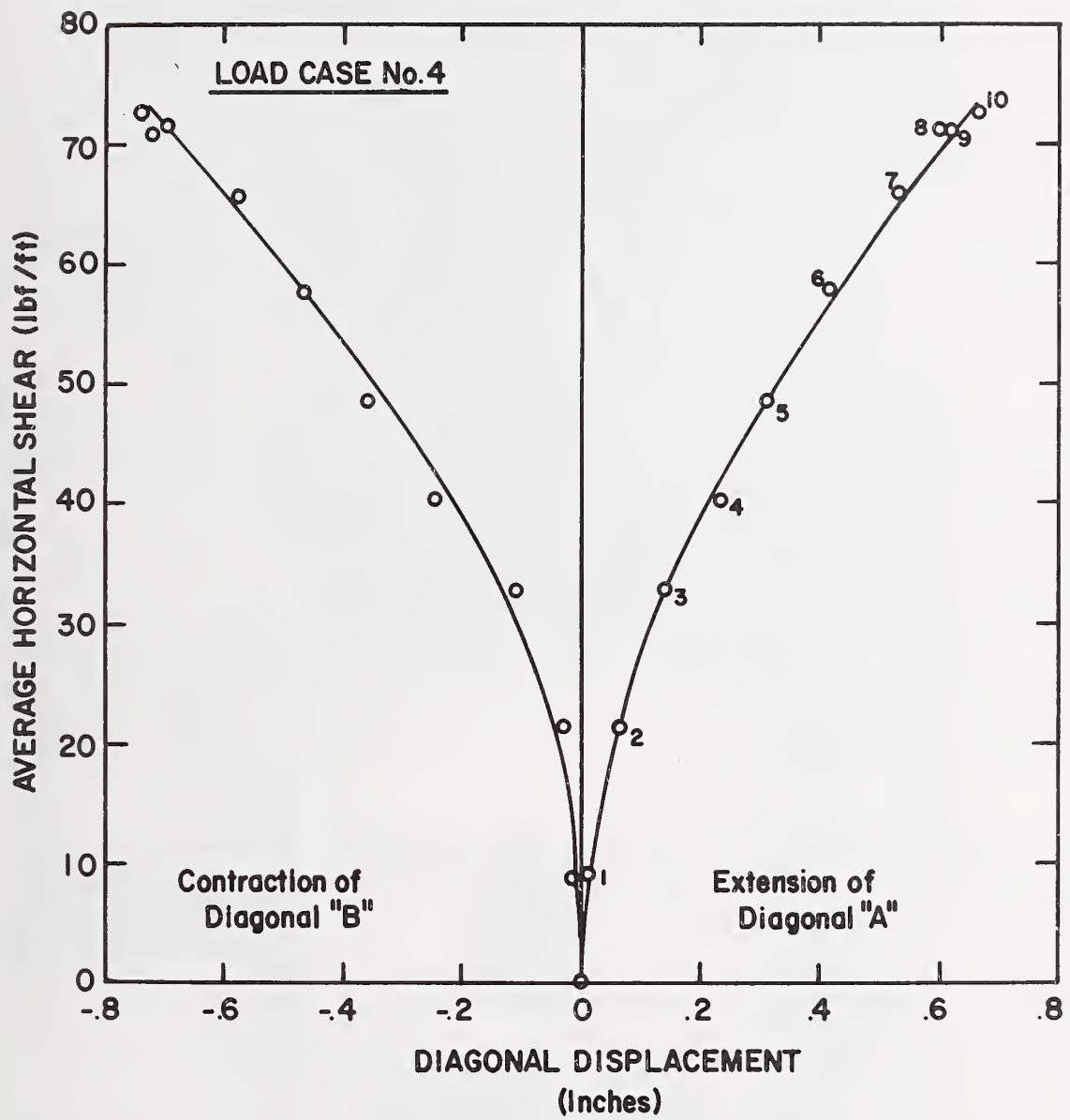


Fig. 7.12 - Load versus Diagonal Displacement for Load Case No. 4

First signs of distress in the mobile home underframe for Load Case No. 4 were observed at load point No. 2 when a weld failed in one of the bar joists, allowing the bottom chord to buckle. This occurred when the sum of the horizontal line loads (applied drag) was approximately 200 lbf/ft (2.9 kN/m). At this same load level, initial yielding was observed in the web of the longitudinal stringer at load point No. 1 where the diagonal tie was connected to the web by means of an eyebolt. No additional failures were observed in the underframe during application of the remaining load increments. However, splitting of the headers in the floor system was observed at points where the bar joists of the underframe were attached by lag screws. A view of the yield lines in the web of the longitudinal stringer at load point No. 1 is shown in Figure 7.13. A short section of steel channel was used at each load point to distribute the load at the eyebolt. The maximum drag load applied to load point No. 1 was 260 lbf/ft (3.8 kN/m).

Load Case No. 5 - This final loading configuration applied to the mobile home consisted only of a horizontal line load acting along the top of the windward wall. The purpose of the test was to examine the failure mechanism of the partition walls and end walls in a simple racking mode. Prior to conducting the test, the system of rams and whiffletrees for applying the vertical line load was removed and 2 x 4 cleats were placed against the inside of the windward wall at the ceiling and were nailed into the bottom chords of the roof trusses. This allowed the roof-to-wall connection, which had been damaged in the previous test, to transfer the upper horizontal line load into the roof trusses. A preload of approximately 500 lbs (2.2 kN) was applied to the over-the-top tie-downs to prevent excessive rotation of the mobile home.

Load-deflection diagrams for points along the leeward wall at the ceiling plane are plotted in Figure 7.14. The deflections are relative to the floor plane and have been corrected for rotation of the mobile home floor system.

Movement of the end walls and partition walls relative to the floor and ceiling was monitored during application of the load increments. Following the application of load increment No. 5 (see Figure 7.14) this relative movement or "slip" averaged 0.1 in (2.5 mm) at both the floor and ceiling for all walls. No significant change was observed for the end walls at load increment No. 7, but averaged about 0.2 in (5 mm) for the partition walls. Vertical separation of the partition walls from the floor became significant during application of load increment No. 8, averaging 0.5 in (13 mm). During the application of load increment No. 9, portions of the interior paneling separated from the front end wall and from most of the partition walls. Also, the exterior sheet on the front end wall developed a pronounced buckle as is shown in Figure 7.15. This was the highest load level attained during the test, it being obvious that no additional resistance to racking could be developed in the superstructure. The separation of the partition walls from the floor averaged 2 in (50 mm) along the hallway and slip averaged 0.4 in (10 mm) at both floor and ceiling. No separation of the end walls from the floor or ceiling was observed. However, the slip after application of load increment No. 9



Fig. 7.13 - Yield Lines in Web of Underframe Stringer at Load Point No. 1

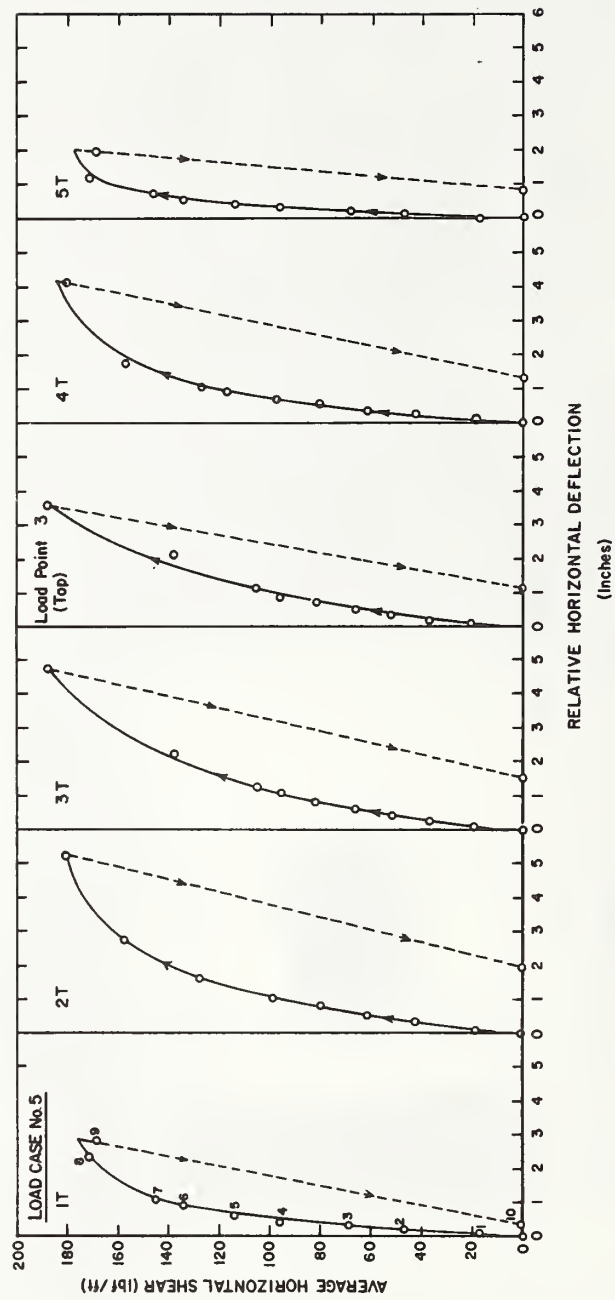


Fig. 7.14 - Load versus Deflection for Load Case No. 5

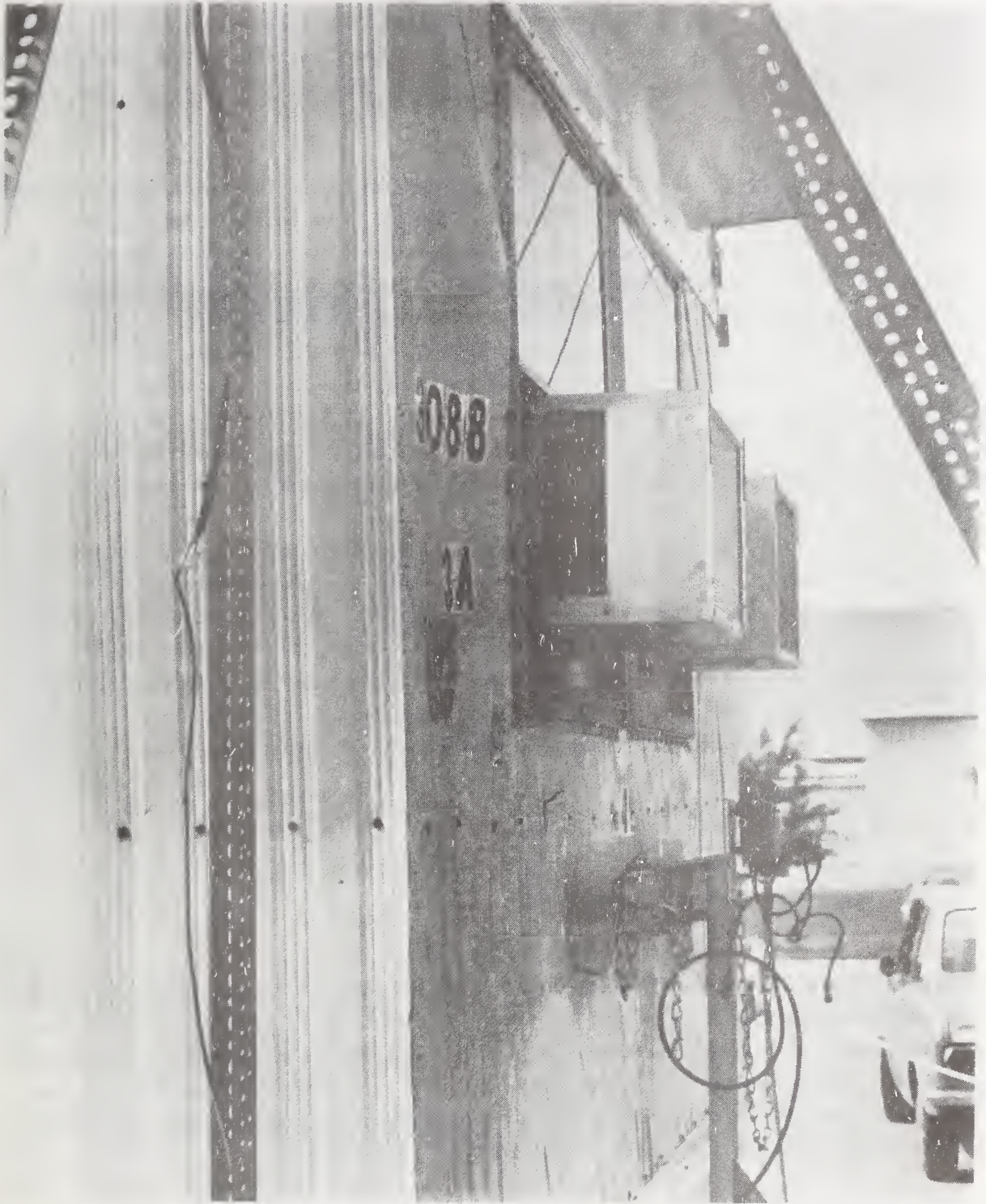


Fig. 7.15 - Condition of Front End Wall at Maximum Load

averaged 0.2 in (5 mm). Diagonal displacements at Section 3 for Load Case No. 5 are plotted against the horizontal load intensity in Figure 7.16. The range of the displacement transducers was exceeded with the application of load increment No. 7 and the remainder of the plot is speculative.

7.3 Stiffness Coefficients - There are several accepted procedures for quantifying stiffness coefficients for nonlinear load-deflection plots. For wood frame construction the load per unit length of structure corresponding to a net deflection of 0.1 in (2.54 mm) has been used [27]. Relevant to any definition of stiffness is the load duration (particularly for wood frame construction) and the anticipated range of structural deformation. The deflections measured in this study correspond to load durations that are substantially longer than those associated with peak wind gusts and tend, therefore, to overestimate the deflections due to actual load fluctuations. However, this consideration is offset somewhat by the fact that deflection limitations usually relate to service conditions rather than to ultimate load conditions and the associated short load durations.

It is usual for codes and standards to specify deflection limitations as fractions of span or length of member, L, typical limitations being L/180 for simple spans and L/90 for cantilevers. For a mobile home of typical dimensions the range of allowable deflections using these criteria would be approximately 0.5 to 1.0 in (13 to 25 mm) for the superstructure. The following stiffness coefficients are proposed as best representing the load-deflection relationships presented in Section 7.2 for the foundation configuration used in this study and for the range of deflections relevant to service conditions.

Racking of end walls	170 (lbs/ft)/in
Racking of central portion of superstructure	100 "
Transverse loading of underframe and foundation system	430 "

Stiffness coefficients for mobile homes constructed in accordance with the provisions of the current federal Mobile Home Construction and Safety Standards can be expected to be substantially greater than the values listed above due to improvements in structural connections and the design of partition walls, floors and ceilings to act as true diaphragms. However, the coefficients determined in this study can serve as a reference by which to judge the effectiveness of recent structural innovations in mobile home construction.

7.4 Forces in Tie-Down Cables - The tie-down scheme used in the load-deflection studies is shown in Figure 7.1. If it is assumed that (1) the load distribution over the mobile home cross-section is known; (2) that the windward pier or pedestal is unloaded; and (3) that the diagonal tie connecting the underframe to the leeward anchor is slack; there are five unknown forces in the mobile home support and tie-down systems. These are valid assumptions when the overturning moment equals or exceeds the restoring moment due to dead load and

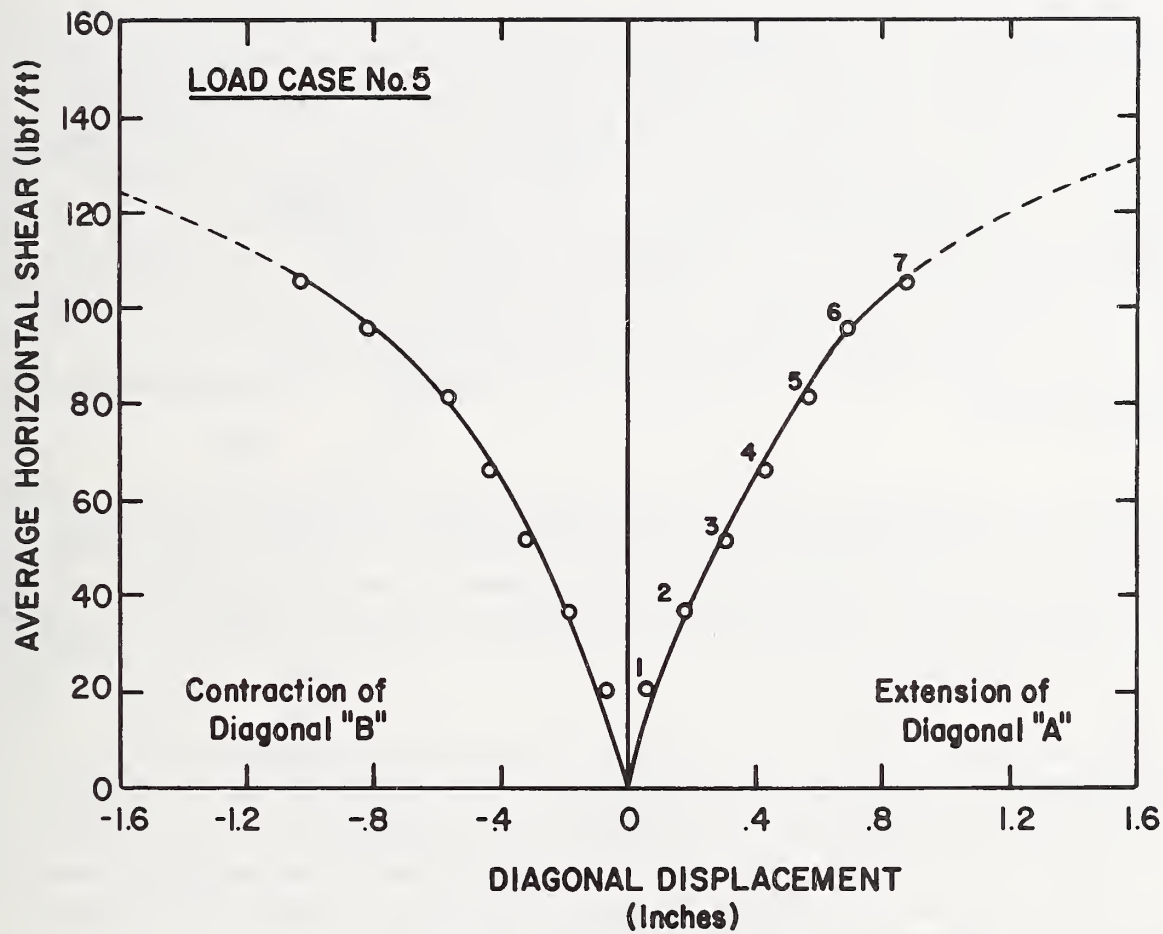


Fig. 7.16 - Load versus Diagonal Displacement for Load Case No. 5

the system of forces becomes statically determinate if two additional assumptions are made; (1) that there is no load acting on the leeward portion of the over-the-top tie and (2) that the coefficient of friction between the mobile home underframe and the leeward pier is known or that the supporting pier is free to rotate and can, therefore, develop no resistance to transverse forces. The forces in the tie-down cables and their variation with applied lift and drag forces are discussed in the following.

Load Case No. 3 - In Figure 7.17 the measured forces in the active diagonal tie and in the over-the-top tie at the windward wall are plotted against the applied drag and lift forces, respectively. It is seen that the force in the diagonal tie increases rapidly when the applied drag load exceeds 82 lbf/ft (1.2 kN/m), indicating that sliding of the longitudinal stringers on the plywood pads covering the support columns has occurred. Beyond this point approximately 65 percent of the increase in the applied drag load is resisted by the diagonal tie. From measurements of vertical forces in the foundation assembly, the change in the vertical reaction at the leeward stringer between load increments 4 and 6 of Figure 7.17 was approximately 500 lbf (2.2 kN), suggesting a coefficient of friction of 0.4 between the plywood pads and the bottom flange of the longitudinal stringer of the mobile home.

The force in the over-the-top tie, while plotted against the vertical line load in Figure 7.17, actually depends upon both the applied drag and lift forces as the restoring moment due to the dead load of the mobile home is exceeded. However, with the drag and lift forces maintained at a constant relative intensity a linear plot should be obtained. This is illustrated by Load Case No. 4.

Load Case No. 4 - With reference to Figure 7.18, the threshold of sliding is not clearly defined, but it has been substantially increased by preloading the over-the-top tie. The relationship between the force in the tie and the applied lift and drag loads becomes highly linear after the fourth load increment. Changes in the overturning moments due to lift and drag and the resisting moment due to the tie-down cable on the windward side differ by approximately 3 percent over the linear range.

On the basis of these results it can be concluded that accurate estimates of tie-down forces under extreme loading conditions which overcome the restoring moment due to dead load can be made with proper choice of friction coefficient and the assumption that the force in the leeward portion of the over-the-top tie is zero. As suggested earlier, the assumption that the supporting piers can resist transverse forces may not always be valid. Given the fluctuating nature of lift and drag forces, it is entirely possible that a mobile home can "walk" across the pier cap if the over-the-top ties are slack, thus subjecting the diagonal tie to the full intensity of the drag load.

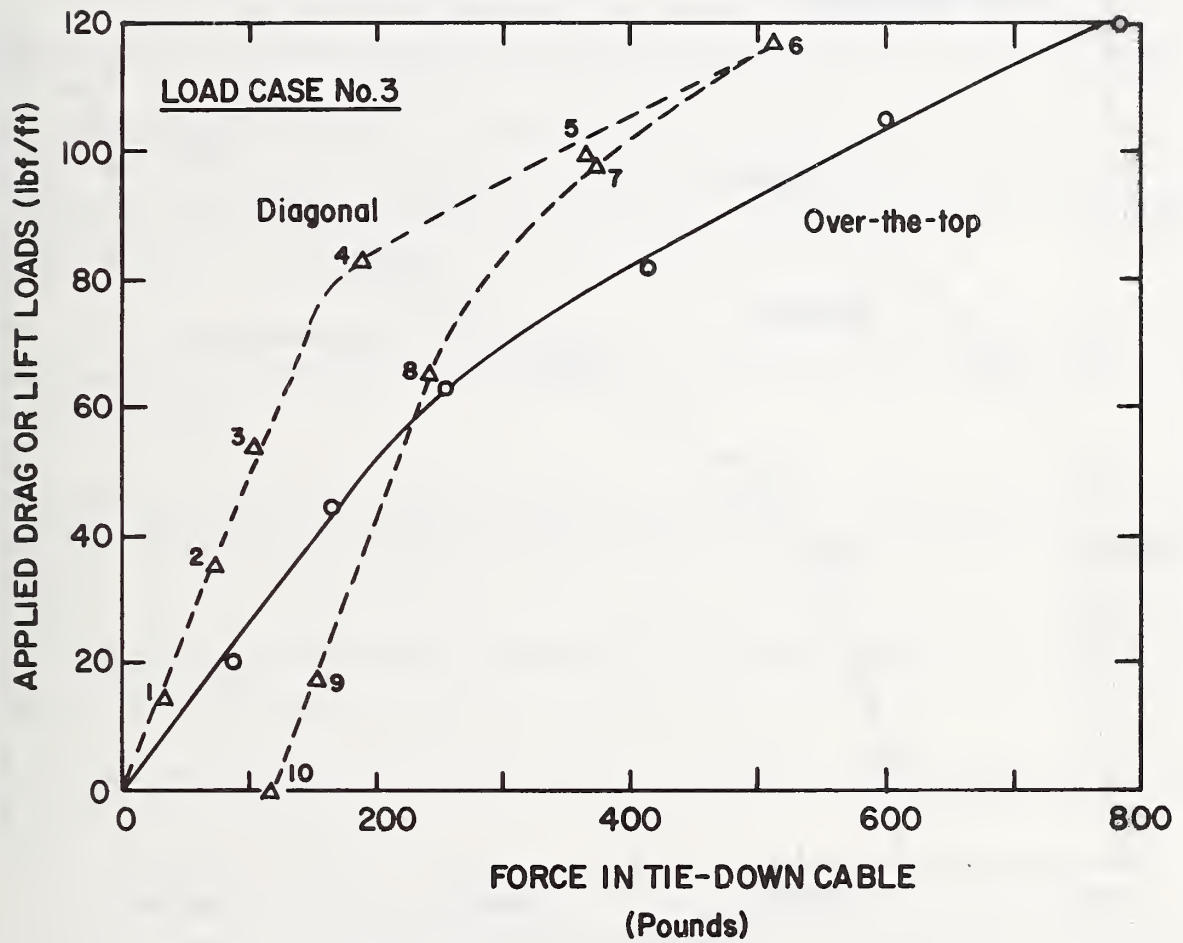


Fig. 7.17 - Forces in Tie-Down Cables for Load Case No. 3

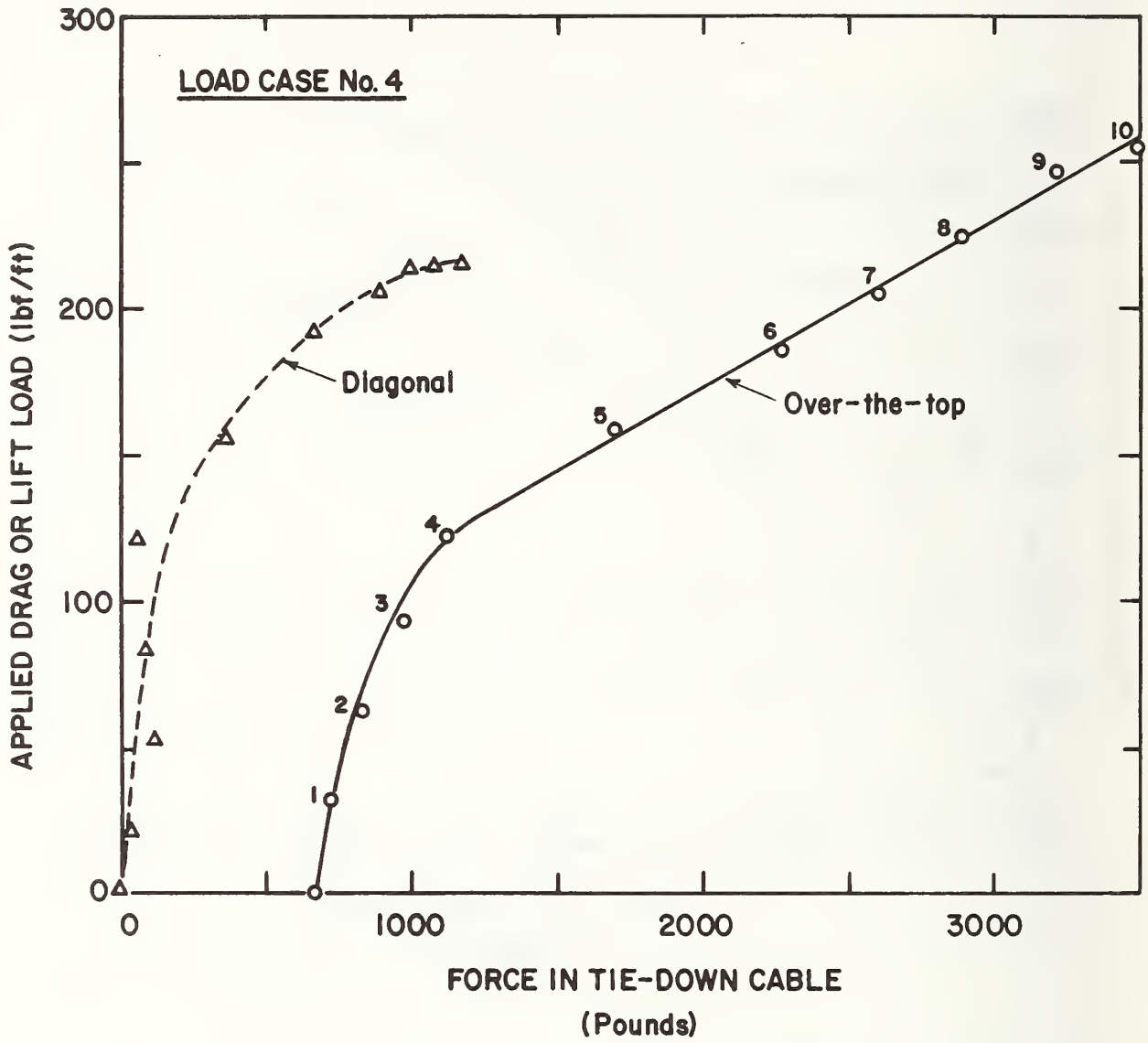


Fig. 7.18 - Forces in Tie-Down Cables for Load Case No. 4

8. CONCLUSIONS AND RECOMMENDATIONS

Based on full-scale measurements of wind speeds and concomitant loads acting on a 12 by 60 ft (3.7 by 18.3 m) mobile home and the behavior of this mobile home under simulated loads corresponding to basic wind speeds of 70 and 90 mph (31 and 40 m/s), the following conclusions can be stated:

(1) The loads listed in Table 15 represent the average maximum values likely to occur for moderately open wind exposures and for basic wind speeds of 70 and 90 mph (31 and 40 m/s).

(2) Measured drag loads tend to confirm the design drag loads currently specified in the federal Mobile Home Construction and Safety Standards (December 1975). For the same basic wind speeds, uplift loads extrapolated from full-scale measurements are approximately 80 percent greater than the design uplift loads currently specified.

(3) Extreme negative pressure fluctuations on the exterior of single-wide mobile homes occur on the end walls and along the perimeter of the roof over strips approximately 2 ft (0.6 m) wide.

(4) Average maximum uplift loads are not strongly influenced by the presence or absence of skirting. Drag loads can be assumed to vary directly with the projected area of the mobile home.

It is felt that the following conclusions will be useful in any future work dealing with wind forces on mobile homes.

(5) The resonant component of response to drag and lift forces is negligible for basic wind speeds up to 90 mph (40 m/s).

(6) The average maximum values of pressure and force coefficients can conveniently be expressed in terms of a mean coefficient and the product of a peak factor and a root-mean-square (r.m.s.) coefficient.

(7) A Weibull distribution satisfactorily describes the probability distribution of peak pressure and load fluctuations.

(8) Accurate estimates of tie-down forces under loading conditions which overcome the dead-load restoring moment can be made on the basis of simplifying assumptions.

The following recommendations are made with regard to the utilization of results obtained from this study and with regard to future research into wind effects on mobile homes.

- (1) The loads listed in Table 15 should form the basis for the design of mobile homes to resist wind forces and wind load provisions of the federal Mobile Home Construction and Safety Standards should be revised as suggested by the wording of Appendix B of this report.
- (2) Consideration should be given to the testing of mobile home scale models of various geometries in wind tunnels to augment the recommended design loads listed in Table 15. Experimental data presented in this report should be used to validate the modeling technique.
- (3) Realistic limitations on structural deflections should be established for service load conditions, taking into account recent innovations in mobile home design and construction.
- (4) Additional research should be conducted to establish an appropriate working stress design equation for tie-down hardware and its interface with the mobile home. Estimates of the coefficient of variation of resistance for various tie-down components should be based on load tests that simulate the mean and fluctuating components of lift and drag forces reported herein.

In conclusion, it must be emphasized that the recommended design wind loads listed in Table 15 and in Appendix B are based on direct field measurements carried out on a full-scale mobile home, the geometry and mass distribution of which are representative of current single-wide mobile home construction. These load recommendations are in no way related to the construction details, load-deflection relationships and failure modes discussed in Section 7 of this report. The measurements presented in Section 7 are exploratory in nature and are not claimed to be representative of structural characteristics of current mobile home construction.

9. ACKNOWLEDGMENTS

Members of the Structures Section staff provided valuable assistance during the course of this experimental investigation, and their contributions are gratefully acknowledged. The author wishes to express his special thanks to the following individuals:

Mrs. Cathy M. Warfield, Administrative Aid, performed the typing of this report.

Dr. R. A. Crist, Chief, Structures Section assisted in the design of the experiment and provided many helpful suggestions during the field studies and during the preparation of this report.

Dr. B. A. Ellingwood and Mr. C.W.C. Yancey, Structural Research Engineers, designed the mobile home support frame, force links and turntable.

Dr. E. V. Leyendecker, Structural Research Engineer, designed the loading system used in the load-deflection studies.

Mr. T. E. Ruschell, Electronics Technician, was responsible for instrument calibration and carried out the A-D conversion and reduction of data.

Messrs. F. A. Rankin, Supervisory Technician, and R. Williams, Physicist, supervised the installation of the mobile home at the test site and the instrumentation-data acquisition system, respectively.

Mr. J. N. Brewer, Chief, Plant Division, arranged for use of the test site and installation of electrical service lines.

10. REFERENCES

1. Dijkers, R. D., Marshall, R. D., and Thom, H. C. S., "Hurricane Camille-August 1969." NBS Technical Note 569, National Bureau of Standards, Washington, D. C., March 1971.
2. Mehta, K. C., et al., "Engineering Aspects of the Tornadoes of April 3-4, 1974." Report prepared for National Research Council, National Academy of Sciences, Washington, D.C., 1975.
3. White, G. F. and Haas, J. E., "Assessment of Research on Natural Hazards." The MIT Press, Cambridge, Massachusetts, 1975.
4. Waldrip, T. G., "Mobile Home Anchoring Systems and Related Construction." Report for Institute for Disaster Research, Texas Tech University, Lubbock, Texas, June 1976.
5. Mobile Home Construction and Safety Standards. Dept. of Housing and Urban Development, Federal Register - Part II, December 1975.
6. Marshall, R. D. and Hsi, G., "Techniques for Measuring Wind Loads on Full-Scale Buildings." Proceedings of Research Seminar on Wind Loads on Structures, University of Hawaii, October 1970, pp. 133-148.
7. Marshall, R. D., "A Study of Wind Pressures on a Single-Family Dwelling in Model and Full Scale." Journal of Industrial Aerodynamics, Vol. 1, No. 2, October 1975, pp. 177-199.
8. Eaton, K. J. and Mayne, J. R., "The Measurement of Wind Pressures on Two-Story Houses at Aylesbury." Journal of Industrial Aerodynamics, Vol. 1, No. 1, June 1975, pp. 67-109.
9. Ambient Pressure Probe, United States Patent 3,950,995, April 1976.
10. Reinhold, T. A., Tieleman, H. W. and Maher, F. J., "Investigation of a Grid Induced Turbulent Environment for Wind Tunnel Testing." Report No. VPI-E-74-30, Virginia Polytechnic Institute and State Univ., Blacksburg, Virginia, December 1974.
11. McMichael, J. M. and Klebanoff, P. S., "The Dynamic Response of Helicoid Anemometers." NBSIR 75-772, National Bureau of Standards, Washington, D. C., November 1975.
12. Tennekes, H., "The Logarithmic Wind Profile," Journal of the Atmospheric Sciences, Vol. 30, 1973, pp. 234-238.
13. Simiu, E., "Logarithmic Profiles and Design Wind Speeds." Journal of the Engineering Mechanics Division, ASCE, Vol 99, No. EM5, Proc. Paper 10100, October 1973, pp. 1073-1083.

14. American National Standard A58.1-1972, Building Code Requirements for Minimum Design Loads in Buildings and Other Structures. American National Standards Institute, Inc., New York, 1972.
15. National Building Code of Canada, Supplement No. 4. Associate Committee on the National Building Code, National Research Council of Canada, 1975.
16. Melbourne, W. H., "Peak Factors for Structures Oscillating Under Wind Action." Proceedings of Conference on Probability Theory of Structural Design, The Institution of Engineers, Australia, November 1974, pp. 35-44.
17. Harris, R. B., "Wind Forces on Mobile Homes." Report prepared for Foremost Insurance Company. Department of Civil Engineering, University of Michigan, June 1962.
18. Cole, H. A., Jr., "On-the-line Analysis of Random Vibrations." AIAA Paper No. 68-288, presented at AIAA/ASME Ninth Structures, Structural Dynamics and Materials Conference, Palm Springs, CA, 1968.
19. Yang, J. C. S. and Caldwell, D. W., "The Measurement of Damping and the Detection of Damages in Structures by the Random Decrement Technique." Presented and published at 46th Shock and Vibration Symposium and Bulletin, San Diego, CA, November 1975.
20. Yang, J. C. S., "The Measurement of Damping in Mobile Homes." Report prepared for the National Bureau of Standards, September 1976.
21. Standard for the Installation of Mobile Homes - Including Mobile Home Park Requirements, NFPA No. 501A, 1975.
22. Durst, C. S., "Wind Speeds Over Short Periods of Time. Meteorological Magazine, Vol. 89, London, 1960, pp. 181-186.
23. Vellozzi, J. W. and Cohen, E., "Gust Response Factors." Journal of the Structural Division, ASCE, Vol. 94, No. ST6, Proceedings Paper 5980, June 1968, pp. 1295-1313.
24. "Wood Handbook," Agricultural Handbook No. 72, Forest Products Laboratory, U.S. Forest Service, August 1974.
25. Galambos, T. V. and Ravindra, M. K., "Tentative Load and Resistance Factor Design Criteria for Steel Buildings." Research Report No. 18, Structural Division, Washington University, September 1973.
26. "Uniform Building Code," International Conference of Building Officials, 1973.

27. Tuomi, R. L. and McCutcheon, W. J., "Testing of a Full-Scale House Under Simulated Snowloads and Windloads." USDA Forest Service Research Paper FPL 234, 1974.

11. APPENDIX A

Illustrative Example - Determination of Design Loads

To illustrate the procedure outlined in Section 6.4, the average maximum pressure coefficients and the recommended design pressure for tributary roof areas (excluding the roof perimeter) are determined for a single-wide mobile home in the following example.

The multiple-point pressure coefficients for Record No. 10-4, taps R8 to R11, are presented in Table 4. These coefficients were computed using a record length of 504 seconds and a mean wind speed of 13.0 mph at the height of the mobile home (see Table 1). Also listed in Table 4 are the peak factor g , the upcrossing rate n_o , the peak rate n_p , and the Weibull parameters c and k . As previously discussed, the values of C_p , C_{ps} , c and k are considered to be invariant with wind speed.

Assuming a basic wind speed of 70 mph, the mean dynamic reference pressure, q_h is obtained from Eq. 21.

$$\bar{q}_h = (0.0011)(70)^2 = 5.4 \text{ psf.}$$

The value of $P(>X)$ is obtained from Eq. 23

$$P(>X) = \frac{13.0}{(660)(0.81)(70)} = 3.5 \times 10^{-4}$$

The associated peak factor, g , can now be determined, either by using Eq. 11 or by resorting to probability paper as shown in Figure 5.6.

From Eq. 11,

$$e^{-\left(\frac{g}{0.50}\right)^{0.72}} = 3.5 \times 10^{-4}$$

and

$$g = 8.6$$

Since negative departures from the mean are of interest for external pressures acting on the roof (suction), the peak factor is based on negative departures from the mean and the peak negative pressure coefficient is obtained as follows:

$$\begin{aligned}
\hat{C}_p &= C_p + g C_{pe} && \text{(see Eq. 22)} \\
&= -0.95 + (-8.6)(0.35) \\
&= -3.96
\end{aligned}$$

These are the values of $P(>X)$, g and \hat{C}_p listed in Table 10 for Record No. 10-4 and for $u_{FM} = 70$ mph. An identical procedure is used to obtain the corresponding values for $u_{FM} = 90$ mph. In determining the internal pressure coefficients, the peak factor is based on positive departures from the mean since this will, when combined with the negative external pressure acting on the roof, produce the most critical pressure combination.

Again with regard to tributary areas of the roof, the values of \hat{C}_p listed in Table 11 are obtained from averaging the relevant multiple point pressure coefficients listed in Table 10 and the internal pressure coefficients listed in Table 9. For $u_{FM} = 70$ mph (Table 11), the values of \hat{C}_p for tributary roof areas and for the maximum internal pressure are -4.30 and $+1.00$, respectively. The corresponding values of \hat{p} (see Eq. 22) for $\bar{q}_h = 5.4$ psf are -23.2 psf and $+5.4$ psf, respectively. Since these pressures both act upward on the roof, the combined pressure is $-23.2 - 5.4 = -28.6$ psf for $u_{FM} = 70$ mph. Finally, applying the load reduction factor of 0.8 for working stress design as is discussed in Section 6.6, the recommended load for the design of trusses, roof membrane and fasteners in the standard wind zone (Table 15) is $(0.8)(-28.6) = -23$ psf.

12. APPENDIX B

Recommended Revisions of Section 280.305 "Structural Design Requirements" - Federal Mobile Home Construction and Safety Standards, December 18, 1975.

The following changes in the rules and regulations of Section 280.305 "Structural Design Requirements" are recommended on the basis of full-scale measurements, design criteria and procedures described elsewhere in this report. The loads indicated in the following paragraphs are equivalent static loads for the design of mobile homes and their anchoring systems to resist wind forces and represent average maximum loads for the conditions stated.

RULES AND REGULATIONS

Sec. 280.305 Structural design requirements.

(a) (See original text)

(b) *Design Loads.* (1) *Design dead loads.* Design dead loads shall be the actual dead load supported by the structural assembly under consideration. (2) *Design live loads.* The design live loads, including wind and snow loads, shall be as specified in this Section and shall be considered to be uniformly distributed. The roof live load or snow load shall not be considered as acting simultaneously with the wind load and the roof live or snow load and floor live loads shall not be considered as resisting the overturning moment or sliding due to wind. (3) When engineering calculations are performed, allowable unit stresses may be increased as provided in the documents referenced in Sec. 280.304 except as shown otherwise in Sec. 280.306(a). (4) The Data Plate posted in the mobile home (See Sec. 280.5) shall show for which structural zone(s) of the USA the mobile home has been designed and the actual design external snow and/or wind live loads. The Data plate shall include reproductions of the Load Zone Maps shown in Sec. 280.305(c) and (d) and related information. The Load Zone Maps shall be not less than one-half the size illustrated.

(c) *Wind Loads.* (1) *Standard Wind (Zone I).* When a mobile home is not designated as "Hurricane-Resistive," the mobile home and each wind resisting part and portion thereof shall be designed for the loads listed under "Standard Wind (Zone I)" in the table below.

(2) *Hurricane Resistive (Zone II).* (i) When a mobile home is designated as "Hurricane Resistive," the home and each wind resisting part and portion thereof shall be designed for the loads listed under "Hurricane Resistive (Zone II)" in the table below. (ii) For exposures in coastal and other areas where wind records indicate significantly higher loads than the loads specified for Zone I and Zone II, the Department may establish more stringent requirements for homes known to be destined for such areas.

(d) *Roof Loads.* (1) Flat, curved and pitched roofs shall be designed to resist the following live loads, applied downward on the horizontal projection as appropriate for the design zone marked on the mobile home:

	Pounds per square foot
North Zone-----	40
Middle Zone-----	30
South Zone-----	20

(2) For exposures in areas (mountainous or other) where snow records or experience indicate significant differences from the loads stated above, the Department may establish more stringent requirements for homes known to be destined for such areas. For snow loads, such requirements are to be based on a roof snow load of 0.6 of the ground snow load for areas exposed to wind and a roof snow load of 0.8 of the ground snow load for sheltered areas.

(e) Design Load Deflection. (See original text)

(f) Fastening of Structural Systems. (See original text)

(g) *Walls.* The walls shall be of sufficient strength to withstand the load requirements as defined in Sec. 280.305(c) and (d) of this part and, when subjected to horizontal loads of 15 and 25 lbs/ft² for Zone I and Zone II, respectively, shall not exceed the deflections as specified in Sec. 280.305(e). The connections between the bearing walls, floor, and roof framework members shall be fabricated in such a manner as to provide support for the material used to enclose the mobile home and to provide for transfer of all lateral and vertical loads to the floor and chassis.

(1) Except where substantiated by engineering analysis or tests, studs shall not be notched or drilled in the middle one-third of their length.

(2) Interior walls and partitions shall be constructed with structural capacity adequate for the intended purpose and shall be capable of resisting a horizontal load of not less than five pounds per square foot. Finish of walls and partitions shall be securely fastened to wall framing.

(h) Floors. (See original text)

(i) *Roofs.* (1) Roofs shall be of sufficient strength to withstand the load requirements as defined in Sec. 280.305(b), (c) and (d) of this part and, when subjected to uplift loads of 9 and 15 lbs/ft² for Zone I and Zone II respectively, or the roof loads of Sec. 280.305(d), shall not exceed the deflections specified in Sec. 280.305(e). The connections between roof framework members and bearing walls shall be fabricated in such a manner to provide for the transfer of design vertical and horizontal loads to the bearing walls and to resist uplift forces.

(2) Roofing membranes shall be of sufficient rigidity to prevent deflection which would permit ponding of water or separation of seams due to wind, snow, ice, erection or transportation forces.

(3) Cutting of roof framework members for passage of electrical, plumbing or mechanical systems shall not be allowed except where substantiated by engineering analysis.

(4) All roof penetrations for electrical, plumbing or mechanical systems shall be properly flashed and sealed. In addition, where a metal roof membrane is penetrated, a wood backer shall be installed. The backer plate shall be not less than 5/16 inch plywood, with exterior glues, secured to the roof framing system beneath the metal roof, and shall be of a size to assure that all screws securing the flashing are held by the backer plate.

Design Loads for Standard and Hurricane Wind Zones

	<u>STANDARD</u> (Zone I)	<u>HURRICANE</u> (Zone II)
ROOF		
Design of trusses, roof membrane and fasteners (except as noted below)	-23 (-18)	-40 (-30)
Roof membrane and fasteners on strip 2 feet wide extending around perimeter of roof	-36	-61
Overhangs (net uplift)	45	77
SIDE WALLS		
Design of studs, doors, windows, exterior wall covering and fasteners (except as noted below)	15	26
Exterior wall covering and fasteners at ends of sidewalls on vertical strips 6 feet wide	-12	-21
	-24	-40
END WALLS		
Design of studs, windows, exterior wall covering and fasteners	15	26
	-32 (-24)	-56 (-40)
FLOOR	6	10
DRAG LOAD		
Load acting on horizontally projected area of structure and used for design of structural subsystems to resist racking (See Note 4)	17 (15)	29 (24)
End sections (1/4 length)	15	24
Central section (1/2 length)		
UPLIFT LOAD		
Load acting vertically upward on plan area of structure and used for design of structural subsystems to resist bending in vertical plane (See Note 5)	16	28

Notes:

1. All pressures in pounds per square foot.
2. Negative sign indicates pressures acting outward.
3. Loads indicated by () are to be applied to double-wide units only.
4. Resultant to be applied at 0.6h above ground level. h is height of roof-wall intersection.
5. Resultant to be applied at 0.4W from windward edge of roof. W is width of mobile home.

U.S. DEPT. OF COMM. BIBLIOGRAPHIC DATA SHEET	1. PUBLICATION OR REPORT NO. NBSIR 77-1289	2. Gov't. Accession No.	3. Recipient's Accession No.
4. TITLE AND SUBTITLE The Measurement of Wind Loads on Full-Scale Mobile Homes		5. Publication Date September 1977	
7. AUTHOR(S) Richard D. Marshall		6. Performing Organization Code	
9. PERFORMING ORGANIZATION NAME AND ADDRESS NATIONAL BUREAU OF STANDARDS DEPARTMENT OF COMMERCE WASHINGTON, DC 20234		8. Performing Organ. Report No. 7415141	
12. SPONSORING ORGANIZATION NAME AND COMPLETE ADDRESS (Street, City, State, ZIP) Division of Energy, Building Technology and Standards Office of Policy Development and Research Department of Housing and Urban Development Washington, D.C. 20410		10. Project/Task/Work Unit No.	
15. SUPPLEMENTARY NOTES <input type="checkbox"/> Document describes a computer program; SF-185, FIPS Software Summary, is attached.		11. Contract/Grant No.	
16. ABSTRACT (A 200-word or less factual summary of most significant information. If document includes a significant bibliography or literature survey, mention it here.) An experimental investigation of wind loads acting on a full-scale mobile home is reported. The objectives of the investigation were (1) the direct measurement of surface pressures and overall drag and lift forces, (2) the formulation of recommended loads for the design of mobile homes and their anchoring systems to resist forces due to wind and (3) the measurement of deflections and the identification of failure modes with application of simulated wind loads. Measurements were obtained for a variety of wind speeds and relative wind directions using a mobile home with nominal plan dimensions of 12 by 60 ft (3.7 by 18.3m). Wind speeds were measured at five levels ranging from 3 to 18m and the mean velocity profiles were found to be best described by a power law with exponent $\alpha = 0.18$. Extreme negative pressure fluctuations were found to occur on the end walls and along the perimeter of the roof. The resonant component of response of the mobile home to drag and lift forces is negligible for basic wind speeds up to 90 mph (40 m/s) and the average maximum lift loads are not strongly influenced by the presence or absence of skirting. Recommended design loads are based on the average maximum event in a time interval of 1000 seconds and are tabulated for assumed basic wind speeds of 70 and 90 mph (31 and 40 m/s) and a moderately open wind exposure.		13. Type of Report & Period Covered Final	
17. KEY WORDS (six to twelve entries; alphabetical order; capitalize only the first letter of the first key word unless a proper name; separated by semicolons) Aerodynamics; building; codes and standards; full-scale testing; mobile homes; wind loads.		14. Sponsoring Agency Code	
18. AVAILABILITY <input checked="" type="checkbox"/> Unlimited <input type="checkbox"/> For Official Distribution. Do Not Release to NTIS <input type="checkbox"/> Order From Sup. of Doc., U.S. Government Printing Office, Washington, DC 20402, SD Stock No. SN003-003- <input checked="" type="checkbox"/> Order From National Technical Information Service (NTIS), Springfield, VA, 22161	19. SECURITY CLASS (THIS REPORT) UNCLASSIFIED	21. NO. OF PRINTED PAGES	
	20. SECURITY CLASS (THIS PAGE) UNCLASSIFIED	22. Price	



